# EXPLOITING THE IMMUNOGENIC CANCER MUTANOME TO ENHANCE ONCOLYTIC VIRUS THERAPY

By

Monique Marguerie Honours BSc.

A thesis submitted in partial fulfillment of the requirements of the degree of

Master's of Science, Specialization in Biochemistry

University of Ottawa

Faculty of Medicine

May 2014

Supervisor

Dr. John C. Bell, PhD

**Abstract**

Oncolytic viruses (OVs) are effective anti-cancer agents, however their abilities to induce anti-tumor immunity are not yet optimal. Mutanome epitopes are a novel source of tumor antigen formed as a result of mutations within the tumor genome. Within this project we attempted to combine B16F10 mutanome vaccination with OV therapy. We confirmed previous findings that significant immune responses to these epitopes can be generated. Furthermore, we designed and cloned a multi-epitope mutanome construct into MG1 Maraba virus and E1-/E3- deleted type 5 Adenovirus to use for heterologous prime-boost vaccination. While we demonstrated that these viruses induced T-cell responses to one mutanome epitope, we failed to detect responses to the other epitopes. Furthermore there was no effect seen on overall survival. This approach warrants further investigation because coupling mutanome vaccination with OV therapy has the potential to exploit the therapeutic effects of the OV while inducing anti-tumor immunity to tumor-unique antigens.

*"I cannot give any scientist of any age better advice that this: The intensity of the conviction that a hypothesis is true has no bearing on whether it is true or not. The importance of the strength of our conviction is only to provide a proportionally strong incentive to find out if the hypothesis will stand up to critical evaluation."*

- Sir Peter B. Medawar, Advice to a Young Scientist [1]

**Acknowledgements**

First and foremost, I would like to thank my supervisor Dr. John Bell for his wisdom and encouragement, and for giving me the opportunity to work and study in his lab. I am also grateful to Dr. Harold Atkins who not only has mentored me throughout my MSc, my summer studentship, and my 4th year honours project, but also gave me my very first opportunity to work in a wet-lab research environment. I would like to generously thank Dr. Rebecca Auer, Dr. Brian Lichty, Dr. Kelley Parato and Dr. Chantal Lemay for their guidance and expertise throughout my degree.

Many thanks are also owed to everyone in the Bell/Atkins/Auer/Diallo labs for making the lab such a friendly and helpful environment. I would like to acknowledge certain people in particular: Kyle Stephenson, for always answering my numerous questions, and for reading my ELISPOT plates; Marie-Claude, for her magic cloning hands and for making this thesis much less painful for you to read; Theresa, for helping me with animal work and making it something that I look forward to; Dr. Robin Parks, for cloning the Ad-MUT virus and for his much-needed advice; Spencer Martin for sequencing our B16 cells; Geeta, for being my very first lab mentor; Almo, Vicki, Maddie and Andrea for help with experiments; and importantly, Jovian, for being my partner-in-crime throughout our MSc's;. Also, a special thank you to Carolina and Laura who involved me in their own research projects and exposed me to other exciting aspects of OV therapy.

Most importantly, I am grateful to my parents and Garrett who have always had faith in me and have supported me unconditionally in my studies and throughout my life.

**Table of Contents**

**List of Abbreviations**

| | |
|---|---|
| AA | Amino acid |
| Ab | Antibody |
| Ad | Adenovirus. Particularly, in the context of this paper Ad refers to E1-/E3- deleted type 5 adenovirus (AdRP2014) |
| Ad-MUT | Ad virus encoding mutanome construct, wild-type ubiquitin |
| APC | Antigen presenting cell |
| BMDC | Bone marrow derived dendritic cell |
| DC | Dendritic cell |
| DCT | Dopachrome tautomerase |
| DMEM | Dubelcco's Modified Eagle's Medium |
| FBS | Fetal bovine serum |
| GFP | Green fluorescent protein |
| IFN | Interferon |
| IM | Intramuscular |
| irrB16 | gamma irradiated B16F10 cells |
| IP | Intraperitoneal |
| IV | Intravenous |
| MG1 | Maraba double mutant virus (M: L123W, G:Q242R) |
| MG1-MUT | MG1 virus encoding mutanome construct, wild-type ubiquitin |
| MG1-MUT-UbMUT | MG1 virus encoding mutanome construct, mutated ubiquitin |
| MHC | Major histocompatibility complex |
| MOI | Multiplicity of infection |

| | |
|---|---|
| NGS | Next Generation Sequencing |
| NK | Natural killer |
| OV | Oncolytic virus |
| PBS | Phosphate-buffered saline |
| PFU | Plaque forming units |
| SLP | Synthetic long peptide |
| SMNC | Splenic mononuclear cells |
| SQ | Subcutaneous |
| TAA | Tumor associated antigen |
| Ub | Ubiquitin |
| VSV | Vesicular Stomatitis Virus |
| WT | Wild type |

## List of Tables

**List of Figures and Illustrations**

# 1 INTRODUCTION

## *1.1 Cancer*

In Canada, almost half of the national population will develop cancer in their lifetime (41% of women and 46% of men), and about a quarter will die as a result of cancer, making it the leading cause of death in Canada in 2013 [2]. While there have been significant advancements in cancer therapeutics over the last few decades, the alarmingly high mortality rate impresses the need for further research and more successful therapies.

Cancer is a deeply complex, diverse and dynamic disease that, even after decades of research, we are still unable to fully understand. A very basic and broad way to describe cancer is as cells that have acquired the ability to grow and divide uncontrollably through genetic and epigenetic changes [3]. Cancer development is quite analogous to Darwinian evolution; as growth advantages are acquired in response to genetic changes, the population slowly shifts from a normal cell population into a population of cancerous ("transformed") cells, possessing increased growth and survival advantages compared to the original cell populations [4].

Two pivotal publications outlined eight biological capabilities of cancer, referred to as the hallmarks of cancer, which result in the cancer-like phenotype. These include sustaining proliferative signaling, evading growth suppressors, resisting cell death, enabling replicative immortality, inducing angiogenesis, activating invasion and metastasis, reprogramming of energy metabolism and evading immune destruction [4, 5]. In addition to increasing our understanding of cancer, these cancer "hallmarks" have proven to be effective therapeutic targets as well. With myriads of therapies targeting

these biological capabilities both in the clinic and in pre-clinical and clinical trials [5], hopefully we are not far away from removing cancer from the top of the list of causes of death for Canadians and people around the world.

### *1.2 Cancer Immunoediting*

As early as 1909, Paul Ehrlich proposed that in long-lived organisms, such as humans, the immune system must have a hand in the prevention of cancer (Ehrlich, 1909). The interaction between cancer and the immune system is very complex and challenging to elucidate. Scientists have spent decades trying to determine whether the immune system is a driving force or a protective force against cancer. As it turns out, we are slowly realizing that the immune system has a hand in both sides: not only can it suppress tumor growth but it can also promote tumor progression.

The immune system plays many crucial roles in the prevention of cancer, not the least of which is immunosurveillance, a process in which the immune system detects and kills tumor cells before they progress to a malignant state [6]. The immune system also acts in a preventative fashion, by sequestering viral infections that could lead to virus induced tumors, and by eliminating pathogens, which, if unresolved could lead to a chronic inflammation and facilitate tumorigenesis [7]. As mentioned, the immune system can also promote cancer progression. The term “cancer immunoediting” has been assigned to the dual role the immune system plays in cancer progression [8]. Cancer immunoediting consists of three phases: the elimination phase (also referred to as immunosurveillance), the equilibrium phase, and the escape phase. The immunoediting process is outlined in **Figure 1.1**. The elimination phase represents what we typically

**Figure 1.1**. **The three phases of cancer immunoediting.**

Summary of the role that the immune system plays in the clearance, shaping and progression of cancer. The elimination phase is the first stage of cancer immunoediting and is when the immune system is working to eliminate transformed cells and prevent tumor outgrowth through various mechanism. This phase will result in either the elimination of the cancer or progression to the equilibrium phase, the second and longest phase of the immunoediting process. During equilibrium, there is a balance between pressures exerted by the tumor and by the adaptive immune system, which is acting to prevent tumor outgrowth. During this phase, the tumor cells may acquire survival advantages through mutations, which may eventually enable the tumors to progress into clinically detectable malignancies and enter the escape phase. Reproduced with permission from Vesely *et al*. [6]

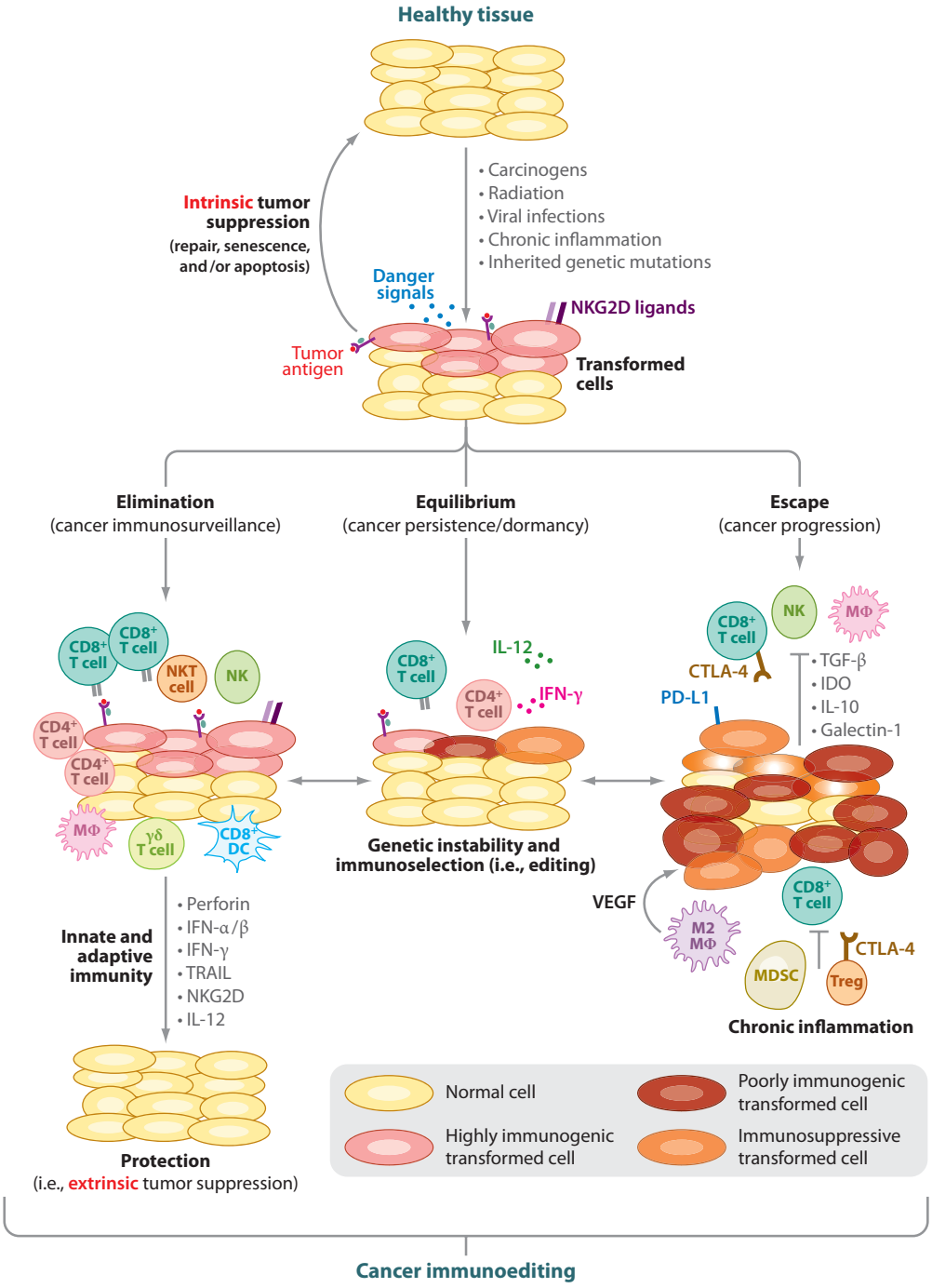
Healthy tissue
• Carcinogens
• Radiation
• Viral infections
• Chronic inflammation
• Inherited genetic mutations
Intrinsic tumor suppression
(repair, senescence, and/or apoptosis)
Danger signals
NKG2D ligands
Tumor antigen
Transformed cells
Elimination
(cancer immunosurveillance)
Equilibrium
(cancer persistence/dormancy)
Escape
(cancer progression)
CD8+ T cell
NKT cell
NK
CD4+ T cell
MΦ
γδ T cell
CD8+ DC
IL-12
IFN-γ
Genetic instability and immunoselection (i.e., editing)
CTLA-4
PD-L1
• TGF-β
• IDO
• IL-10
• Galectin-1
VEGF
M2 MΦ
MDSC
Treg
Chronic inflammation
Innate and adaptive immunity
• Perforin
• IFN-α/β
• IFN-γ
• TRAIL
• NKG2D
• IL-12
Protection
(i.e., extrinsic tumor suppression)
Normal cell
Poorly immunogenic transformed cell
Highly immunogenic transformed cell
Immunosuppressive transformed cell
Cancer immunoediting

understand to be encompassed within immunosurveillance; it is characterized by competent adaptive and innate immune responses destroying transformed cells before the tumors become clearly visible [9]. Transformed cells can be detected by the CD8+ effector cells through the presentation of tumor antigens on MHC class I molecules or by NK cells through their NKG2D ligands [10]. Tumor cells may also express stress-induced molecules such as surface calreticulin [11] or they may release endogenous damage-associated molecular patterns (DAMPs) to enhance the immune system's recognition of cancer cells [12]. In addition, IFNγ has been identified as a critical player in the development of anti-cancer immune functions, and mice depleted of IFNγ are more susceptible to tumor establishment and progression [9].

Tumor specific antigens have also been identified as players in the process of cancer elimination [13]. Tumors that have not been exposed to the immune system have a tendency to be highly immunogenic. For example, if a tumor that has developed in an immune deficient mouse is then seeded in an immune competent mouse, the cells are unlikely to establish a tumor due to immune responses against them [14, 15]. Schreiber's group recently demonstrated that in immune competent mice, tumors lacking strong antigens will fail to be rejected by the host, while tumors which possess the strong antigens will successfully be rejected through T-cell mediated immunoselection [13].

Despite all of the safeguards in place to eliminate tumor cells, sometimes the immune system fails to eliminate the transformed cells. When this occurs the cells progress to a dynamic intermediate stage of cancer immunoediting, during which time they are kept in a state of functional dormancy by the host immune system. This stage,

referred to as the equilibrium phase [6, 10, 16], is understood to be the longest of the immunoediting phases. During this phase the tumor acquires its most immunoevasive mutations. The adaptive immune system, through strong anti-tumor immune responses is able to contain the cancer, however it is unable to eradicate it. Anti-tumor cytokines such as IFNγ and IL-12 work to promote tumor elimination, whereas tumor promoting cytokines such as IL-23 and IL-10 enable the tumor to persist [17]. Depletion of T-cells or the use of antibodies that block immune-mediating cytokines such as IFNγ and IL-12, causes the tumors to enter the escape phase and grow out [16]. In contrast, the innate immune system has been shown to be non-essential for maintaining tumors in equilibrium [16].

The third and final stage of immunoediting is the escape phase. In this phase the balance between tumor and immune system has tilted towards the tumor due to the acquired ability of the tumor cells to evade immune pressure; the result of which is the progression into a clinically evident disease [18]. The mechanisms involved in evading the immune system are complex and very differently in each tumor. Suppressing proinflammatory danger signals to prevent dendritic cell maturation [19] and inducing the loss of ligands for the NK cell effector molecules are both mechanisms which have been shown to be involved in immune evasion [20]. In addition, because more immunogenic tumor variants are likely to be eliminated from the tumor population through immunoediting early in cancer progression, the remaining cells may be invisible to the immune system [6, 10].

Tumors can also acquire defects in their antigen processing and presentation pathways. For example some tumors experience a down regulation in MHC I expression

[21] while others may develop insensitivity to IFNγ [18, 22, 23]. By applying selective pressure and eliminating the more immunogenic tumor variants, the immune system has caused the tumor population to evolve and become less immunogenic. This has simultaneously given the tumor a survival advantage and promoted tumor cell proliferation [6]. Due to the plasticity of cancer, some immunotherapies can also lead to immunoediting and evolution of the cancer population towards tumor variants insensitive to therapy [9]. For this reason, combination therapy approaches and immunotherapies with multiple targets are more likely to be successful and reduce the probability of tumor relapse. Within the context of this thesis we combine oncolytic virus therapy and immunotherapy approaches in attempt to enhance tumor control.

### *1.3 Generating an anti-tumor immune response*

Cancer related antigens that the immune system may respond to include: neoantigens created as a result of accumulation of mutations in cancer; products of non-mutated genes that are preferentially expressed by cancer cells; or antigens from the cancer's tissue of origin that are not yet tolerized [24, 25]. Dendritic cells (DC) are specialized antigen-presenting cells and are one of the key components in the induction of anti-tumor immune responses. They take up antigens from surrounding environments, which they process internally and present on their MHC molecules at the cell surface. If the DCs do not receive maturation signals concurrent to antigen uptake, such as TLR stimulation, the result will be T-cell tolerance instead of the production of an effective anti-tumor response [26, 27]. CD4+ T-cells recognize MHC class II molecules and are known for their functions producing the cytokines necessary for the effector functions of other immune cells. CD8+ cytotoxic T-cells recognize MHC class I

molecules on target cells and can act to kill these cells. Both CD4+ T-cells and CD8+ T-cells have been shown to generate antigen-specific immune reactions that can play a role in tumor regression [18, 28-31].

### *1.4 Cancer Immunotherapy*

The current standard of care for many cancers today is chemotherapy drugs designed to target rapidly dividing cells, like cancer cells. The problem with chemotherapy drugs is that they also cause toxicity for non-cancerous cells, resulting in many unwanted side effects. While rapid cell division is a well-known characteristic of cancer cells, there are also many other traits that can be targeted [4, 5]. Cancer immunotherapy, a branch of cancer therapy focused on enhancing an individual's immune response to cancer, focuses on doing just that. There are three main areas that cancer immunotherapy generally focuses on in order to enhance an individuals anti-cancer immune response: 1 – promoting the antigen presentation abilities of DCs, 2 – enhancing the protective T-cell responses and 3 – overcoming mechanisms of tumor immunosuppression [32].

There has been a great deal of research that has gone into understanding and promoting the antigen presentation abilities of DCs *in vivo* [33]. Dendritic cells are corner stones in the generation of antigen specific immune responses and as such DC adoptive transfer is a key area that has undergone significant investigation. Many DC vaccine therapy trials have demonstrated a clinical benefit [34], and the first DC therapy was approved by the FDA in 2010 for metastatic prostate cancer [35].

Enhancing T-cell responses has been another main focus of cancer immunotherapy. Adoptive transfer of antigen-specific T lymphocytes has been very

successful for some types of cancer, however more immunosuppressive cancers have not been as responsive to this therapy [36]. T-cells that have been modified *ex vivo* to express chimeric antigen receptors, commonly referred to as CAR T-cells, have resulted in significant improvements in therapeutic efficacy as well some quite astounding clinical outcomes in response to treatment [37-39].

Enhancing DC ability to prime effector immune cells is one example of how we can therapeutically enhance anti-tumor immunity. There are also many other mechanisms through which this can also be accomplished. Anti-tumor immune responses can be enhanced through vaccination with whole cell and infected cell vaccines [40], recombinant proteins [41], synthetic peptides [42, 43], and messenger RNA [44]. Furthermore, we can use next generation genome sequence techniques in order to identify novel tumor specific mutations within the cancer genome for immunizing against. This approach will be discussed more in detail in the following section.

### *1.4.1 The Cancer "Mutanome"*

It is broadly understood that DNA mutations are one of the primary causes of cancer [5, 45]. Human cancers carry 10s to 100s of nonsynonymous mutations and these mutations can function as a novel source of antigens within the tumor [46, 47]. The term "mutanome" refers to the library of somatic mutations that are present within a given tumor, and "mutanome antigens" refers to the neo-antigens that have developed as a result of these mutations [43].

The mutanome of different cancers can be identified by "next-generation sequencing" (NGS) technology, a method of ultrafast and high-throughput sequencing,

followed by computational analysis to identify mutations found within a cancer that are not found within normal tissue [43, 47]. Rapid identification of the mutanome has huge implications for personalized cancer therapies. It enables us to quickly identify patient-specific neoantigens that can then be targeted by immunotherapeutic approaches.

There are some trials investigating the administration of cancer vaccines targeting tumor associated antigens (TAA). The limiting factor with this approach is that the antigens being targeted are from self-epitopes which are subject to central tolerance [48]. Tumor specific "mutanome" antigens would not be as heavily subjected to central tolerance mechanisms, supporting why there have been immune responses detected towards these neoantigens in cancer patients [46]. There has been evidence that if the immune system is able to generate sufficient immune responses to cancer neoantigens than it can lead to control of cancer progression [13, 49-51].

The sequencing of the first entire mouse genome in 2011 [52] showed that it was feasible to use mice as a pre-clinical model organism for investigation of the cancer mutanome. In 2012, Ugur Sahin's group was the first group to sequence a mouse tumor exome [43]. They successfully identified hundreds of nonsynonymous somatic point mutations expressed in genes of the B16F10 cell line and showed that many of these nonsynonymous somatic mutations found in tumors have immunogenic potential. Impressively, they also demonstrated that some of the immune responses induced to these mutanome antigens lead to effective B16F10 tumor control and increased survival duration [43].

Of note, none of the mutations that were identified in this study were present in the four known melanoma oncogenes [43, 47], but mutations were found in established

tumor suppressor genes, DNA repair associated genes, and in genes associated with known cancer pathways [43]. Significantly, there was no evidence that the oncogenicity of the target molecule was related to its immunogenic potential. Thus the immunogenicity of a mutanome antigen has no relation to whether the mutation is cancer driver mutation or a bystander mutation [47].

The exciting findings outlined in this study support the notion that a patients' mutanome can provide us with many useful vaccination targets. With rapid advances in technology and even faster methods of genome sequencing being developed every year, it may soon be possible for a cancer patient to have their tumors sequenced to identify and subsequently target personalized neoantigens. The focus of the project outlined within this thesis is to improve vaccination against mutanome antigens through OV therapy. The characterization of the B16F10 mutanome by Castle *et al* served as our starting point [43].

### *1.4.2 Peptide vaccination strategies*

Preventative vaccination strategies are widely viewed as one of the most successful medical advances in history. Vaccinations against smallpox, polio, measles, and diphtheria have saved millions of lives worldwide since their implementation. While we have observed tremendous successes with preventative vaccination, we have not had nearly the same success for therapeutic vaccination. For cancer in particular we have had limited clinical success with tumor vaccination [53].

There have been many different attempts at therapeutic vaccination strategies over the years including vaccination with recombinant proteins [54, 55], recombinant viral vectors encoding TAAs or viral antigens [56, 57], DNA encoding antigens [58, 59],

antigen-loaded dendritic cells [60, 61] and synthetic peptides [62, 63]. In order for therapeutic vaccines to work, they must be able to induce strong immune responses in the host [42].

Two of these therapeutic vaccination approaches were assessed in this project: synthetic peptides and viral vectors, the latter of which will be discussed later on in this introduction. Treatment with synthetic peptides is more efficient than vaccination with some other DNA vaccines because it eliminates the intermediate step of RNA transcription [42]. An advantage of using peptides for vaccination instead of whole proteins is that whole proteins contain T-cell epitopes that are inaccessible in whole protein form but could otherwise generate T-cell responses [42]. Thus peptide vaccination has the potential to generate responses to a larger repertoire of target sequences relative to whole protein vaccination.

Administration of synthetic peptides with an appropriate adjuvant is one therapeutic vaccination strategy [62, 63]. Two types of peptides used in peptide vaccination are synthetic long peptides (SLP) and short minimal peptides. Short peptides are typically 8-10 amino acids in length, the exact size for presentation by MHC class I molecule. This provides the advantage of external loading of the peptide onto the MHC molecules without having to first internalize the antigen [58, 62]. While vaccination with minimal epitopes has demonstrated some promising results [64-67] it often leads to immunological tolerance instead of immunity [68]. Vaccination with SLPs on the other hand have many advantages over vaccination with short peptides. SLPs are too long to bind exogenously to MHC molecules and thus must be taken up by APCs and processed before they can be presented [69]. This leads to a longer duration of *in*

*vivo* epitope presentation by APCs [70, 71] and enhanced T-cell responses [72, 73]. Furthermore, unlike minimal epitope binding on MHC class I molecules, vaccination with SLPs results in antigen loading to both MHC class I and MHC class II molecules [42].

There has been a great deal of research to enhance the immunogenicity of peptide vaccination [42], but one of the most significant findings was that using long peptides for vaccination instead of minimal epitopes resulted in more robust and effective T-cell responses [74, 75]. As a result we used SLPs in our characterization of mutanome responses throughout this project.

### *1.4.3 Designing a multi-epitope construct*

The generation of T-cell mediated immune responses to TAAs is essential in mediating tumor regression. There have been many vaccination strategies that have been shown to induce productive antigen specific T-cell responses, however the targeting of individual epitopes has resulted in the emergence of antigen loss variants [69]. Antigen loss variants occur when the tumor population evolves to eliminate tumor cells containing an antigen of interest, but retains other tumor variants. Since single antigen targeting has proven generally insufficient in establishing durable cures [76], efforts have been redirected to vaccinate against multiple tumor antigens. The use of polypeptides encoding multiple antigenic epitopes is an approach that has been investigated with significant success [69]. Like in the case of vaccination with long peptides, polypeptide vaccination results in MHC loading through intracellular mechanisms, a longer duration of epitope presentation and thus superior T-cell responses [71].

There are a number of things to consider when designing a polypeptide. The efficiency that a particular epitope is generated through intracellular processing and its subsequent binding affinity for MHC molecules are both important in the formation of T-cell responses to antigens [77]. Proteasomal cleavage of peptides is very strongly influenced by the adjacent amino acid residues to a given epitope [77, 78]. Both the C-terminal residue and the immediate flanking residue of an epitope possess significant signals affecting proteasome cleavage specificity [79] and immunogenic potential [77]. To increase the probability of a polypeptide sequence being properly processed within the proteasome, defined flanking sequences, also known as spacer sequences, can be used. Spacer sequences increase the therapeutic potential of the polypeptides and increase the immune responses towards individual epitopes compared to sequences without spacers [80]. Importantly for our study, by inducing cleavage between peptides of interest, this should eliminate the formation of neo-antigens and the potential of any misdirected immune responses.

Careful consideration and selection of flanking sequences is necessary because while some sequences will lead to more accurate processing of epitopes, others may actually prevent proper antigen processing [81, 82]. The artificial spacer sequence AAY (Alanine-Alanine-Tyrosine), has been well documented to enable proper cleavage, processing and presentation of peptides to T-cells [69], as well as significantly enhance therapeutic efficacy of a multi-epitope DNA vaccine in a cervical cancer model [80]. Alanine is a small hydrophobic residue, and hydrophobic residues are associated with proteasomal cleavage at the carboxyl (P1) site of the residue [78] and enhanced CTL responses to the epitope [77]. The two side-by-side alanine residues in the AAY linkage

sequence support C-terminal cleavage of an epitope while the tyrosine residue induces a strong N-terminal cleavage site for the adjacent epitope [80]. AAY is the cleavage sequence used within our multi-epitope construct design.

While cleavage sequences between epitopes may promote proper processing within the proteasome, it does nothing to ensure that the polypeptide will reach the proteasome in the first place. Rodriguez *et al* have demonstrated that targeting DNA-based multi-epitope constructs to the protein degradation pathway results in increased proteolysis and increased CTL precursor frequencies [83]. Another group showed that proteasome targeting was crucial for the therapeutic treatment of established tumors with a DNA multi-epitope construct [80].

Targeting a DNA construct to the 26S proteasome degradation pathway can be achieved by adding ubiquitin to the construct design [83]. Fusion of ubiquitin to a multi-epitope construct has lead to elevated class I MHC presentation, enhanced immunogenicity and increased therapeutic effect as a result of polyubiquitination and targeting to the proteasome [83]. The conjugation of ubiquitin, a 76 amino acid protein, to eukaryotic proteins is an obligatory step for proteasome degradation [84]. Elongation of the ubiquitin chain leads to the targeting of the complex to the proteasome, only if the polyubiquitination occurs through bonds with lysine 48 of the preceding ubiquitin molecule [85]. If this K48 is mutated to another residue, such as arginine, this inhibits targeting to the proteasome degradation pathway [86]. It has further been demonstrated that mutation of all lysines in ubiquitin to arginine except for lysine 48, thus preventing the formation of other types of polyubiquitin chains, leads to superior proteasomal targeting relative to wild-type ubiquitin [87].

In our attempts to potentiate anti-tumor immune responses we encode a multi-epitope construct within an oncolytic virus. We employ many of the approaches discussed here, including the use of cleavage sequences and ubiquitination, to optimize processing of our multi-epitope construct. Our strategy for designing this multi-epitope construct for insertion into our oncolytic virus is further discussed in the *Results*.

### *1.5 Oncolytic Viruses*

Oncolytic viruses (OVs) are an emerging type of cancer therapeutic that have shown significant success in preclinical and clinical trials [88]. OVs are replication competent, tumor-selective viruses that have the ability to eliminate malignancies through direct and indirect killing of tumor cells. Today, there are many different types of viruses under investigation for oncolytic and anti-cancer effects. OVs can be either naturally selective for tumor cells, such as for Newcastle disease virus and mumps virus, or they can be engineered through different mechanisms to be tumor-selective, as is the case for adenovirus, vesicular stomatitis virus (VSV), Maraba virus, herpes simplex virus and vaccinia virus [88-90].

The first observations of viruses being able to disseminate disease caused by cancer were reported as early as 1904 in a case report in which a leukemia patient went into remission after an influenza infection [91]. Since then there have been many more case reports of similar phenomena [92] and even some clinical trials, unethical by todays standards, in the mid-twentieth century reported that cancer patients could be administered infectious bodily fluids from other patients and this would in some cases control cancer burden [93]. While some remissions were observed, most were only short-lived and many patients experienced toxicity as a result of infection. In the last

couple of decades, there has been massive advances in our understanding of the mechanisms of action of oncolytic viruses, in the safety of the viruses as well as in their therapeutic efficacy [88].

Today, some of the major barriers that scientists and clinicians are working to overcome to improve clinical efficacy of OV therapy include improving virus delivery to the tumor, enhancing the intratumoral spread, minimizing viral clearance, and enhancing virus induced antitumor immunity [88].

### *1.5.1 Maraba virus & Vesicular Stomatitis virus*

Maraba virus and Vesicular Stomatitis Virus (VSV) are both members of the *Rhabdoviridae* family and were both used throughout this project. Rhabdoviruses are rarely associated with disease in humans and as a result, pre-existing immunity, a major hurdle in oncolytic virus therapy [88], is considerably rare [89]. Maraba and VSV are negative-strand RNA viruses that do not proceed through a DNA intermediate, eliminating the risk of integration of the viral DNA into the genome when used as an oncolytic agent [89, 94, 95]. These viruses replicate rapidly in mammalian cells and can be genetically modified to enhance tumor specificity or to encode therapeutic transgenes [89]. They also are relatively small in size and thus would more readily extravasate from blood vessels into the parenchyma of the tumor [96]. All of these properties make both Maraba virus and VSV very effective oncolytic agents.

Aside from rabies virus, Lyssavirus, VSV is probably the most characterized virus of the *Rhabdoviridae* family. It is an arthropod-borne virus that primarily affects rodents, cattle, swine and horses. [97]. The genome of VSV is 11 kilobases long and is

comprised of five proteins: a nucleocapsid (N), polymerase proteins (P & L), a surface glycoprotein (G) and a peripheral matrix protein (M) [94].

Interferons (IFN) are very important with regards to the innate antiviral immunity and VSV is strongly inhibited by its presence. In fact, infection of mice defective in type I IFN signaling with wild-type VSV (wtVSV) can be lethal [94, 98]. However, deletion of methionine 51 in the matrix protein of VSV (VSVΔ51) attenuates the virus by inducing host cells to produce more IFN while maintaining its oncolytic ability and efficacy [99]. The production of IFN in response to virus infection protects the host cells against infection and enhances the safety of the oncolytic virus.

Compared to other rhabdoviruses Maraba virus is more potent and effective for killing human tumor cells [89]. Like VSV, Maraba is a vesiculovirus containing the N, P, M, G and L genes. In order to improve safety and therapeutic potential of the virus, Maraba was engineered to contain two mutations, one in the matrix protein, L123W, and one on the G protein, Q242R. This double mutant form of Maraba virus is commonly referred to as MG1 [89]. These mutations resulted in the MG1 virus being able to replicate more quickly during the early phase of infection, while simultaneously being significantly more attenuated on primary cells compared to the wild type Maraba [89]. As an oncolytic agent, MG1 is more effective and less toxic than VSVΔ51 as confirmed in both *in vitro* and *in vivo* experiments [89].

### *1.5.2 Oncolytic virus therapy and immunotherapy collide*

Despite the misleading name, oncolytic virus therapeutic efficacy is the result of many more factors than just their ability to lyse tumor cells. It is now widely understood that antitumor efficacy of an OV also significantly depends on its ability to

stimulate antitumor immunity [100]. In a clinical trial in which melanoma patients were injected intratumorally with oncolytic vaccinia virus, some of the patients' non-injected distant tumors also decreased in tumor burden [101], suggesting that systemic anti-tumor immune responses may be responsible for this efficacy [100]. Moreover Reovirus, another oncolytic virus currently in phase 3 clinical trials, does not even require direct tumor oncolysis in order to result in therapeutic efficacy, further implicating antitumor immune activity [102].

In some cases, transient expression of tumor antigens as a result of OV tumor destruction may be sufficient to generate immune responses [103]. This immune responses is made possible by the pathogen associated molecular patterns (PAMPs) of the OV that signal the immune system to respond to the imposed threat upon the host [104]. However despite the concurrent presentation of PAMPs, the TAAs of most human tumors will be too weak to induce strong enough immune effector functions to control tumor progression [105]. As a solution to this problem oncolytic viruses can be engineered to enhance general immune stimulation, like in the case of viruses encoding granulocyte macrophage colony stimulating factor (GMCSF) [40, 106] or interferon-β (IFN-β) [107-109], or to stimulate antigen directed immune responses, like in the case of viruses encoding tumor associated antigens [110-112].

A unique approach to combining immunotherapy with OV therapy was carried out by Richard Vile's group. A cDNA library derived from a normal human prostate was cloned into VSV and it was found that vaccination with the library encoding VSV could cure the majority of mice with established prostate tumors [113]. Despite encoding multitudes of self-antigens within the virus, multiple rounds of vaccinations could be

administered to the mice without observing any signs of autoimmunity [113]. Furthermore, a similar strategy encoding the cDNA library of a melanoma cell line into VSV was able to cure mice with these established melanoma tumors [114]. The successful translation of these virally-expressed cDNA libraries across tumor types is particularly noteworthy. Another very impressive approach to immunovirotherapy is with a heterologous prime-boost vaccination approach as described in the following section.

### *1.6 Heterologous Prime-Boost Vaccination*

The ability of the immune system to generate tumor-directed T-cell responses is somewhat compromised in the presence of an oncolytic virus because the viral epitopes compete with tumor epitopes and often result in the generation of stronger anti-viral responses than anti-tumor responses [42]. The use of a heterologous prime-boost vaccination approach, with two different viruses encoding the same tumor antigen, has been shown to ameliorate this effect. A group at McMaster University has approached this challenge by using a replication incompetent, E1- and E3- deleted recombinant human type 5 adenovirus as a priming vector followed by VSVΔ51 or MG1 Maraba virus as a boosting vector, with both vectors encoding human dopachrome tautomerase (hDCT) [110, 115-117].

#### *1.6.1 Adenovirus vector as an immune priming vector*

While some adenoviruses have been evaluated for their oncolytic potential, the ones used throughout this thesis are replication incompetent. These viruses are used to prime the immune system towards certain antigens rather than as oncolytic vectors.

The recombinant adenovirus variants are all E1-/E3- deleted serotype 5 adenoviruses, commonly referred to as first-generation adenoviruses.

The E1 gene of adenovirus plays an important role in viral replication [118]. Deletion of this E1 region leaves the virus replication defective [119]. The E3 region of adenovirus is non-essential for viral replication and its deletion increases the cloning capacity of this virus from 5kbp to 8kbp [120].

These first-generation, replication deficient adenoviruses have been shown to be very effective vaccination vectors [117, 121, 122]. Vaccination with transgene expressing adenoviruses results in prolonged presentation of antigens and CD8+ T-cell responses sustained for a long period of time relative to other methods of immunization [122]. As such, antigen expressing adenoviruses are very efficient immune priming vectors, generating immune responses that have been shown be successfully boosted through antigen expressing OVs [116, 123]

### 1.6.2 Efficacy of the heterologous prime-boost vaccination approach

DCT is a melanoma associated antigen and as such is highly expressed in the melanoma mouse-derived cell line, B16F10. In both a lung B16F10 tumor model and an intracranial model the heterologous prime-boost therapeutic approach successfully increased the antitumor immunity while simultaneously diminishing the antiviral attenuating responses normally associated with VSV vaccination [110, 115]. Increased tumor-infiltrating lymphocytes and T-cell recognition of epitopes of other TAAs were also observed [110]. Corresponding efficacy experiments showed that these antitumor immune responses also lead to significantly increased survival benefits, in the mice with intracranial B16F10 tumors and in mice with B16F10 lung tumors [115, 116].

The prime-boost therapeutic platform was also tested with a prime of Ad-hDCT followed by a boost of MG1-hDCT. MG1 was found to induce significantly stronger antigen specific T-cell responses as an oncolytic boosting vector than VSV [111]. In fact, there are currently preparations underway by John Bell, Brian Lichty and David Stojdl to bring this prime-boost therapeutic approach into clinical trials. Toxicology and immunological studies have been conducted with cynomolgus macaques using an adenovirus and MG1 Maraba virus encoding MAGE A3, a known human TAA, and so far results have been quite promising [123]. MAGE A3 is associated with many tumors types of various histological types [124] and thus is a very promising target for immunotherapy. Hopefully, if all proceeds as planned, we should see this MAGE A3, prime-boost oncolytic virus therapy in humans, within the context of a Phase I clinical trial, before the end of the summer.

## 2 HYPOTHESIS AND OBJECTIVES

*Hypothesis*

I hypothesized that combining mutanome epitope vaccination with oncolytic virus therapy in a heterologous prime-boost therapeutic approach would result in a superior therapeutic outcome than either vaccination approach on its own.

*Objectives*

1. Confirm the presence of the previously described mutanome antigens in our B16F10 cells, and confirm the immunogenicity of these epitopes
2. Design a multi-epitope construct containing the mutanome peptide sequences and clone it into MG1 Maraba virus and E1-/E3- type 5 adenovirus
3. Test the ability of these mutanome viruses to induce mutanome specific anti-tumor immune responses in mice, and to confer tumor control and survival advantage upon treated mice

## 3 MATERIALS AND METHODS

### *3.1 Mice and cell lines*

Female 6-week old C57Bl/6 mice were purchased from Charles River Laboratories. Mice were treated, housed, and euthanized according to the rules and regulations set in place by the University of Ottawa Animal Care and Veterinary Service. Mice were euthanized at the end of the experiment or when they exhibited certain health states such as exhibiting hind limb paralysis, respiratory distress, or bearing tumors greater than 15mm x 15mm.

Cell lines Vero (ATCC CCL-81), HeLa (ATCC CCL-2), SNB-19 (ATCC CRL-2219), and the B16-F10 melanoma (ATCC CRL-6475) were all purchased from the American Type Culture Collection. Cells were cultured in 150mm polystyrene plates in Dulbecco's Modified Eagle's Medium (DMEM) (Corning Cellgro, VA, USA) supplemented with 10% fetal bovine serum (FBS) (Thermo Scientific, Utah, USA). Cell stocks were tested for mycoplasma contamination prior to use.

### *3.2 Viruses*

MG1-GFP, MG1, VSVΔ51, VSVΔ51-IFNγ, VSVΔ51-GMCSF, MG1-hDCT, MG1-MUT and MG1-MUT-UbMut were propagated in Vero cells cultured in grown in 150mm polystyrene plates. Cells were infected at an MOI of 0.05 and culture supernatants were filtered through 0.22μm pore Millipore Stericup® Filter Units (Millipore, MA, USA) and concentrated by centrifugation at 14,000rpm for 1.5hours. Virus pellets were resuspended in PBS, aliquotted, stored at -80°C, used once and then discarded. The Maraba MG1 virus contains two mutations sites (M-protein: Q242R; G-protein: L123W) compared to the wild-type Maraba virus (Brun, 2010). VSVΔ51-GMCSF was originally

cloned by Chantal G Lemay, PhD, and the VSVΔ51-IFNγ virus was cloned and provided by Marie-Claude Bourgeois-Daigneault, PhD. MG1-hDCT was provided by Dr. Brian Lichty at McMaster University.

MUT and MUT-UbMut constructs, the sequences of which are described in more detail in the *Results* section (**Figure 4.16**), were ordered in plasmids from GeneArt® Gene Synthesis, a service provided by Life Technologies (Carlsbad, CA). The MG1 shuttle vector and backbone were kindly provided by David Stojdl PhD. The MUT plasmids as well as the MG1 shuttle vector were digested with the MluI restriction enzyme and the inserts were sub-cloned into the MG1 shuttle vector. Positive colonies were identified by PCR using primers located upstream and downstream of the MluI restriction site on the MG1 shuttle vector. Sequencing was performed using the same primers at the Ottawa Hospital StemCore Facilities to ensure proper orientation of the insert and to confirm the sequence cloned. A portion of the shuttle vector containing our sequence of interest was cut out of the MG1 shuttle vector and subcloned into the Maraba MG1 backbone vector using the KpnI and NheI restriction sites. Positive colonies were identified by PCR using the same primers.

Rescues were performed by infecting Vero cells with vaccinia virus expressing T7 polymerase at a multiplicity of infection (MOI) of 3 for 2 hours. The virus inoculum was removed and cells were transfected with the MG1-MUT or MG1-MUT-UbMut plasmid and pCI-Neo T7 driven plasmids encoding Maraba N, P, and L genes at ratios of 2: 1: 1.25: 0.25 as described elsewhere (Brun et al., 2010). Transfections were performed using lipofectamine 2000 according to the manufacturer's protocol (Thermo Scientific, Waltham, MA). Supernatants were collected 48 hours after transfection and

filtered through a 0.22μm filter to remove vaccinia virus. The supernatant was added to fresh Vero cells and visible cytopathic effects observed 24 hours later indicated the presence of the virus. The supernatants were collected, titered, and frozen at -80°C.

Ad-hDCT was provided by Brian Lichty PhD (McMaster University, Hamilton ON), and was grown as previously published (Bridle, 2010). AdRP2014 [125] is the empty vector E1-/E3- deleted type 5 control adenovirus used throughout this thesis; herein referred to as Ad. Both Ad and Ad-MUT were cloned by Robin Parks PhD (Ottawa Hospital Research Institute, Ottawa ON). The Ad-MUT virus (AdRP3117) was cloned using the constructs ordered from GeneArt according to the previously published protocol [126]. Adenoviruses were exclusively administered intramuscularly, based on evidence suggesting that this was the most effective route of administration [127].

### *3.3 Tumor models*

Subcutaneous tumors were established in C57Bl/6 mice by injecting $7.5x10^4$ B16-F10 cells, reconstituted in 100μL PBS, into the right hind flank of the mouse. Lung tumors were seeded in C57Bl/6 mice by injecting $7.5x10^4$-$2.5x10^5$ B16-F10 cells, reconstituted in 100μL PBS, through intravenous administration. Exact cell concentrations can be found in figure captions throughout this text. In survival studies, sub-cutaneous tumors were measured every 2-3 days. Tumor volume was calculated according to the following equation: tumor volume = $\frac{1}{2}(\text{width})^2(\text{length})$, with length representing the larger of the two measurements.

### *3.4 Peptides*

The immunodominant peptide from of DCT (DCT180-188, SVYDFFVWL) was synthesized by Biomer Techology (Pleasanton, CA), as was the 27 amino acid DCT peptide (DCT169-197, GTQPQIANCSVYDFFVWLHYYSVRDTL) and the immuno-dominant epitope from the N protein of VSV (RGYVYQGL), referred to as the VSV-N peptide. Twenty-seven amino acid long SLPs were designed to encode the point mutation at amino acid 14 with thirteen flanking amino acids from the B16F10 genome. These mutanome peptides are listed in **Table 2.1**. We received orders of the mutanome peptides from both Biomer Technology and Pepscan (Lelystad, Netherlands). All peptides were provided as a lyophilized powder with >90% purity. Peptides were resuspended in 100% DMSO at a concentration of 10mg/mL and were aliquotted in 20µL volumes and stored at -80°C. The peptides were not used following more than one freeze-thaw.

### *3.5 Viral plaque assay*

The titer – the amount of infections virus per unit of measurement – of Maraba and VSV viruses was determined by standard plaque assay on Vero cells with overlays composed of a 1:1 ratio of 1% agarose and 2x DMEM (Gibco) containing 20% FBS. Viruses were titered in 10-fold and half-log increments in serum free DMEM and 200µL of the virus containing media was added to each well of a six well plate. Virus concentration (PFU/mL) was quantified 24 hours after infection by counting the number of plaques formed per well and calculating the input virus concentration according to the following equation: PFU/mL = (# plaques in well)(dilution of input virus)/(volume of input virus).

**Table 2.1. List of mutanome peptides, and corresponding amino acid sequences, used throughout this thesis.**

Peptides were previously characterized by Castle et al. [43] Described in more detail in Table 4.1.

| Mutation | 27AA peptide sequence |
|---|---|
| MUT05 | FVVKAYLPVNESFAFTADLRSNTGGQA |
| MUT17 | VVDRNPQFLDPVLAYLMKGLCEKPLAS |
| MUT20 | FRRKAFLHWYTGEAMDEMEFTEAESNM |
| MUT22 | PKPDFSQLQRNILPSNPRVTRFHINWD |
| MUT24 | TAYITPPTTTTKKARVSTPKPATPSTD |
| MUT25 | STANYNTSHLNNDVWQIFENPVDWKEK |
| MUT28 | NIEGIDKLTQLKKPFLVNNKINKIENI |
| MUT29 | IPSGTTILNCFHDVLSGKLSGGSPGVP |
| MUT30 | PSKPSFQEFVDWENVSPELNSTDQPFL |
| MUT44 | EFKHIKAFDRTFANNPGPMVVFATPGM |
| MUT46 | NHSGLVTFQAFIDVMSRETTDTDTADQ |
| MUT48 | SHCHWNDLAVIPAGVVHNWDFEPRKVS |

### *3.6 Splenocyte preparation & ex vivo stimulation*

Spleens were harvested from mice at predetermined time points as indicated in the results section. Spleens were mashed through a 100μM filter to create a single cell suspension and red blood cells were lysed using ACK lysis buffer (0.15mM $NH_4Cl$, 10mM $KHCO_3$, 0.1mM $Na_2EDTA$, pH 7.3). Splenocytes were resuspended in cRPMI, Hyclone RPMI 1640 media supplemented with 10% HyClone Fetal Bovine Serum and 1x Pen Strep (Gibco® Life Technologies Penicillin Streptomycin), and chilled on ice or at 4°C until ready for use.

Splenocytes were restimulated *ex vivo* by the addition of 2-10μg/mL of peptide and 0.4μL/well of CD28 (BD Pharmingen) to cells in a total volume of 200μL per well in a 96-well plate. Peptides used for *ex vivo* restimulation of splenocytes include the VSV-N peptide, the DCT 9AA and 27AA peptides, and the following mutanome peptides: MUT05, MUT17, MUT20, MUT22, MUT24, MUT25, MUT28, MUT29, MUT30, MUT44, MUT46, and MUT48 (for peptide sequences, refer to **Table 2.1**).

### *3.7 Flow Cytometry*

For IFNγ intracellular staining, two million splenocytes were restimulated with designated antigen for 1.5-4hours (as indicated) at 37°C before GolgiPlug (BD Biosciences) was added to the cells and cells were incubated for another 3.5hours at 37°C. After the incubation, the cells were surface stained with antibodies CD4-PE (clone GK1.5, BD Bioscience, 1/500 dilution) and CD8-PECy5.5 (clone 53-6.7, BD Bioscience, 1/100 dilution). Cells were then permeabilized and fixed using the BD Cytofix/Cytoperm kit (BD Bioscience, Cat# 554714) according to the kit protocol, and stained with an antibody against IFNγ-FITC (clone XMG1.2, eBioscience, 1/200

dilution). Cells were assessed by flow cytometry using a Beckman Coulter CyAn™ ADP Analyzer and all data analysis was performed using the Beckman Coulter Kaluza Analysis Software, version 1.2. Between 20,000 and 200,000 events were accumulated and analyzed per sample depending on the experiment.

### *3.8 IFNγ ELISpot assay*

The mouse IFN-γ ELISpot$^{PLUS}$ kit (ALP) with pre-coated plates was purchased from MabTech (Cincinnati USA). Prior to loading splenocytes and antigen, plates are washed with PBS and pre-conditioned in cRPMI for 30minutes. Three to five hundred thousand splenocytes were loaded per well with corresponding antigens of interest and incubated overnight (18-20hours) at 37°C, 5% $CO_2$. After incubation, the splenocytes were removed and the ELISpot plate was processed according to the manufacturer's directions. Briefly, the splenocytes were washed off of the plate with PBS and the wells were incubated with the following reagents in succession, separated by thorough washes with PBS: biotinylated detection mAb, streptavidin-ALP, and BCIP/NBT-plus substrate. Following a final wash with water, individual spots were visible in each well. Each spot corresponds to one splenocytes that was secreting IFNγ in response to antigen stimulation. Number of spots per well is quantified using the ImmunoSpot® ELISpot plate reader (Cellular Technology Limited, Shaker Heights, OH). Data is presented as a ratio of the number of spots per number of cells added to each well.

### *3.9 Single- and Multi-step Growth Curves*

Vero cells were seeded in 6-well plates at a density of $2.5x10^5$ cells per well. It was assumed that the cells would approximately double overnight so infections were

calculated based on a cell concentration of $5x10^5$ cells/well. Cells were infected in duplicate at an MOI of 10 or an MOI of 0.001 for the single- and multi-step growth curves respectively. Cells were initially infected in serum-free DMEM, and one hour later supernatants were aspirated, cells were washed twice with PBS and 1mL of DMEM containing 10% FBS was added to the cells – this was considered as time 0. Supernatants were subsequently collected 3, 6, 9, 12 and 24 hours later for the single-step growth curve and 12, 24, 36, 48 and 72 hours later for the multi-step growth curve. Supernatants were frozen at -80°C until they were titered.

### *3.10 Generating Bone Marrow Derived Dendritic Cells*

To generate bone marrow derived dendritic cells (BMDCs), bone marrow was harvested from the tibias and femurs of naïve C57Bl/6 mice. Red blood cells were lysed with ACK lysis buffer and counted with a hemocytometer. From this point, BMDCs were cultured according to two different methods; methods that were later compared as described in the *Results* section.

*Method 1*

BMDCs were cultured as previously described [128]. Briefly, cells were seeded in non-tissue coated 100mm polystyrene petri dishes at a density of $2x10^5$ cells/mL in 10mL of RPMI containing 40ηg/mL rmGM-CSF. Six days later, 5mL of media supplemented with 40ηg/mL of rmGM-CSF was added.

*Method 2*

BMDCs were cultured as previously published [129]. Briefly, cells were seeded in 100mm polystyrene dishes at a density of $2x10^5$ cells/mL in 10mL of RPMI media containing 20ηg/mL rmGM-CSF (R&D Systems, Minneapolis, MN). Three days later,

another 10mL of RPMI media containing 20ηg/mL rmGM-CSF was added to the cells. Three days after that, half of the cell culture was collected, centrifuged and resuspended in fresh media containing 20ηg/mL rmGM-CSF. Cells were returned to the original plate until they were mature on day 9 after bone marrow harvesting.

*Maturing the BMDCs*

BMDCs were matured either through the addition of 100ng/mL LPS (Sigma, St. Louis, MO), or 100ηg/mL CPG (ODN1826) (InvivoGen, San Diego, CA) to the cell culture 18 hours prior to use.

### *3.11 Statistical Analysis*

All statistical analyses were conducted using Prism 5 for MAC OS X (GraphPad Software, La Jolla, CA), version 5.0a. Where applicable, data is presented as mean + SEM. Statistical analysis tests used throughout this thesis include: student t-tests, one-way ANOVAs with Bonferroni or Dunnett's multiple comparison post-tests, and Mantel-Cox tests. Specific tests used in each case are indicated in the figure legend. In all cases: * = $P < 0.05$, ** = $P < 0.01$, *** = $P < 0.001$.

### *3.12 Next Generation Sequencing and Analysis*

Exome sequencing on the B16 mouse tumor line and normal C57Bl/6 splenocytes was performed by Spencer Martin in Dr. Brad Nelson's lab at the BC Cancer Agency (Victoria, BC) to identify genetic mutations and for comparison with previously presented findings [43]. The procedure used was as follows:

The Agilent SureSelectXT All Mouse Exon Enrichment Kit (Aligent Technologies, Santa Clara, CA) was used to enrich for 50 Mb of DNA covering over 24,000 genes, and this was sequenced on the Illumina Hi-Seq2000 sequencer. Approximately 80 million

paired-end 100bp reads, or eight billion bases, of each of the mouse exome's were sequenced. Sequences were aligned to the mouse genome (build mm9) using Burrows Wheeler Aligner [130]. Bam files were indexed using Samtools Index, duplicate reads were removed using Samtools Rmdup, and remaining reads were compiled using Samtools Pileup [131]. Variants were first filtered to remove those with low base call quality and those with low mapping quality. Next, Samtools VarFilter was used to filter out variants with low depth of coverage of the variant or low depth of coverage at the variant position. Variants were filtered to remove single nucleotide polymorphisms identified in DbSNP128, and confirmed by visual inspection using Integrative Genomics Viewer [132]. Finally, variants were annotated using Annovar [133] on the UCSC mm9 Knowngene database. Coverage statistics were assessed using BedTools [134]. Variants present in the tumor that were not present in the normal C57Bl/6 splenocytes were identified as mutants. In addition, RNA-seq was performed on the B16 tumor line to identify which of the exome seq identified mutations were expressed at the RNA level, and to identify fusion transcripts. *De novo* assembly of the RNA-seq reads was performed using Trans-AbySS [135] (PMID: 20935650), and the transcripts were visually inspected using IGV and the UCSC Genome browser (http://genome.ucsc.edu/cgi-bin/hgGateway?hgsid=377831071_XlMvycPULgYxZnS2gHYNCU7dM1Xh&clade=mammal&org=Mouse&db=mm9).

## 4. RESULTS

*4.1 BMDCs are unnecessary in the ELISPOT assay.*

ELISPOT immune assay is a commonly used assay for detecting and quantifying immune responses to antigens of interest. The ELISPOT assay is significantly more sensitive than the more commonly used ELISA assay or flow cytometry and can thus be used to measure small immune responses that may not be detected by other methods. The process for conducting an ELISPOT assay is described in detail in the *Materials and Methods* section. Previous studies conducting ELISPOT assays with synthetic long peptides [43] have used bone-marrow dendritic cells as additional antigen presenting cells in the cultures to process and present antigen to T-cells. We observed that using BMDCs in the ELISPOT generated substantial background so we tested different methods to reduce this background. Importantly, we confirmed that sufficient antigen presentation does occur in the presence of only splenocytes for the purposes of an ELISPOT assay, and that adding BMDCs may not be necessary.

**Figure 4.1** illustrates the high background that is present when BMDCs are added to the splenocytes culture. **Figure 4.1A** shows in quantitative measures how many IFNγ spots were generated in control and restimulation wells of the ELISPOT. Unpulsed BMDCs mixed with splenocytes from untreated mice should be the assay's negative control however over 150 spots were generated, seemingly as a result of the presence of BMDCs. While co-cultures of splenocytes from DCT treated mice and DCT pulsed BMDCs result in significantly higher responses, it is possible that weaker immune responses would go undetected due to high background levels. Representative images of ELISPOT wells are displayed in **Figure 4.1B**.

**Figure 4.1. ELISPOT assays using BMDCs as professional antigen presenting cells results in significant and potentially misleading background.**

C57Bl/6 mice were primed and boosted with 100μg 9AA DCT peptide and 50μg poly(I:C) administered SQ in order to generate anti-DCT specific immune responses. (a) Number of IFNγ secreting cells per $5x10^5$ splenocytes from treated and untreated mice incubated without BMDCs (no BMDCs), coincubated with unpulsed BMDCs (unpulsed), or BMDCs pulsed with DCT (DCT pulsed). Data is presented as mean + SEM (N=2). Asterisks indicate a statistically significant different response to restimulation by DCT pulsed BMDCs compared to unpulsed BMDCs. (Student t-test: ns = not significant, * = $P < 0.05$, ** = $P < 0.01$, *** = $P < 0.001$). (b) Images of ELISPOT wells depicting data quantified in (a).

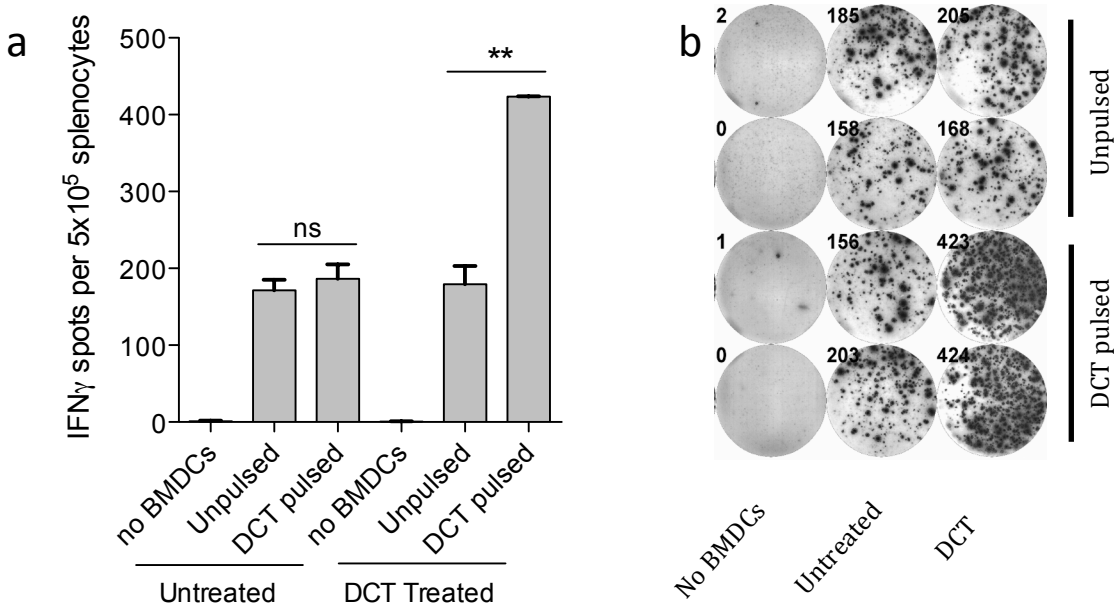
a
IFNγ spots per 5x10^5 splenocytes
500
400
300
200
100
0
ns
**
no BMDCs
Unpulsed
DCT pulsed
no BMDCs
Unpulsed
DCT pulsed
Untreated
DCT Treated
b
2
185
205
0
158
168
1
156
423
0
203
424
Unpulsed
DCT pulsed
No BMDCs
Untreated
DCT

Contaminating cell populations in the BMDC cultures could potentially lead to this high background. Two different BMDC culture methods, Method 1 [128] and Method 2 [129] reported in the literature were tested to determine which would result in a DC population of highest purity. Flow cytometry data displayed in **Figure 4.2A** shows that culturing bone marrow according to Method 2 results in a more pure population of DCs than Method 1. Also, two different TLR agonists, used to induce DC activation were tested. LPS, a TLR4 agonist, not only more efficiently activated the DC populations than CPG, a TLR9 agonist (flow cytometry data not shown), but it also resulted in less non-specific IFNγ production (**Figure 4.2B**).

In order to elucidate whether BMDCs were necessary for an ELISPOT assay at all we conducted an ELISPOT with splenocytes from mice vaccinated with 9AA DCT or 27AA DCT, using either splenocytes alone restimulated with peptide (**Figure 4.3A**), or splenocytes cultured with peptide-pulsed BMDCs (**Figure 4.3B**). In the absence of BMDCs, both the 9AA and 27AA DCT peptide restimulations resulted in significant antigen specific responses (**Figure 4.3A**) suggesting that BMDCs are unnecessary for assay success. Significantly, if you take into account the non-specific IFNγ production in each assay, the net response generated to restimulation is higher in the splenocytes only assay (**Figure 4.3A**) than it is in the splenocytes + BMDCs assay (**Figure 4.3B**). These results support that BMDCs can confound assay results, and that elimination of the BMDCs will result in a clearer and more accurate ELISPOT assay.

**Figure 4.2. Optimizing a BMDC culture and maturation method for use in ELISPOT assays.**

BMDCs were derived and cultured according to Method 1 and Method 2 as described in the *Materials and Methods*. C57Bl/6 mice were vaccinated twice with DCT and spleens were harvested. (a) Flow cytometry analysis was conducted on the BMDCs, stained for CD11c to determine the dendritic cell purity of the BMDC cell culture. (b) DCs matured with CPG or LPS, were used in an ELISPOT assay with splenocytes from DCT vaccinated mice to compare background levels generated as a result of the two maturation methods. Asterisks indicate statistically significant different responses. (Student t-test: ns = not significant, * = $P < 0.05$).

a

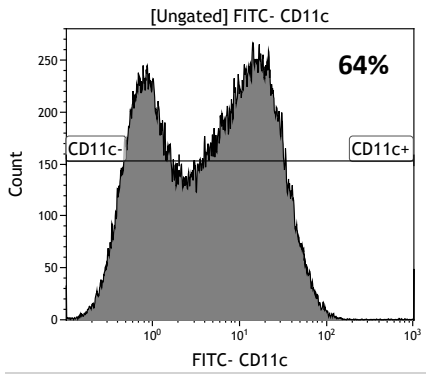


| Gate | Number | %Total | %Gated |
|---|---|---|---|
| All | 106,332 | 100.00 | 100.00 |
| CD11c- | 38,135 | 35.86 | 35.86 |
| CD11c+ | 68,327 | 64.26 | 64.26 |

**Method 1**

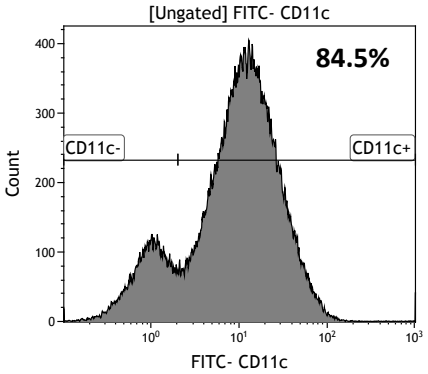


| Gate | Number | %Total | %Gated |
|---|---|---|---|
| All | 101,659 | 100.00 | 100.00 |
| CD11c- | 15,707 | 15.45 | 15.45 |
| CD11c+ | 86,017 | 84.61 | 84.61 |

**Method 2**

b

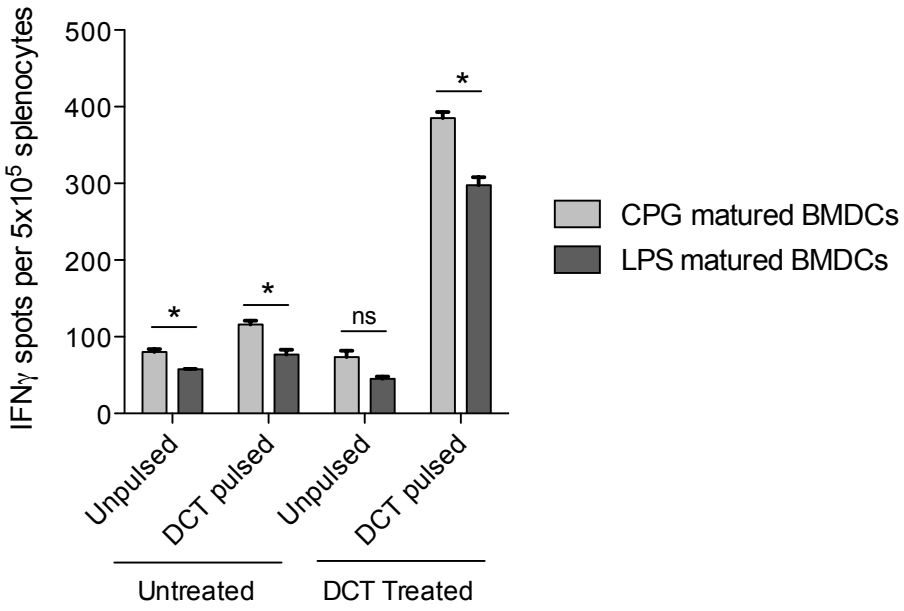

**Figure 4.3. Co-culturing splenocytes with BMDCs is unnecessary to conduct an ELISPOT immune assay.**

C57Bl/6 mice were vaccinated SQ on day 0 and day 7 with 100μg of either 9AA DCT peptide or 27AA DCT peptide in combination with 50μg poly(I:C). On day 14, mice were euthanized, and spleens were harvested, processed and restimulated with nothing, 9AA DCT peptide or 27AA DCT peptide. Splenocytes were restimulated either in (a) the absence of BMDCs or (b) in the presence of them.

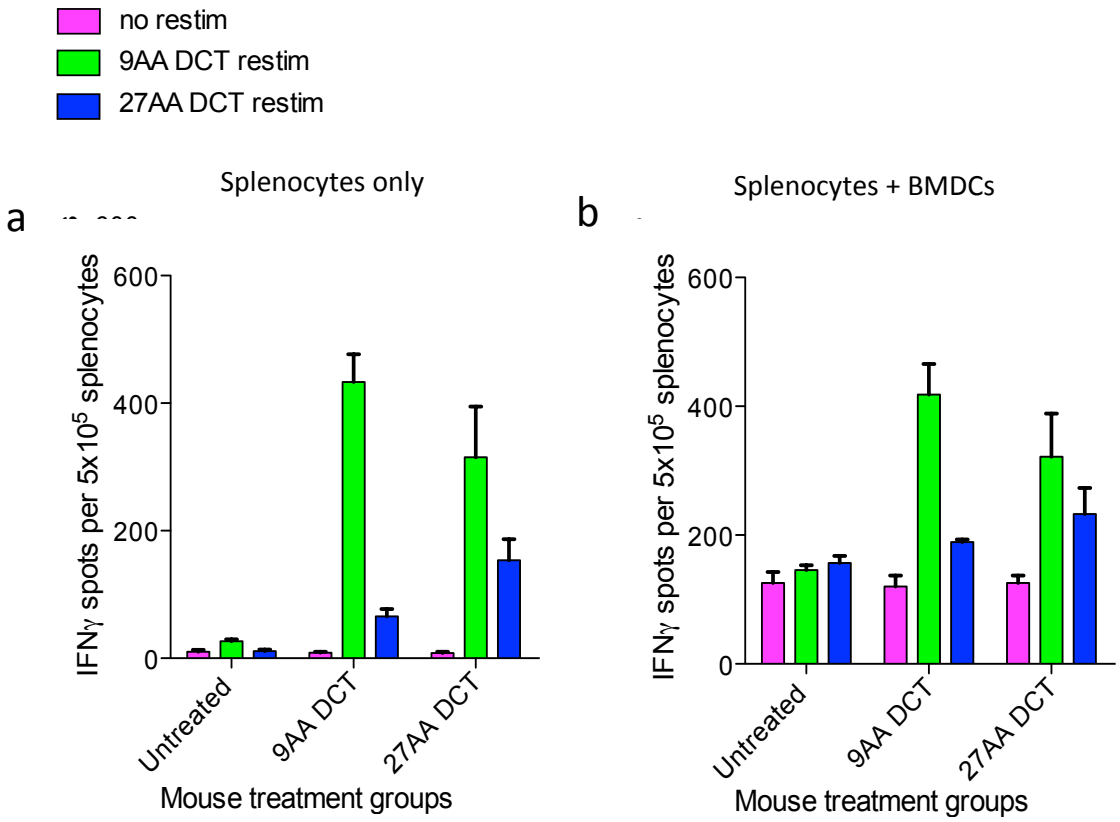
no restim
9AA DCT restim
27AA DCT restim
a
Splenocytes only
IFNγ spots per 5x10^5 splenocytes
600
400
200
0
Untreated
9AA DCT
27AA DCT
Mouse treatment groups
b
Splenocytes + BMDCs
IFNγ spots per 5x10^5 splenocytes
600
400
200
0
Untreated
9AA DCT
27AA DCT
Mouse treatment groups

*4.2 Subcutaneous injection is the most immune stimulatory route of peptide administration.*

While we knew that different routes of administration could affect the subsequent response to treatment, it was unclear which route would generate the greatest number of antigen specific T-cells in response to peptide vaccination. We tested this by treating mice (timeline in **Figure 4.4A**) with DCT peptide mixed with poly(I:C), and delivering these treatments subcutaneously (SQ), intravenously (IV), intramuscularly (IM) and intraperitoneally (IP). Spleens were harvested and restimulated *ex vivo.* Immune responses were measured by ELISPOT (**Figure 4.4B**). SQ administration proved to induce the greatest number of antigen specific T-cells and so was used for subsequent peptide vaccinations in this study, unless otherwise indicated. Representative ELISPOT wells are presented in **Figure 4.4C.**

*4.3 B16F10 "mutanome" peptides successfully generate immune responses in mice.*

As previously mentioned, the cancer "mutanome" is a source of novel TAAs that can be exploited to induce anti-tumor immunity. A collaborator at the BC Cancer Agency in Dr. Brad Nelson's lab, Spencer Martin, conducted Next Generation Genome Sequencing (NGS) on our B16F10 cells to confirm the presence of the previously characterized immunogenic B16F10 mutanome sequences [43]. We confirmed that 12 of the 16 mutations were expressed in our B16F10 cells (**Table 4.1**). Mutations highlighted in grey were found not to be expressed while expression was confirmed for the remaining sequences. The "mutation name" listed in **Table 4.1** is what each mutation will be referred to as throughout this thesis. The gene in which the mutation was found and the amino acid alteration are also listed.

**Figure 4.4. SQ peptide administration elicited the greatest T-cell activation relative to other routes of administration.**

C57Bl/6 mice were treated according to the following timeline with 100μg DCT peptide and 50μg poly(I:C). Routes of administration IP, IV, IM, and SQ. (b) Number of IFNγ secreting cells per $5x10^5$ splenocytes upon DCT *ex vivo* restimulation as measured by ELISPOT assay. Data is presented as mean +SEM with all groups containing an N of 3 mice per group, except for the untreated groups which have an N of 2 mice. Asterisks indicate a statistically significant difference between the untreated control and the treated groups (One-way ANOVA, p-value=0.0004; Dunnett's post-test: * = $P < 0.05$, ** = $P < 0.01$, *** = $P < 0.001$). (c) Representative images of ELISPOT wells quantified in (b).

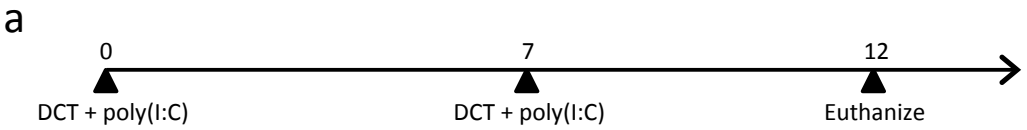
a
0
7
12
DCT + poly(I:C)
DCT + poly(I:C)
Euthanize

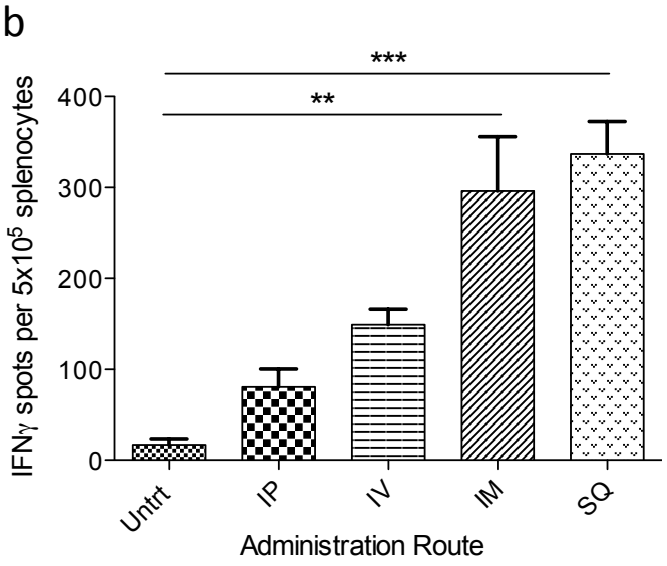
b
***
**
400
300
200
100
0
IFNγ spots per 5x10^5 splenocytes
Untrt
IP
IV
IM
SQ
Administration Route

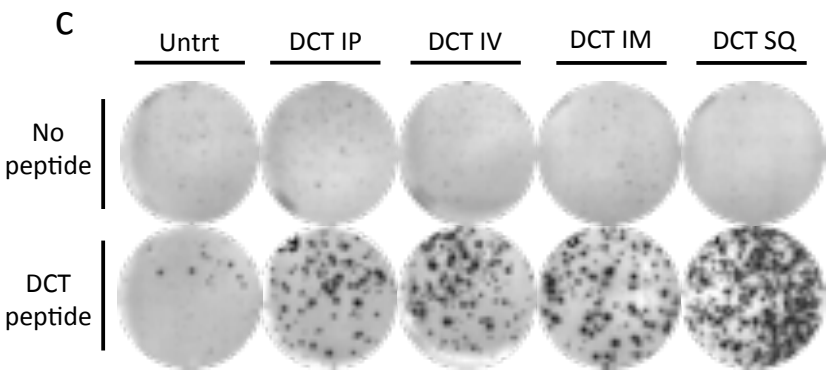
c
Untrt
DCT IP
DCT IV
DCT IM
DCT SQ
No peptide
DCT peptide

**Table 4.1. Confirmation of the presence of previously characterized immunogenic mutanome mutations by NGS.**

Included in this table are the mutation names, the gene in which each mutation is located, the point mutation amino acid change, and the 27AA mutanome peptide sequences. Underlined amino acids indicate the point mutation within the sequence. As determined by NGS, rows highlighted in grey are mutations identified by Castle e*t al* [43] that are not expressed in our B16F10 cells.

| Mutation | Gene | AA substit. | 27AA peptide sequence | Present in exome?* | Present in RNA?* |
|---|---|---|---|---|---|
| MUT05 | Eef2 | p.G795A | FVVKAYLPVNESFAFTADLRSNTGGQA | ✔ | ✔ |
| MUT12 | Gnas | p.S112G | | ✔ | ✗ |
| MUT17 | Tnpo3 | p.G504A | VVDRNPQFLDPVLAYLMKGLCEKPLAS | ✔ | ✔ |
| MUT20 | Tubb3 | p.G402A | FRRKAFLHWYTGEAMDEMEFTEAESNM | ✔ | ✔ |
| MUT22 | Asf1b | p.A141P | PKPDFSQLQRNILPSNPRVTRFHINWD | ✔ | ✔ |
| MUT24 | Dag1 | p.P425A | TAYITPPTTTTKKARVSTPKPATPSTD | ✔ | ✔ |
| MUT25 | Plod2 | p.F530V | STANYNTSHLNNDVWQIFENPVDWKEK | ✔ | ✔ |
| MUT28 | Ppp1r7 | p.L170P | NIEGIDKLTQLKKPFLVNNKINKIENI | ✔ | ✔ |
| MUT29 | Mthfd1l | p.F294V | IPSGTTILNCFHDVLSGKLSGGSPGVP | ✔ | ✔ |
| MUT30 | Kif18b | p.K739N | PSKPSFQEFVDWENVSPELNSTDQPFL | ✔ | ✔ |
| MUT36 | Tm9sf3 | p.Y382H | | ✔ | ✗ |
| MUT44 | Cpsf3l | p.D314N | EFKHIKAFDRTFANNPGPMVVFATPGM | ✔ | ✔ |
| MUT45 | Mkrn1 | p.N346Y | | ✗ | ✗ |
| MUT46 | Actn4 | p.F835V | NHSGLVTFQAFIDVMSRETTDTDTADQ | ✔ | ✔ |
| MUT48 | Def8 | p.R255G | SHCHWNDLAVIPAGVVHNWDFEPRKVS | ✔ | ✔ |
| MUT50 | Sema3b | p.L663V | | ✔ | ✗ |

Rows highlighted in grey are mutations identified by Castle *et al* that were found not to be expressed in our B16F10 cells

Rows in white are mutations identified by Castle *et al* that were confirmed to be expressed in our B16F10 cells

* Next-generation whole genome sequencing was performed by Spencer Martin at the BC Cancer Agency.

T-cell responses generated to each of the 12 expressed mutanome sequences were examined through SLP vaccination and subsequent ELISPOT analysis. Findings are summarized in **Figure 4.5**. **Figure 4.5A** displays the restimulated results relative to the non-restimulated controls. **Figure 4.5B** shows the results normalized to the unstimulated controls (unstimulated wells subtracted from stimulated wells). In our hands, MUT25 peptide elicits the strongest T-cell response, followed closely by MUT05 and MUT44.

*4.4 No evidence of epitope competition to generate T-cell responses when mice are vaccinated with multiple mutanome peptides.*

One concern we had about vaccinating against multiple antigens simultaneously was epitope competition. We were concerned that vaccination with two or more peptides would reduce the T-cell responses generated to each individual antigen. This concern was somewhat alleviated when we vaccinated mice against 1, 2, or 4 different peptides (timeline in **Figure 4.6A**) and still observed that the immune response to an individual peptide remained consistent (**Figure 4.6B**).

We further investigated if vaccinating mice with multiple peptides in multiple locations would lead to a greater T-cell response to each antigen compared to vaccination in a single location. Vaccination in multiple locations may provide the advantage of accessing more draining lymph nodes than vaccination in a single location. Mice were vaccinated SQ against 4 mutanome peptides, all in the same location (right hind flank) or in four different locations as depicted in **Figure 4.7B**. No significant difference in T-cell response was detected between the two groups

**Figure 4.5. T-cell responses elicited to mutanome peptide vaccination.**

C57Bl/6 mice were immunized with 100μg of a single mutanome SLP + 50μg of poly(I:C) SQ in bilateral flanks. (a and b) IFNγ ELISPOT analysis of splenocytes from vaccinated mice. Columns represent means +SEM. All groups have an N of 3 mice per group except for MUT05, MUT17, MUT20, MUT30 and MUT44 which have an N of 4 mice per group. (a) Splenocytes were either not restimulated (nothing) or they were restimulated with the mutanome peptide to which the mice were vaccinated (peptide). Asterisks indicate a statistically significant difference between mutanome peptide restimulation and the non-restimulated control (Student t-tests: * = $P < 0.05$, ** = $P < 0.01$, *** = $P < 0.001$). (b) Data from graph in (a) is normalized to the non-restimulated controls. Asterisks indicate a statistically significant difference in the T-cell responses between mice mutanome peptide vaccinated mice and naïve mice (One-way ANOVA: p-value <0.0001; Dunnett's multiple comparison post-test: * = $P < 0.05$, ** = $P < 0.01$, *** = $P < 0.001$).

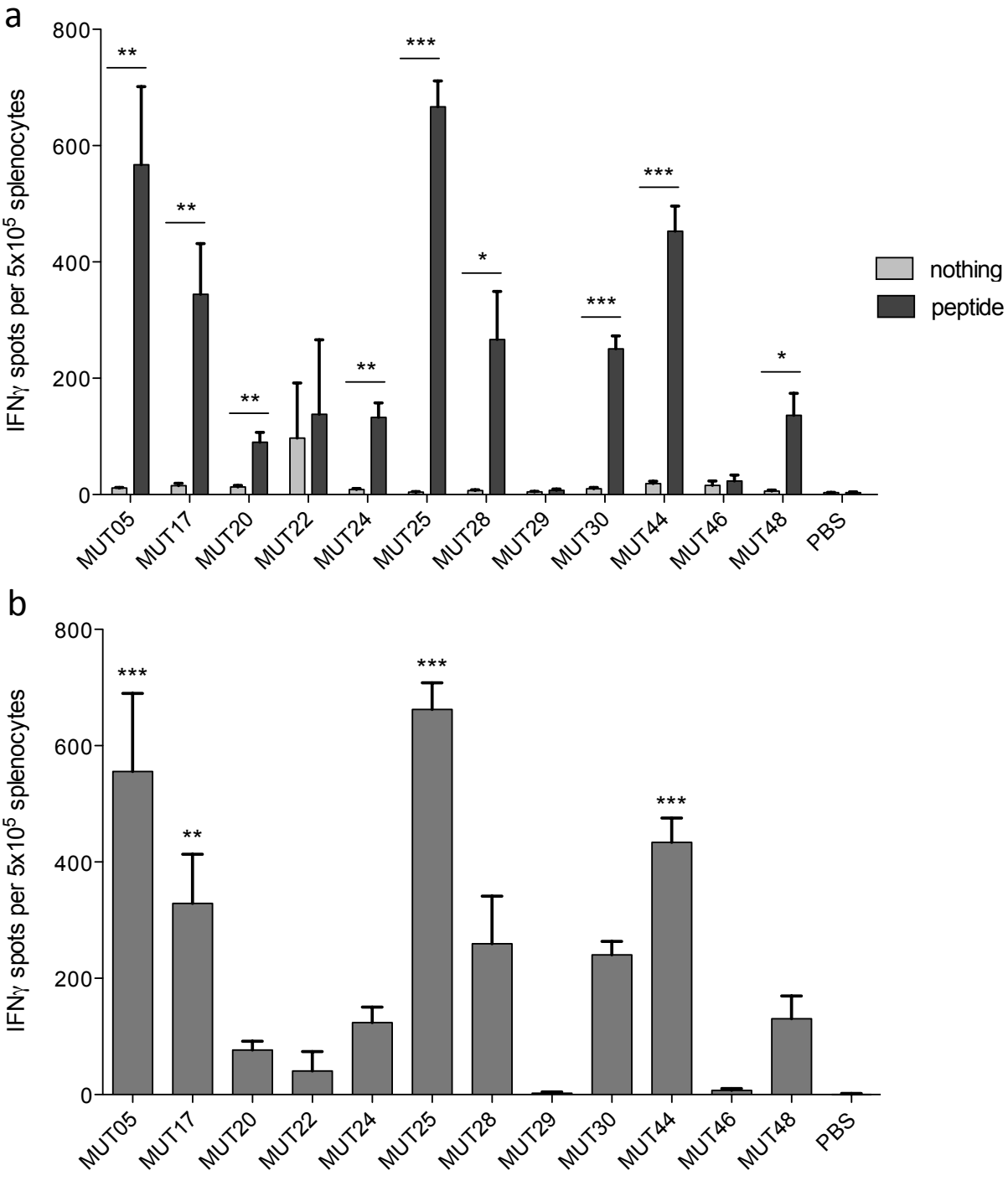
a
IFNγ spots per 5x10^5 splenocytes
800
600
400
200
0
**
**
**
**
***
*
***
***
*
nothing
peptide
MUT05
MUT17
MUT20
MUT22
MUT24
MUT25
MUT28
MUT29
MUT30
MUT44
MUT46
MUT48
PBS
b
IFNγ spots per 5x10^5 splenocytes
800
600
400
200
0
***
**
***
***
MUT05
MUT17
MUT20
MUT22
MUT24
MUT25
MUT28
MUT29
MUT30
MUT44
MUT46
MUT48
PBS

**Figure 4.6. No evidence of epitope competition to generate T-cell responses**.

C57Bl/6 mice were treated SQ with 100μg of MUT30, or each MUT30 and MUT17, or of each MUT30, MUT17, MUT44 and MUT05 with 50μg poly(I:C). (b) IFNγ ELISPOT analysis of $5x10^5$ splenocytes from vaccinated or control mice. Splenocytes were restimulated against MUT30. All data is presented as mean +SEM with all groups containing an N of 3 mice per group, except for the untreated groups which have an N of 2 mice. (One-way ANOVA: ns = $P > 0.05$)

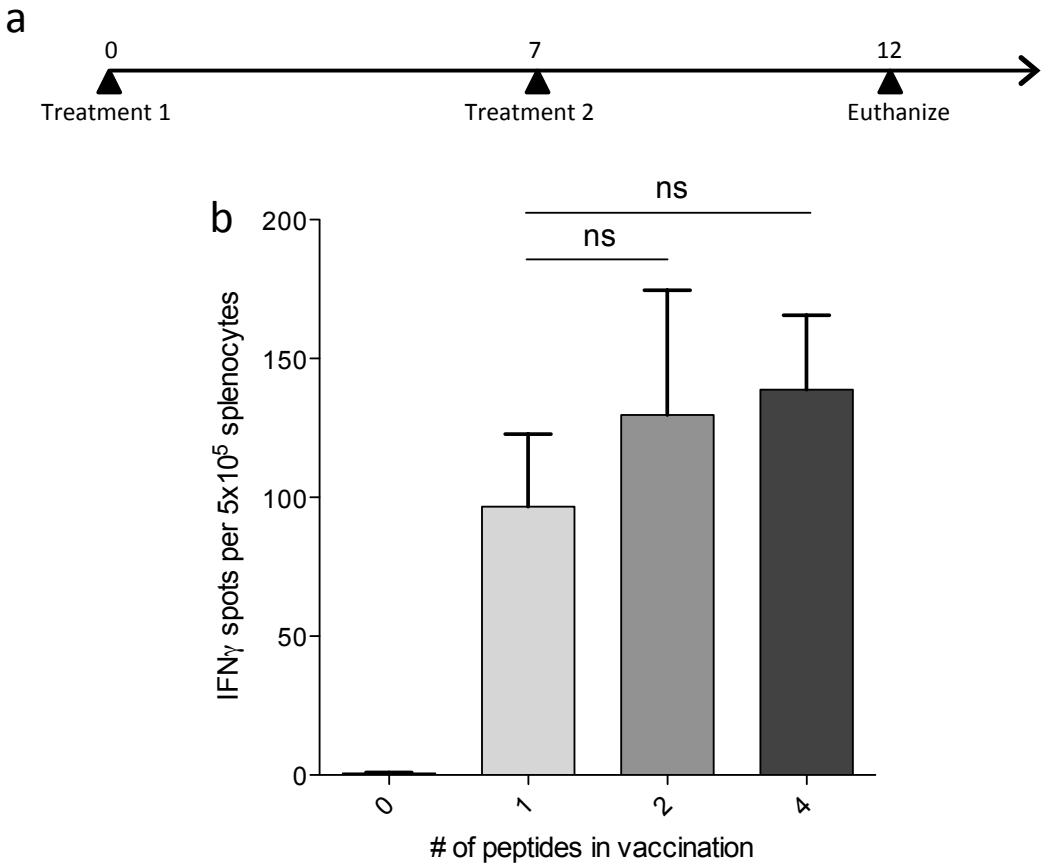
a
0
7
12
Treatment 1
Treatment 2
Euthanize
b
ns
ns
200
150
100
50
0
IFNγ spots per 5x10^5 splenocytes
0
1
2
4
# of peptides in vaccination

**Figure 4.7. Vaccinating with multiple peptides in distinct locations provides no added T-cell response relative to vaccination in the same location**

C57Bl/6 mice were treated according to the indicated timeline with 100μg of each of MUT05, MUT17, MUT30 and MUT44 peptides and 50μg poly(I:C). All peptides were administered SQ together in the same location (Same) or individually in different locations (Different) as displayed in (b). (c) IFNγ ELISPOT analysis of splenocytes from mice vaccinated with mutanome peptides. Data is presented as mean +SEM with groups containing an N of 3 mice, except for the untreated groups which have an N of 2 mice. (Student t-test: ns = $p > 0.05$)

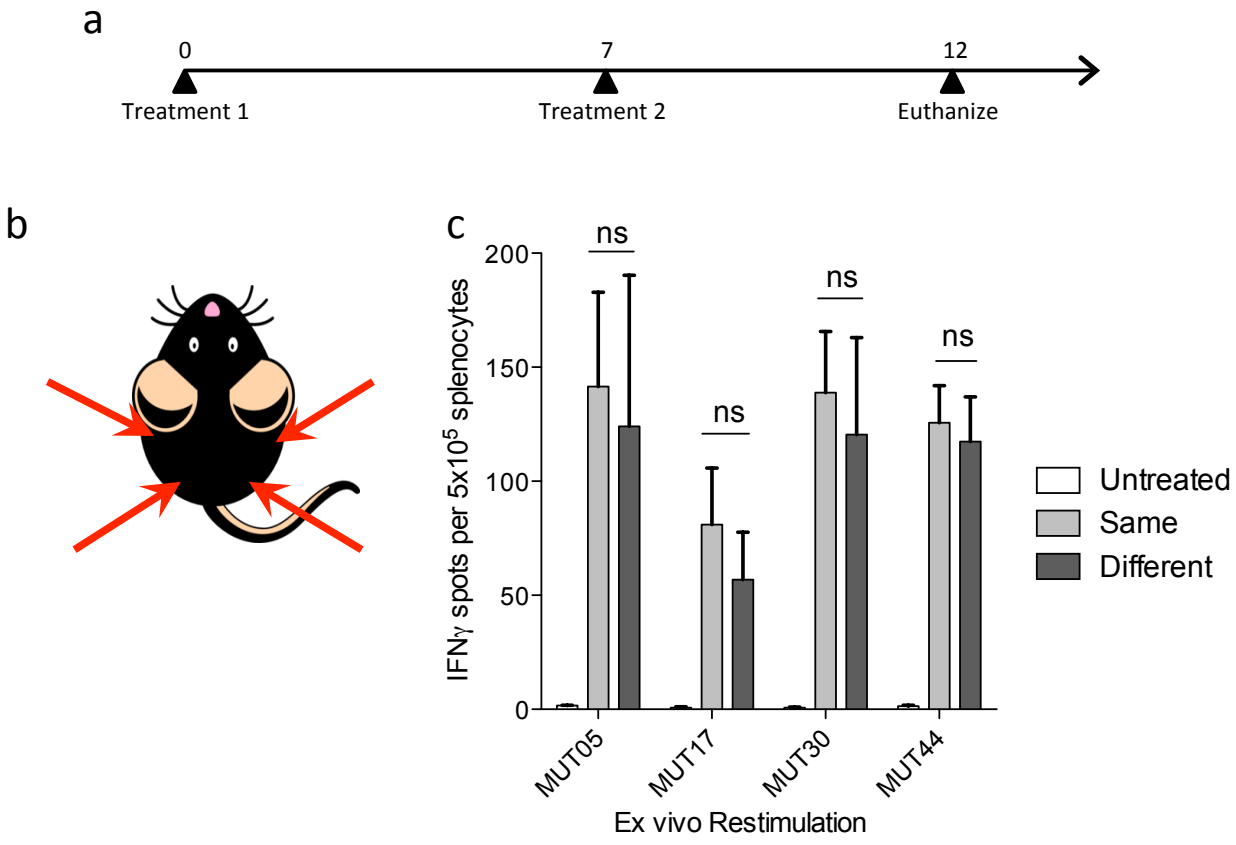
a
0
7
12
Treatment 1
Treatment 2
Euthanize
b
c
ns
ns
ns
ns
200
150
100
50
0
IFNγ spots per 5x10^5 splenocytes
MUT05
MUT17
MUT30
MUT44
Ex vivo Restimulation
Untreated
Same
Different

(**Figure 4.7C**). Thus vaccination at just one site is sufficient for generating immunity to multiple antigens.

*4.5 Some cross-reactivity of mutanome specific T-cells can be observed to wild-type peptide sequences.*

The results so far have demonstrated that vaccination with mutanome SLPs can induce significant immune responses in mice, even when mice are vaccinated with multiple peptides at once. However vaccination against more than four mutanome peptides has not yet been investigated, so we vaccinated mice with a peptide cocktail containing all twelve mutanome peptides of interest. **Figure 4.8A** displays immune responses, evaluated by ELISPOT, that were generated in response to *ex vivo* stimulation with each individual mutanome peptide. Measurable responses were detected to the majority of peptides in the vaccination cocktail with MUT05, MUT24, MUT25, MUT28 and MUT44 eliciting the strongest responses. While the apparent number of reactive T-cells to each peptide restimulation appears to be lower in **Figure 4.8A** than in **Figure 4.5B**, the highest and lowest response rates from each ELISPOT have approximately equivalent spot density. The difference is due to the settings of the ELISPOT plate reader. Measurements shown in **Figure 4.8A** were taken with more stringent spot detection limits than **Figure 4.5B** as these settings were found to give a more accurate representation of each well. In general, the relative trends observed in the T-cell response strength to each mutanome peptide are similar between **Figure 4.8A** and **Figure 4.5B**. Responses are observed to the majority of antigens not just a single immunodominant peptide.

**Figure 4.8B** depicts the T-cell cross-reactivity that occurs to self-epitopes, measured by *ex vivo re*stimulation with the wild-type peptide sequences corresponding to the mutanome peptides. **Figure 4.8B** demonstrates that most of the mutanome immune responses cross-react with their wild-type sequence, but in general these responses are notably lower than T-cell responses towards the mutanome peptides in **Figure 4.8A**. Wild-type peptides corresponding to MUT24, MUT25, and MUT28 mutanome antigens elicit the greatest self-responses and thus would be prime suspects if any autoimmune reactivity was observed. However there has been no significant evidence of autoimmunity yet in this study.

*4.6 Vaccination with mutanome peptides does not have an affect, positive or negative, on B16F10 tumor progression*

It has previously been reported that vaccination with individual mutanome encoding SLPs can induce control over subsequent tumor growth in the B16F10 model [43] however we were unable to replicate these results (**Figure 4.9B & C**) despite identical timelines and treatments being used (**Figure 4.9A**). We further examined whether vaccination against multiple mutanome peptides could confer control over tumor progression, according to the timeline in **Figure 4.9A.** Treatment with these mutanome peptide cocktails was also unable to confer any survival advantage (**Figure 4.9D**) or tumor control (**Figure 4.9E**) in treated mice.

A subsequent study tested whether vaccination with a combination of all 12 mutanome peptides would result in tumor control (timeline in **Figure 4.10A**). Mice were treated prophylactically with the mutanome peptide cocktail and challenged IV with B16F10 cells. IV challenge, as opposed to SQ tumor challenge, was selected

**Figure 4.8. T-cell responses to self- and mutanome- epitopes elicited by vaccination of mice with mutanome peptides.**

C57Bl/6 mice were immunized with a cocktail of 100μg of each of the 12 mutanome peptides with 50μg poly(I:C). All groups have an N of 3. (a) IFNγ ELISPOT analysis of splenocytes from vaccinated mice, restimulated with individual mutanome peptides. Columns represent means +SEM. (One-way ANOVA, p-value < 0.0001). (b) IFNγ ELISPOT analysis of pooled splenocytes from mice vaccinated with the mutanome peptide cocktail and restimulated *ex vivo* against wild-type self-peptides. (One-way ANOVA, p-value < 0.0001) Asterisks indicate a statistically significant difference between the T-cell responses generated to peptide restimuations compared to the non-restimulated (nothing) control (Dunnett's Multiple Comparison post-test: * = P < 0.05, ** = P < 0.01, *** = P < 0.001).

a

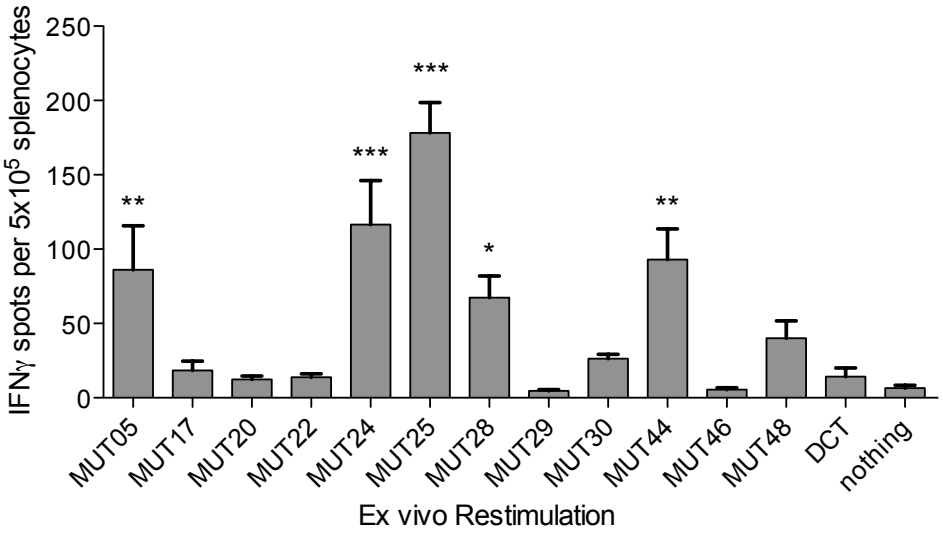
IFNγ spots per 5x10^5 splenocytes
250
200
150
100
50
0
**
***
***
*
**
MUT05
MUT17
MUT20
MUT22
MUT24
MUT25
MUT28
MUT29
MUT30
MUT44
MUT46
MUT48
DCT
nothing
Ex vivo Restimulation

b

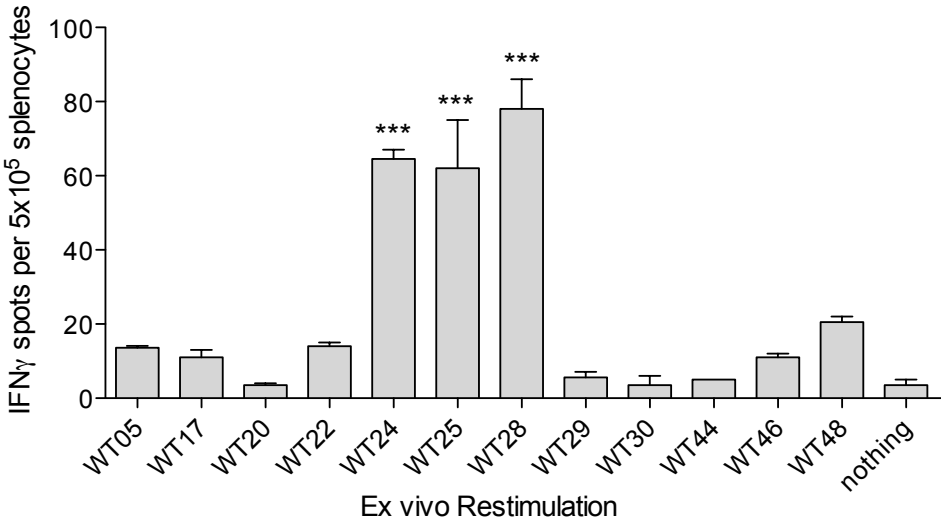
IFNγ spots per 5x10^5 splenocytes
100
80
60
40
20
0
***
***
***
WT05
WT17
WT20
WT22
WT24
WT25
WT28
WT29
WT30
WT44
WT46
WT48
nothing
Ex vivo Restimulation

**Figure 4.9. Mutanome peptide vaccination does not confer tumor control or prolong survival in a B16F10 SQ tumor model.**

C57Bl/6 mice were treated according to the timeline shown in (a) with priming and boosting immunizations of 100μg peptide and 50μg poly(I:C), SQ. (b) Kaplan Meier curve of mice survival after vaccination with PBS, poly(I:C) only, MUT30 & poly(I:C) or DCT & poly(I:C). No significant difference in trends according to log-rank, Mantel-Cox, test. (c) Tumor growth curves corresponding with treatment groups in (b) expressed as the mean tumor size per group +SEM. (d) Kaplan Meier curve of mouse survival after being vaccinated with 100μg of each peptide and 50μg of poly(I:C) SQ. MUT combo 1 is a combination of MUT30, MUT44, MUT20, and MUT17. MUT combo 2 is a combination of MUT12, MUT24, MUT29, and MUT36. No significant trends according to log-rank, Mantel-Cox, test. (e) Tumor growth curves corresponding with treatment groups in (d) are expressed as the mean size per group +SEM. Treatment groups are the same as in (d). All groups had an N of 5 mice per group.

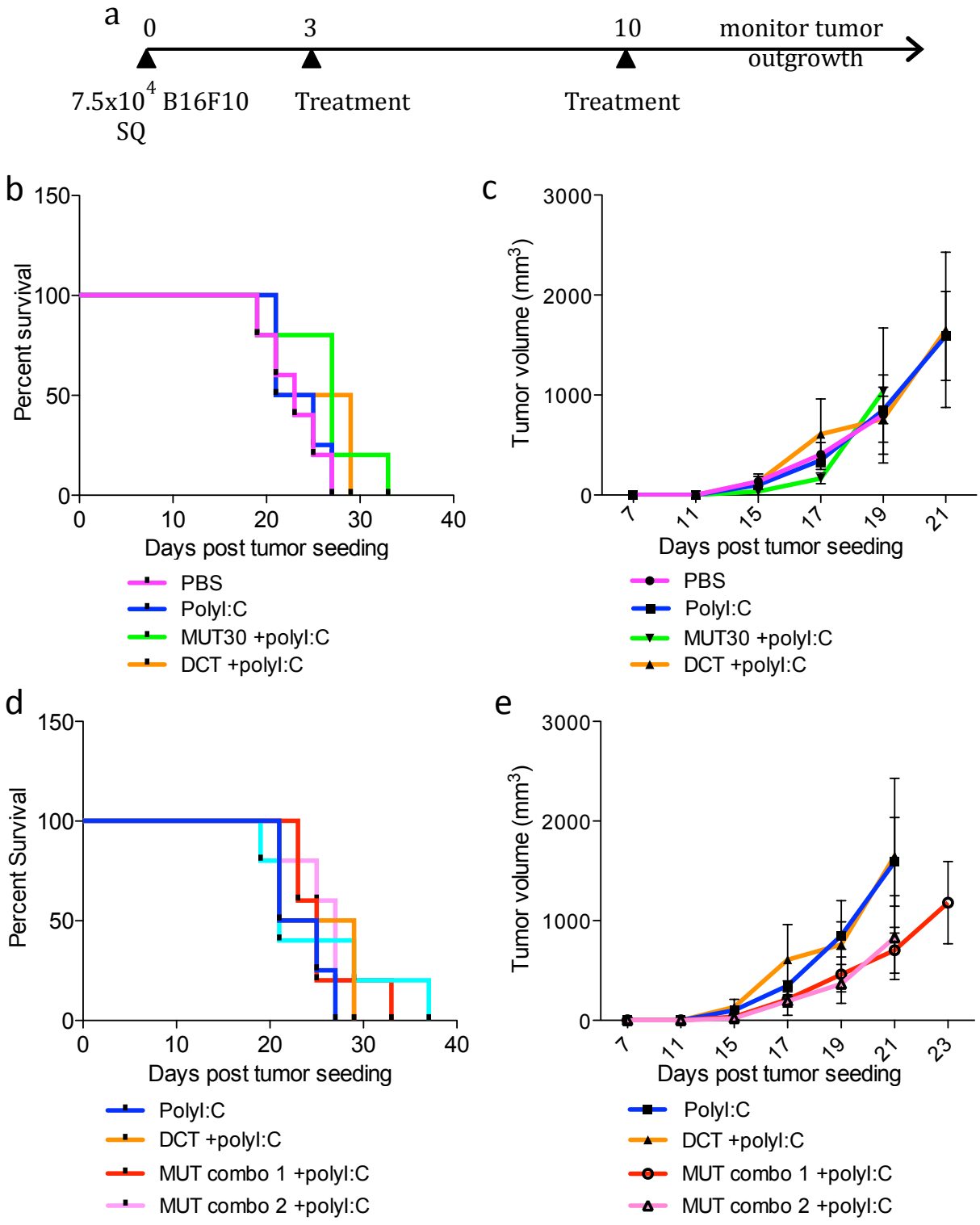
a
0
3
10
monitor tumor outgrowth
7.5x10^4 B16F10 SQ
Treatment
Treatment
b
Percent survival
Days post tumor seeding
PBS
PolyI:C
MUT30 +polyI:C
DCT +polyI:C
c
Tumor volume (mm3)
Days post tumor seeding
PBS
PolyI:C
MUT30 +polyI:C
DCT +polyI:C
d
Percent Survival
Days post tumor seeding
PolyI:C
DCT +polyI:C
MUT combo 1 +polyI:C
MUT combo 2 +polyI:C
e
Tumor volume (mm3)
Days post tumor seeding
PolyI:C
DCT +polyI:C
MUT combo 1 +polyI:C
MUT combo 2 +polyI:C

vaccination with a cocktail of mutanome peptides is insufficient to confer survival advantage to treated mice. This suggested to us that a more robust method of vaccination is needed to induce effective tumor control.

*4.7 TAA vaccination in combination with OV therapy results in superior anti-tumor immunity.*

As a proof of concept we showed that vaccination against MG1 virus encoding dopachrome tautomerase (MG1-hDCT) generates a significantly stronger antigen T-cell response than does vaccination with the DCT peptide mixed with poly(I:C) adjuvant (**Figure 4.11A**). This suggests that encoding the mutanome antigens within MG1 Maraba virus may also result in a stronger antigen specific and perhaps a more therapeutically relevant response. Interestingly, according to the results displayed in **Figure 4.11B**, it appears that having the antigen encoded within the virus may not be necessary. Co-administration of the peptide and MG1 also generates a significantly enhanced antigen specific T-cell response.

VSVΔ51, VSVΔ51 encoding GMCSF cytokine (VSVΔ51-gmcsf), and VSVΔ51 encoding IFNγ (VSVΔ51-IFNγ) were also tested for their ability to further stimulate a T-cell response to peptide vaccination as compared with the poly(I:C) adjuvant. Results from this experiment are displayed in **Figure 4.12**. Surprisingly, VSV turned out to be a much less potent immune stimulator than Maraba, despite both being members of the *Rhabdoviridae* family and being very similar in structure. So, while the encoded therapeutic transgenes may have slightly increased the antigen specific immune responses in comparison to VSVΔ51, Maraba MG1 was still a more efficient immune stimulator.

**Figure 4.10. Mutanome peptide vaccination does not confer tumor control or prolong survival in a B16F10 SQ model.**

C57Bl/6 mice were treated according to the timeline shown in (a) with priming and boosting immunizations composed of 30μg of each peptide and 50μg poly(I:C). (b) Kaplan Meier curve of mouse survival after being vaccinated with PBS, poly(I:C), or a cocktail of all twelve mutanome peptides (MUT peps) & poly(I:C). No significant trends are present according to log-rank, Mantel-Cox, test.

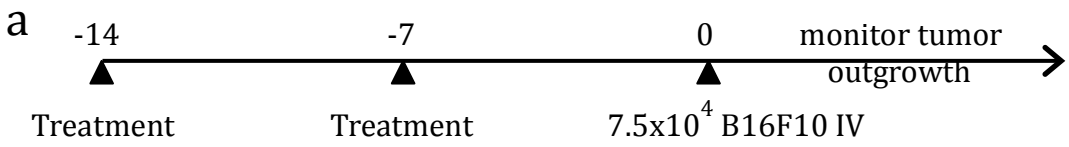
a
-14
-7
0
monitor tumor outgrowth
Treatment
Treatment
7.5x10^4 B16F10 IV

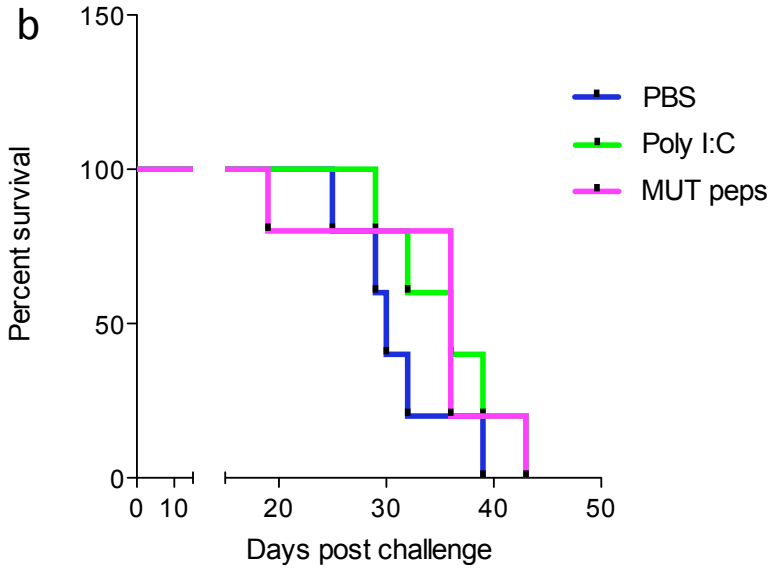
b
150
100
50
0
Percent survival
0
10
20
30
40
50
Days post challenge
PBS
Poly I:C
MUT peps

**Figure 4.11. Immune responses generated to DCT when DCT is presented in combination with virus or poly(I:C)**

C57Bl/6 mice were immunized with $1x10^8$ MG1-hDCT or 30μg of DCT in combination with $1x10^8$pfu MG1-GFP or 50μg poly(I:C). Immunizations were administered IV or SQ as indicated on the graphs. All groups have an N of 5 mice per group. Columns represent means +SEM. Asterisks indicate a statistically significant different immune response to *ex vivo* restimulation by DCT peptide compared to the non-restimulated control (One-way ANOVA, p-value<0.0001; Dunnett's Multiple Comparison post-test: ns = not significant, * = P < 0.05, ** = P < 0.01, *** = P < 0.001). (a) IFNγ ELISPOT analysis comparing the immune response generated to DCT when it is encoded within MG1 versus when it is co-administered with poly(I:C) adjuvant. (b) IFNγ ELISPOT analysis comparing the immune response generated to DCT when it is encoded within MG1, coadministered with MG1 or co-administered with poly(I:C).

a

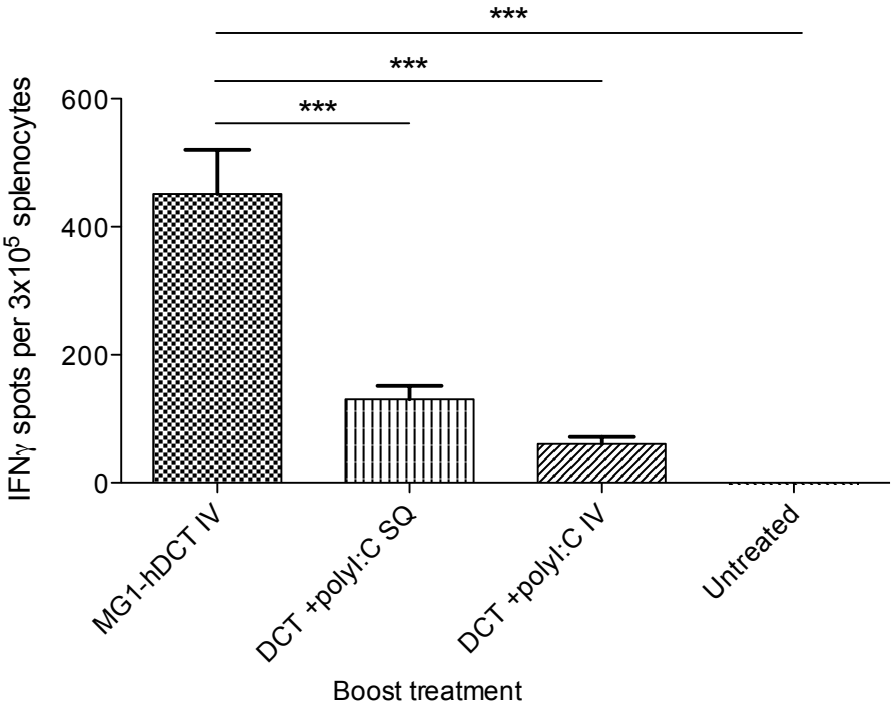
***
***
***
600
400
200
0
IFNγ spots per 3x10^5 splenocytes
MG1-hDCT IV
DCT +polyI:C SQ
DCT +polyI:C IV
Untreated
Boost treatment

b

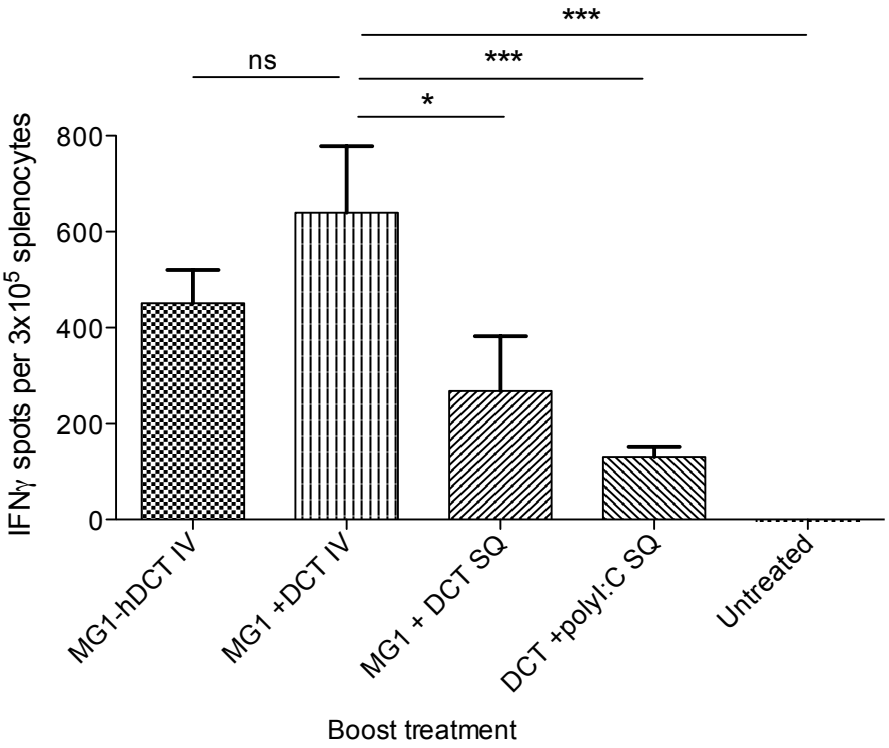
***
ns
***
*
800
600
400
200
0
IFNγ spots per 3x10^5 splenocytes
MG1-hDCT IV
MG1 +DCT IV
MG1 + DCT SQ
DCT +polyI:C SQ
Untreated
Boost treatment

**Figure 4.12. Co-administration of peptide with Maraba virus leads to a superior T-cell response relative to co-administration with VSV.**

All C57Bl/6 mice were vaccinated with 100μg DCT + 50μg poly(I:C) SQ on day 0. On day 7, mice were administered nothing (untreated), 100μg DCT and 50μg poly(I:C), or 100μg DCT and $1x10^8$pfu of MG1, VSVΔ51, VSVΔ51-gmcsf, or VSVΔ51-IFNγ. On day 14 mice were euthanized and splenocytes were restimulated *ex vivo* with 9AA DCT and VSVn peptides. Immune responses were quantified with ELISPOT. Asterisks indicate a statistically significant different immune response between treatment groups (One-way ANOVA, p-value<0.0001; Bonferroni post-test: *** = P < 0.001).

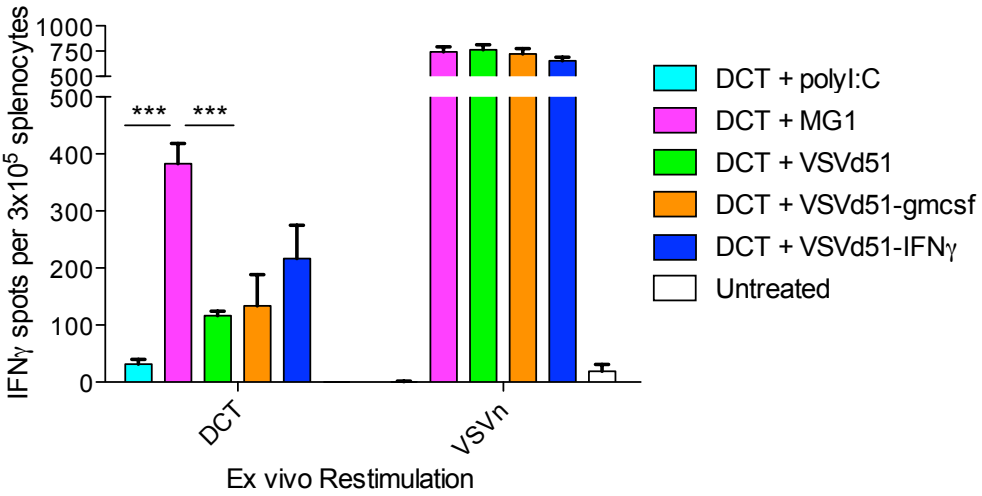
IFNγ spots per 3x10^5 splenocytes
1000
750
500
500
400
300
200
100
0
***
***
DCT
VSVn
Ex vivo Restimulation
DCT + polyI:C
DCT + MG1
DCT + VSVd51
DCT + VSVd51-gmcsf
DCT + VSVd51-IFNγ
Untreated

In *Section 4.2* it was demonstrated that SQ peptide vaccination resulted in stronger T-cell responses than vaccination through other routes (**Figure 4.4**). In contrast, the results in **Figure 4.11B** suggest that IV vaccination with peptide mixed with virus results in a greater T-cell responses than SQ delivery. These opposing results raise the question of whether it is necessary to administer the virus and peptide by the same route, or if IV administration of virus and SQ administration of peptide would also result in a strong antigen specific immune response. **Figure 4.13** demonstrates that in fact virus and peptide need to be administered together to effectively stimulate antigen specific T-cell responses.

We have already demonstrated by ELISPOT that 9AA DCT mixed with Maraba MG1 results in a stronger immune response than 9AA DCT combined with poly(I:C) (**Figure 4.11**) and we confirmed this by flow cytometry, gated on CD8+ cells (**Figure 4.14A**). Furthermore we tested this finding using the 27AA DCT peptide to determine whether MG1 can also enhance T-cell response to 27AA peptides relative to poly(I:C) adjuvant. We found that 27AA DCT mixed with MG1 virus resulted in a superior T-cell response to DCT relative to when it was mixed with poly(I:C) (**Figure 4.14B**). Based on these observations we predicted that MG1 would also boost the T-cell responses towards our 27AA synthetic long mutanome peptides relative to poly(I:C), however this was not the case. As displayed in **Figure 4.15** MG1 did not enhance T-cell reactivity towards mutanome peptides relative to poly(I:C) for MUT30 (**Figure 4.15B**), MUT25 (**Figure 4.15C**) or MUT22 (**Figure 4.15D**). We decided to move forward and test our original hypothesis that encoding these mutanome peptides within an

**Figure 4.13. Co-administration of virus and peptide result in a strong T-cell response relative to administration through separate routes**

Mice in all groups were primed with 50μg poly(I:C) + 30μg of 9AA DCT peptide SQ and boosted with nothing, $1x10^8$pfu MG1-hDCT IV, $1x10^8$pfu MG1 + 30μg 9AA DCT IV, or $1x10^8$ MG1 IV while 30μg 9AA DCT was administered SQ in the same mice. One week later, spleens were harvested, processed, and restimulated with either 9AA DCT or VSVn peptide, stained for CD8+ cells and IFNγ and analyzed by flow cytometry. Data is presented as means +SEM. Asterisks indicate a statistically significant difference in immune response between treatment groups (One-way ANOVA, p-value<0.0075; Bonferroni post-test: ns = not significant, * = $P < 0.05$).

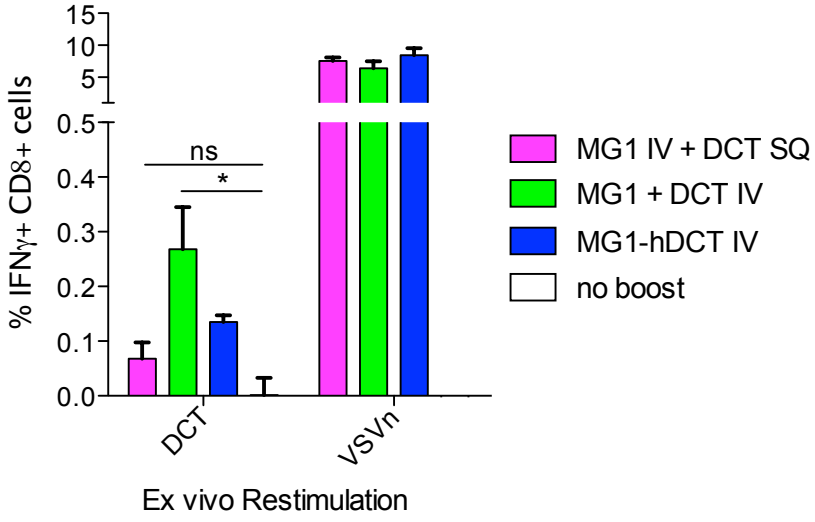
15
10
5
0.5
0.4
0.3
0.2
0.1
0.0
% IFNγ+ CD8+ cells
ns
*
DCT
VSVn
Ex vivo Restimulation
MG1 IV + DCT SQ
MG1 + DCT IV
MG1-hDCT IV
no boost

**Figure 4.14. Co-administration of MG1 induces stronger T-cell responses to both the 9AA and the 27AA DCT relative to poly(I:C).**

Mice in all groups were primed with 30μg DCT + 50μg poly(I:C) administered SQ on day 0. On day 7 mice were administered either nothing, 30μg DCT + 50μg poly(I:C) SQ, or 30μg DCT + $1x10^8$pfu MG1 IV. 7 days after receiving their boost, mice were euthanized, spleens were harvested, processed and stained with CD8+ and IFNγ for analysis by flow cytometry. The observations were consistent in mice that were treated and *ex vivo* restimulated with the 9AA DCT peptide (a) as well as with the 27AA DCT peptide. Data is presented as means +SEM.

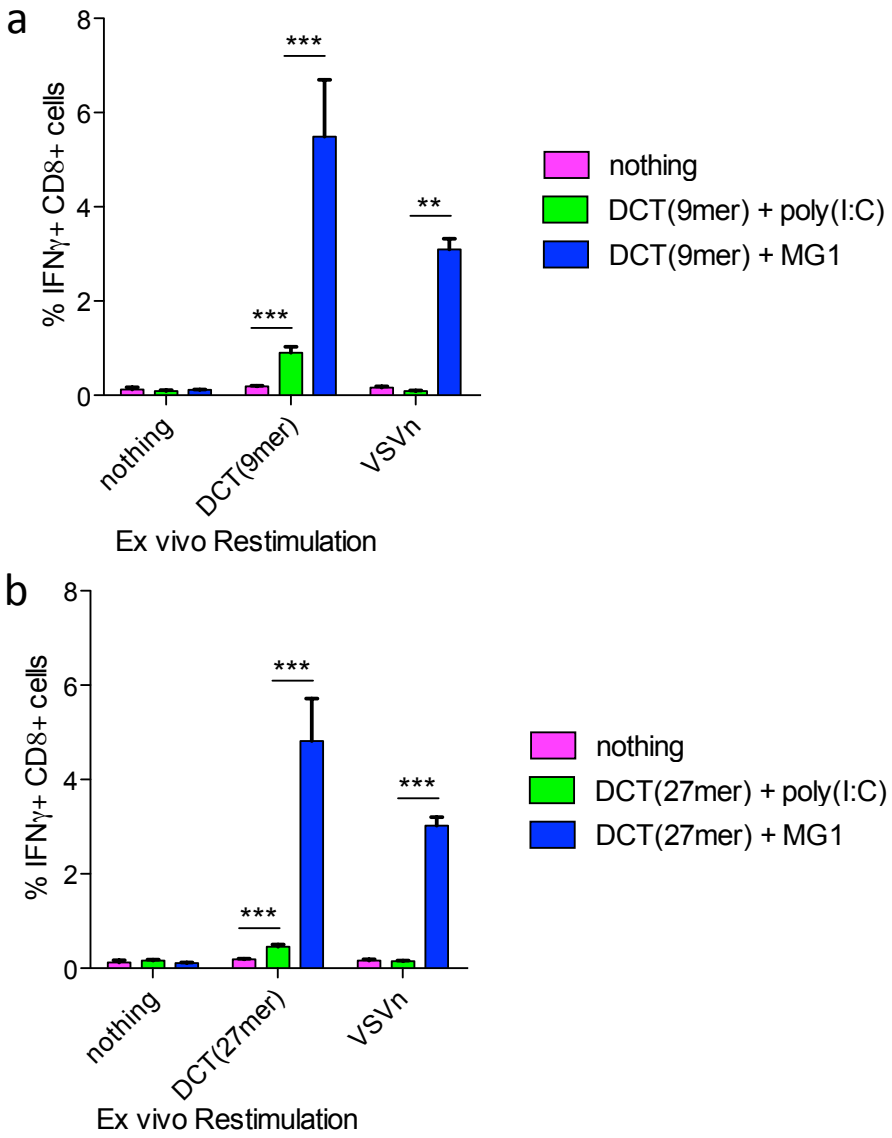
a
% IFNγ+ CD8+ cells
0
2
4
6
8
***
***
**
nothing
DCT(9mer)
VSVn
Ex vivo Restimulation
nothing
DCT(9mer) + poly(I:C)
DCT(9mer) + MG1
b
% IFNγ+ CD8+ cells
0
2
4
6
8
***
***
***
nothing
DCT(27mer)
VSVn
Ex vivo Restimulation
nothing
DCT(27mer) + poly(I:C)
DCT(27mer) + MG1

oncolytic virus would induce superior anti-tumor immunity relative to peptide vaccination and empty virus vaccination.

*4.8 Designing and cloning the mutanome multi-epitope construct into MG1 Maraba virus and E1/E3 deleted, type 5 Adenovirus.*

Previous work by our collaborators at McMaster has demonstrated that a heterologous prime-boost vaccination approach with Adenovirus followed by Maraba virus, both encoding the same tumor antigen, is a very effective way to induce protective anti-tumor T-cell responses while minimizing anti-viral responses, as well as confer a survival advantage to vaccinated animals [111, 116, 117]. We designed a multi-epitope construct encoding sequential sequences of the identified mutanome antigens to be inserted into a virus. The construct design is depicted in **Figure 4.16A**. We arranged the 12 mutanome sequences of interest, identified in **Table 4.1**, in order sequentially from MUT05 to MUT48. Each mutanome sequence is separated by an alanine-alanine-tyrosine (AAY) cleavage sequence, which should enhance proteasomal cleavage of the mutanome construct into individual mutanome peptides [69, 80]. We also tagged the multi-epitope construct with ubiquitin on the C-terminus in order to enhance proteasomal degradation of the sequence [83]. As explained in more detail in the *Introduction,* the substitution of all of ubiquitin's lysines (K) to arginine (R) except for lysine 48, should further enhance processing of the construct by the proteasome [86]. Thus we also designed a sequence identical to the one shown in **Figure 4.16A**, but with all of the lysines in ubiquitin altered to arginine except for lysine 48 (**Figure 4.16B**).

**Figure 4.15. Co-administration of MG1 virus does not induce superior T-cell responses to mutanome SLPs relative to poly(I:C).**

(a) Experimental timeline in days. Mice were treated SQ with 100μg of mutanome peptide (MUT30, MUT25 or MUT22) with 50μg poly(I:C) on day 0; on day 7 mice were boosted with 100μg of mutanome peptide combined with 50μg poly(I:C) or $1x10^8$pfu MG1 virus, administered SQ or IV as indicated. (b,c,d) Columns represent means +SEM. There is no significant difference (determined by One-way ANOVA with Bonferroni post-test) between groups vaccinated with mutanome peptide +poly(I:C) SQ and groups vaccinated with mutanome peptide + MG1 IV for any of the peptides. (b) Experiment vaccinations and *ex vivo* restimulations performed with MUT30, a moderately immunogenic peptide. N=3. (c) Experiment vaccinations and *ex vivo* restimulations performed with MUT25, a highly immunogenic peptide. N=4. (d) Experiment vaccinations and *ex vivo* restimulations performed with MUT22, a poorly immunogenic peptide. N=4.

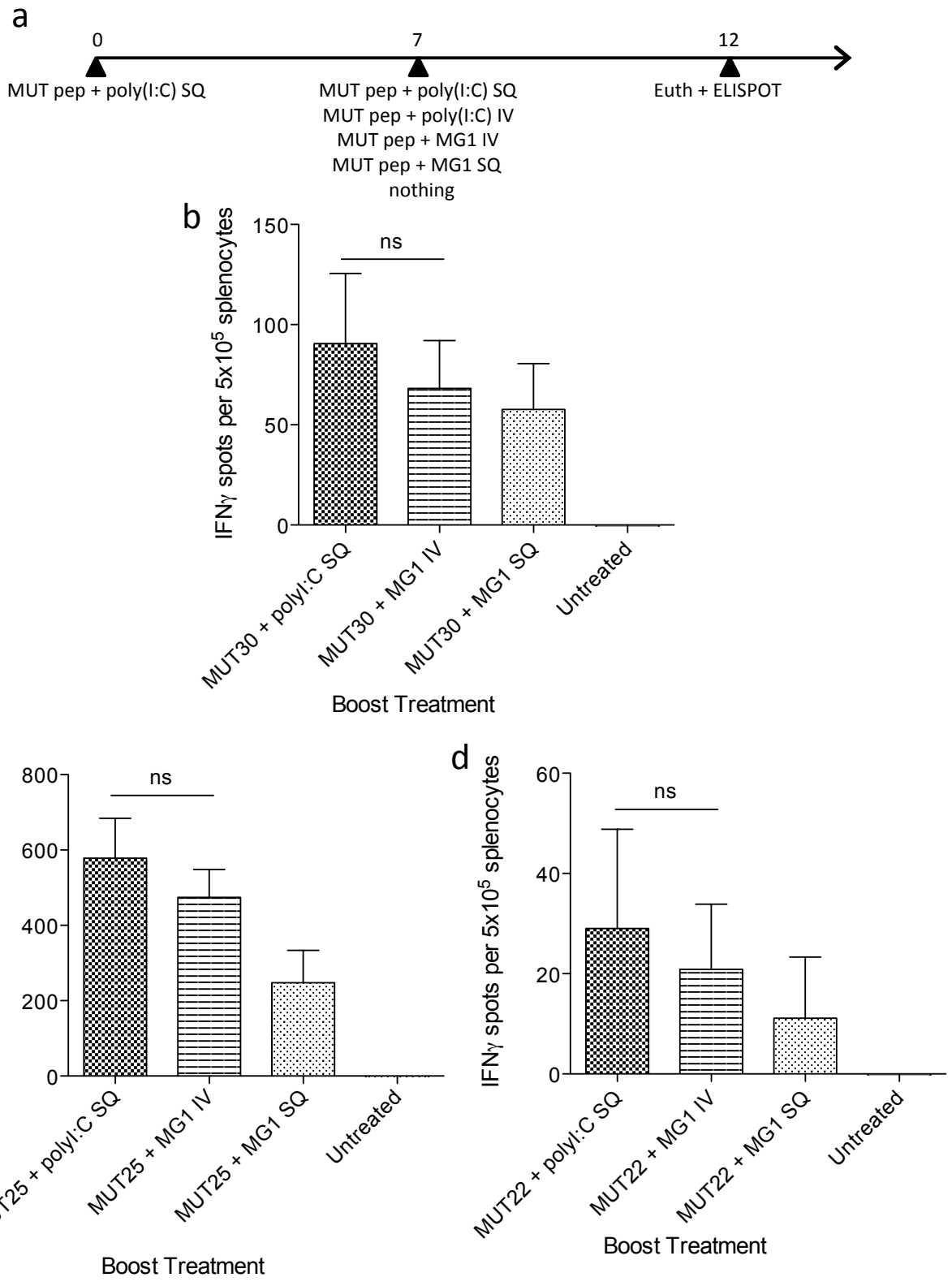
a
0
7
12
MUT pep + poly(I:C) SQ
MUT pep + poly(I:C) SQ
MUT pep + poly(I:C) IV
MUT pep + MG1 IV
MUT pep + MG1 SQ
nothing
Euth + ELISPOT
b
IFNγ spots per 5x10^5 splenocytes
150
100
50
0
ns
MUT30 + polyI:C SQ
MUT30 + MG1 IV
MUT30 + MG1 SQ
Untreated
Boost Treatment
c
IFNγ spots per 5x10^5 splenocytes
800
600
400
200
0
ns
MUT25 + polyI:C SQ
MUT25 + MG1 IV
MUT25 + MG1 SQ
Untreated
Boost Treatment
d
IFNγ spots per 5x10^5 splenocytes
60
40
20
0
ns
MUT22 + polyI:C SQ
MUT22 + MG1 IV
MUT22 + MG1 SQ
Untreated
Boost Treatment

**Figure 4.16. Design of the multi-epitope mutanome construct to be inserted into Maraba virus and Adenovirus.**

All 12 mutanome epitopes of interest are encoded within this muti-epitope construct. Each 27AA mutanome sequence is separated by an AAY linker sequence, and the construct is tagged with ubiquitin. (b) Two different mutanome constructs were generated: one containing regular ubiquitin, displayed in orange, and one containing "mutated" ubiquitin, displayed in blue. The mutated ubiquitin has the same 76AA sequence as the regular ubiquitin however all of its lysines, with the exception of lysine 48, are altered to arginine in order to enhance the targeting of this multi-epitope construct to the proteasome.

a

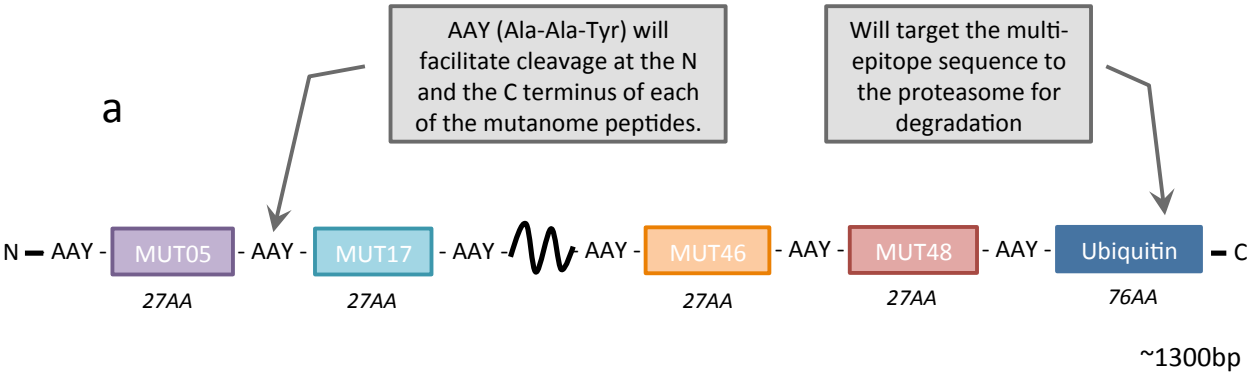
AAY (Ala-Ala-Tyr) will facilitate cleavage at the N and the C terminus of each of the mutanome peptides.
Will target the multi-epitope sequence to the proteasome for degradation
N
AAY -
MUT05
- AAY -
MUT17
- AAY -
AAY -
MUT46
- AAY -
MUT48
- AAY -
Ubiquitin
C
27AA
27AA
27AA
27AA
76AA
~1300bp

b

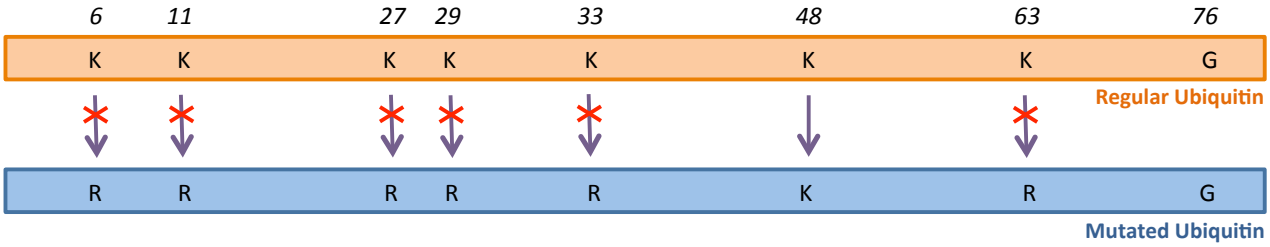
6 11 27 29 33 48 63 76
K K K K K K K G
Regular Ubiquitin
R R R R R K R G
Mutated Ubiquitin

The multi-epitope construct was inserted into both MG1 Maraba virus and E1/E3 deleted, type 5 Adenovirus. **Figure 4.17** illustrates the empty recombinant MG1 Maraba virus genome (MG1) [89] (**Figure 4.17A**), and the Maraba virus genome containing the multi-epitope mutanome construct with regular ubiquitin (MG1-MUT) (**Figure 4.17B**) and with mutated ubiquitin (MG1-MUT-UbMut) (**Figure 4.17C**). **Figure 4.17D** and **E** show the Ad and the Ad-MUT genomes respectively.

As shown by single step growth curves in **Figure 4.18A** and multi-step growth curves in **Figure 4.18B,** the newly cloned MG1-MUT and MG1-MUT-Mut viruses have very similar growth kinetics to MG1 in Vero monkey kidney cells. Thus any differences observed in therapeutic effect of the mutanome expressing Maraba viruses is likely not due to viral growth kinetics.

*4.9 Mutanome virus vaccination results in selective T-cell responses to mutanome epitopes.*

We vaccinated mice with our priming vector, Ad-MUT, and 9 days later harvested the spleens and evaluated the immune responses to each mutanome peptide encoded within the virus. **Figure 4.19A** shows the flow cytometry data from *ex vivo* restimulation of splenocytes from mice vaccinated with Ad-MUT, Ad-BHG, Ad-DCT or nothing. This data is complemented by ELISPOT immune analysis of the same mice, shown in **Figure 4.19B**. Vaccination against Ad-DCT and restimulation with the 9AA DCT peptide is the experimental positive control while restimulation with nothing is the negative control. Both **Figure 4.19A** and **Figure 4.19B** indicate that there is a T-cell response is generated to the MUT25 peptide as a result of vaccination with the Ad-MUT virus. Given that the positive responses to restimulation with the MUT20 epitope

**Figure 4.17. Genomic organization of recombinant Maraba and Adenoviruses.**

Maraba virus engineered to contain two mutations: one in the matrix protein L123W and one on the G protein Q242R. Commonly referred to as MG1. (b) MG1 virus engineered to express the mutanome construct (detailed figure found in *Figure 4.16*) tagged with ubiquitin, between genes G and L. Referred to as MG1-MUT (c) MG1 virus engineered to express the mutanome construct tagged with "mutated" ubiquitin. Construct cloned into MG1 genome between genes G and L. Referred to as MG1-MUT-UbMut. (d) Empty E1/E3 deleted, serotype 5 adenovirus used as an experimental control throughout this thesis. Referred to throughout as Ad. (e) Recombinant type 5 E1/E3 deleted adenovirus, engineered to encode the mutanome construct containing non-altered ubiquitin with a CMV promoter.

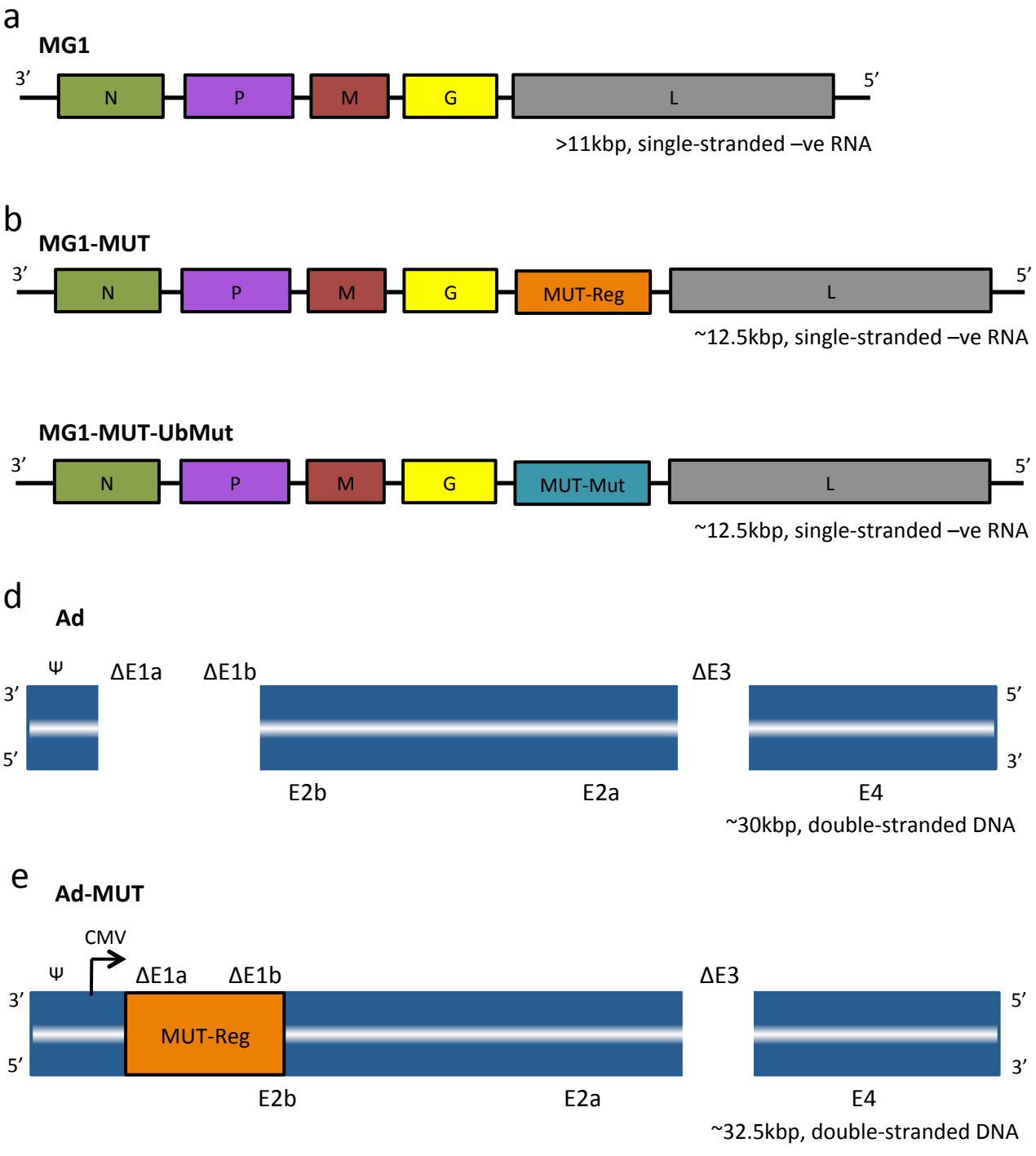
a
MG1
3’
N
P
M
G
L
5’
>11kbp, single-stranded –ve RNA
b
MG1-MUT
3’
N
P
M
G
MUT-Reg
L
5’
~12.5kbp, single-stranded –ve RNA
MG1-MUT-UbMut
3’
N
P
M
G
MUT-Mut
L
5’
~12.5kbp, single-stranded –ve RNA
d
Ad
Ψ
ΔE1a
ΔE1b
ΔE3
3’
5’
5’
3’
E2b
E2a
E4
~30kbp, double-stranded DNA
e
Ad-MUT
CMV
Ψ
ΔE1a
ΔE1b
ΔE3
3’
MUT-Reg
5’
5’
3’
E2b
E2a
E4
~32.5kbp, double-stranded DNA

**Figure 4.18. Viral growth kinetics of mutanome viruses are comparable to that of empty Maraba virus.**

Single-step and (b) multi-step growth curves were performed with the mutanome Maraba viruses, MG1-MUT and MG1-MUT-UbMut, and the empty Maraba virus, MG1, in duplicate. Vero cells were infected at an MOI of 10 and of 0.001 for the single and multi-step growth curves respectively. Supernatants were collected at indicated times post-infection and titered.

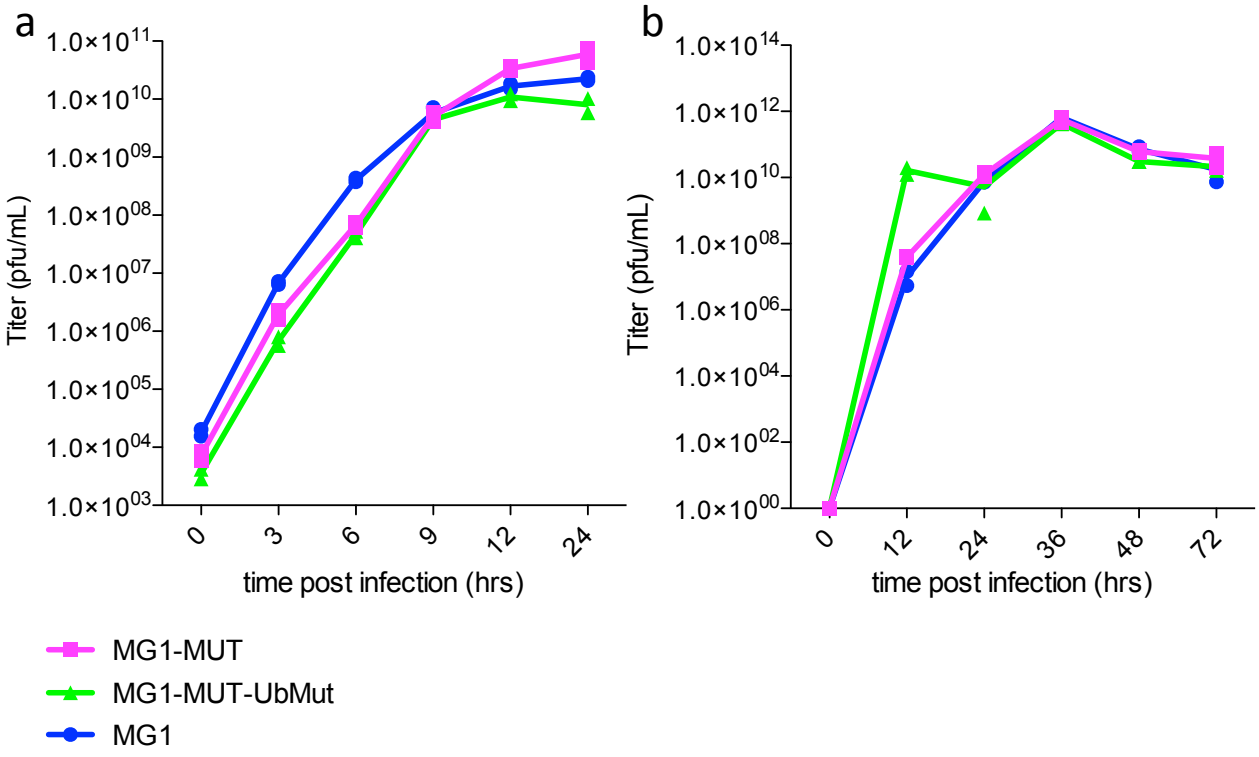
a
1.0×10^11
1.0×10^10
1.0×10^09
1.0×10^08
1.0×10^07
1.0×10^06
1.0×10^05
1.0×10^04
1.0×10^03
Titer (pfu/mL)
0
3
6
9
12
24
time post infection (hrs)
b
1.0×10^14
1.0×10^12
1.0×10^10
1.0×10^08
1.0×10^06
1.0×10^04
1.0×10^02
1.0×10^00
Titer (pfu/mL)
0
12
24
36
48
72
time post infection (hrs)
MG1-MUT
MG1-MUT-UbMut
MG1

seen in **Figure 4.19A** are not also observed by ELISPOT assay in **Figure 4.19B**, it is possible that these responses are the result of contamination, or a figment of the assay itself. There is no evident reason why we would detect an antigen specific immune response by flow cytometry but not by the more sensitive ELISPOT assay. In contrast, while small responses generated to MUT22, MUT24, MUT25, MUT28, and MUT29 were detected by ELISPOT in response to Ad-DCT vaccination, it is possible that these responses were not robust enough to be detected by flow cytometry. However, responses to these antigens were not detected in any subsequent experiments, suggesting that the responses observed here are inconclusive.

While an ELISPOT assay can be a valuable immunological assay it is not an appropriate assay for measuring responses to tumor antigens encoded within the MG1 Maraba virus. Splenocytes are non-specifically activated in response to MG1 vaccination and thus secrete high levels of IFNγ even without being restimulated to any antigen (data not shown). This high level of background stimulation makes it impossible to interpret whether there are any antigen specific T-cell responses elicited. Flow cytometry eliminates this confounding effect by enabling us to look at responses of specific T-cell populations while gating out other cell populations.

Flow cytometry data of tumor bearing mice treated according to the timeline displayed in **Figure 4.20A** is displayed in **Figure 4.20B**. VSVn peptide restimulation of Maraba vaccinated mice is the experimental positive control. Restimulation of splenocytes from MG1-MUT boosted mice with MUT25 and MUT48 peptides both generate a positive response, indicating T-cell specificity to these antigens in response

**Figure 4.19. Ad-MUT induces T-cell responses to one of the B16F10 mutanome epitopes.**

Mice were administered bilateral IM injections of $1x10^8$pfu Ad-MUT, Ad, Ad-hDCT or nothing (no treatment) and 9 days later were euthanized and splenocytes were used for T-cell response analysis. Splenocytes were restimulated *ex vivo* with nothing, DCT peptide, or each of the mutanome peptides. SMNCs were either (a) stained and examined by flow cytometry for CD8+ cells and IFNγ or (b) examined by ELISPOT for relative T-cell activation for each restimulation. Data are presented as means +/- SEM with 3 mice per group for Ad-MUT and Ad-BHG and 2 mice per group for Ad-hDCT and no treatment (nothing) group.

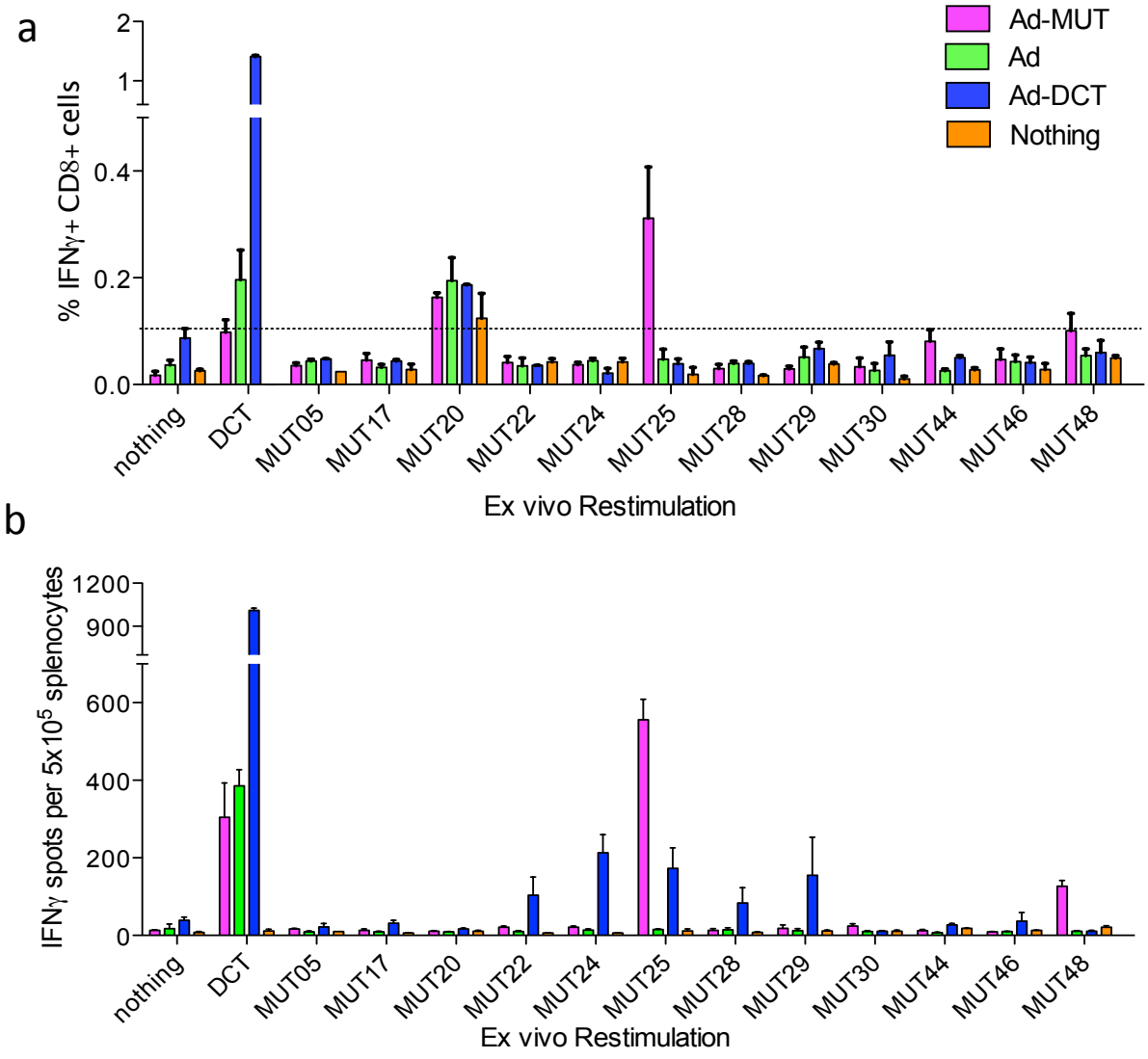
a
Ad-MUT
Ad
Ad-DCT
Nothing
% IFNγ+ CD8+ cells
2
1
0.4
0.2
0.0
nothing
DCT
MUT05
MUT17
MUT20
MUT22
MUT24
MUT25
MUT28
MUT29
MUT30
MUT44
MUT46
MUT48
Ex vivo Restimulation
b
IFNγ spots per 5x10^5 splenocytes
1200
900
600
400
200
0
nothing
DCT
MUT05
MUT17
MUT20
MUT22
MUT24
MUT25
MUT28
MUT29
MUT30
MUT44
MUT46
MUT48
Ex vivo Restimulation

to vaccination with MG1-MUT virus. Interestingly, there were some cell populations visible by flow cytometry that were secreting IFNγ that were not CD8+ cells as presented by the flow cytometry plots in **Figure 4.20C**. We hypothesized that these cells were likely CD4+ T-cells since they are also known to secrete IFNγ in response to antigen specific restimulation [29]. Therefore in all other experiments we decided to also stain for CD4+ cells and assess these cells for IFNγ production.

Prime-boost vaccinations with our mutanome viruses (outlined in **Figure 4.21A**) yielded results similar to previous experiments testing each individual mutanome encoding virus (**Figure 4.21**). Antigen specific responses were detected towards the MUT25 peptide in mice primed with Ad-MUT and boosted with MG1-MUT. Interestingly, both CD8+ and CD4+ cells elicited MUT25 antigen specific responses (**Figure 4.21B** and **Figure 4.21C**). VSVn peptide restimulation is the positive control in this experiment. No T-cell responses were detected towards any of the other mutanome epitopes.

*4.10 Driving out individual mutanome immune responses generated to MG1-MUT*

To determine whether we can force T-cell responses to mutanome peptides other than MUT25, we primed mice with just one mutanome peptide and then boosted the mice with the MG1-MUT virus. **Figures 4.22A & B** display data for mice primed against MUT25, **Figures 4.22C & D** show data for mice primed against MUT44, and **Figures 4.22E & F** show data for mice primed against MUT48. Priming the immune system with MUT25 and MUT48 followed by MG1-MUT resulted in an antigen specific CD8+ T-cell response however priming with MUT44 and boosting with MG1-MUT did not. Of note however, the mice that were both primed and boosted with peptide and

**Figure 4.20. MG1-MUT vaccination induces T-cell responses to two mutanome epitopes encoded within the virus**

Experimental timeline. Lung tumors were seeded through IV injection of $2.5x10^5$ B16F10 cells in C57Bl/6 mice. Mice were primed SQ on day 5 with 30μg of each of the 12 mutanome peptides, mixed with 50μg poly(I:C). On day 12 the mice received $5x10^8$pfu MG1-MUT IV (n=3), $5x10^8$pfu MG1 IV (n=4), 30μg of each mutanome peptide +50μg poly(I:C) (n=4), or nothing (n=2). On day 19 post tumor seeding, mice were euthanized and spleens were harvested for immune analysis. (b) Splenocytes were restimulated *ex vivo* with VSVn peptide, DCT peptide, and each of the mutanome peptides. Analyzed by flow cytometry. Data is presented as means +SEM. (c) Flow plots from select *ex vivo* restimulations demonstrating that there is a portion of activated splenocytes which are not CD8+ T-cells.

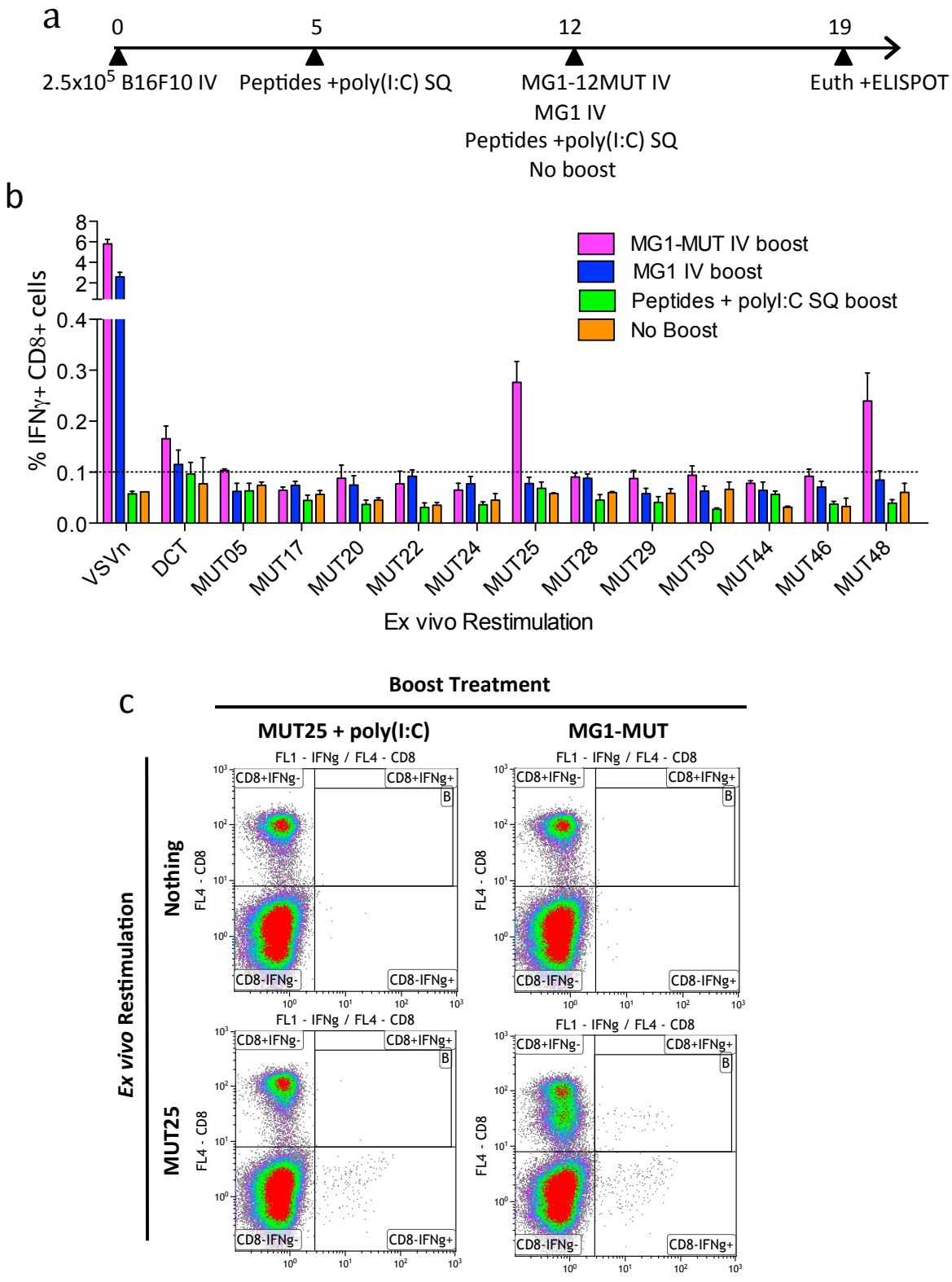
a
0
5
12
19
2.5x10^5 B16F10 IV
Peptides +poly(I:C) SQ
MG1-12MUT IV
MG1 IV
Peptides +poly(I:C) SQ
No boost
Euth +ELISPOT
b
% IFNγ+ CD8+ cells
MG1-MUT IV boost
MG1 IV boost
Peptides + polyI:C SQ boost
No Boost
VSVn
DCT
MUT05
MUT17
MUT20
MUT22
MUT24
MUT25
MUT28
MUT29
MUT30
MUT44
MUT46
MUT48
Ex vivo Restimulation
c
Boost Treatment
MUT25 + poly(I:C)
MG1-MUT
Ex vivo Restimulation
Nothing
MUT25
FL1 - IFNg / FL4 - CD8
FL4 - CD8
CD8+IFNg-
CD8+IFNg+
CD8-IFNg-
CD8-IFNg+
B

**Figure 4.21. Heterologous prime-boost vaccination with the mutanome viruses induces a T-cell response to one of the B16 mutanome epitopes**

Experimental timeline. C57Bl/6 mice were seeded with B16F10 lung tumors on day 0; on day 5 mice were primed IM with $1x10^8$pfu Ad-MUT, Ad, or nothing. On day 19, mice were boosted IV with $5x10^8$pfu MG1-MUT. On day 12 mice were euthanized and immune analysis was performed on splenocytes. Splenocytes were restimulated *ex vivo* with nothing, VSVn peptide, DCT peptide, and each of the mutanome peptides. SMNCs were stained and examined by flow cytometry for (b) CD8+ cells and IFNγ or (c) CD4+ cells and IFNγ. Data are presented as means +SEM with 5 mice per group (n=5).

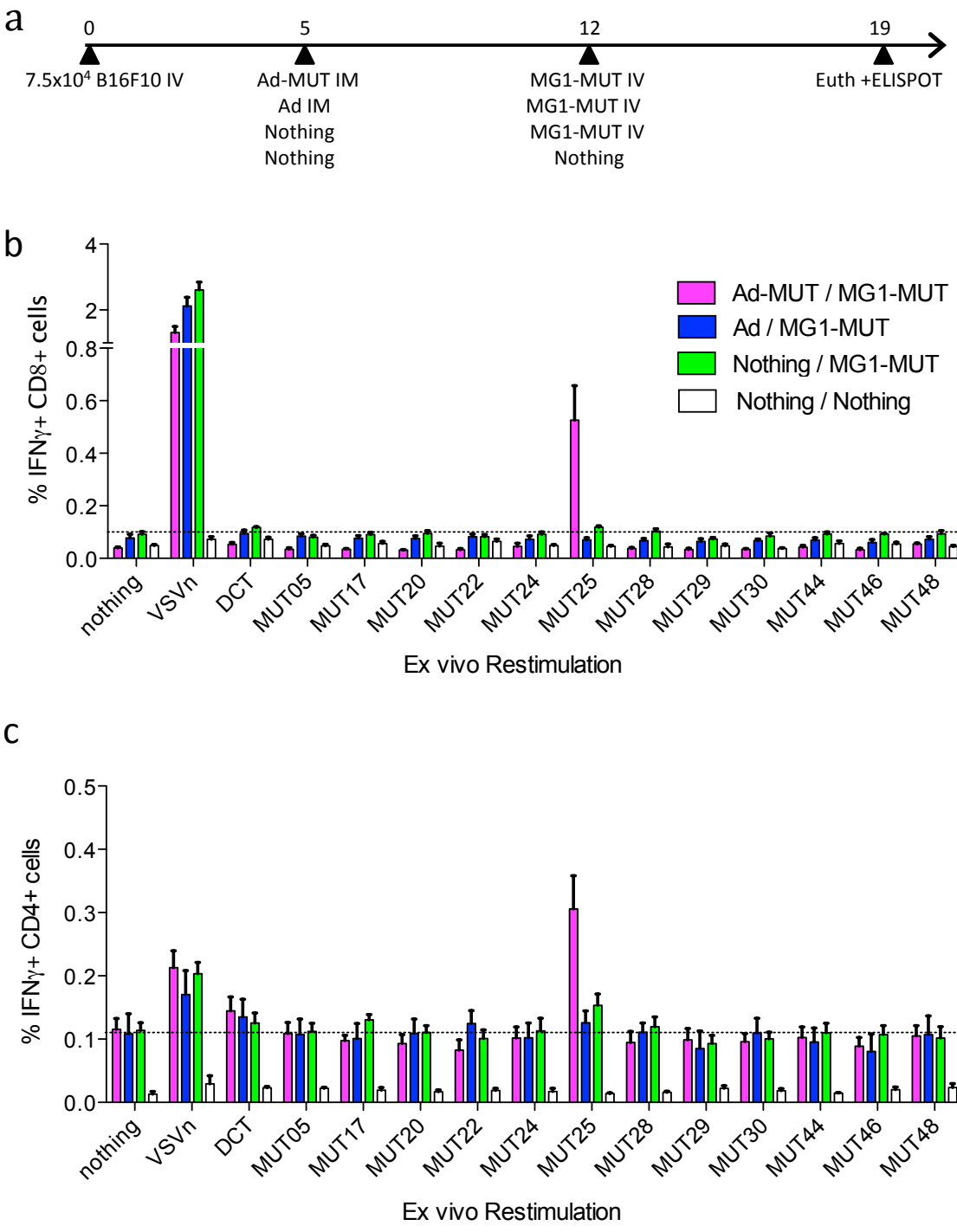
a
0
5
12
19
7.5x10^4 B16F10 IV
Ad-MUT IM
Ad IM
Nothing
Nothing
MG1-MUT IV
MG1-MUT IV
MG1-MUT IV
Nothing
Euth +ELISPOT
b
% IFNγ+ CD8+ cells
Ad-MUT / MG1-MUT
Ad / MG1-MUT
Nothing / MG1-MUT
Nothing / Nothing
nothing
VSVn
DCT
MUT05
MUT17
MUT20
MUT22
MUT24
MUT25
MUT28
MUT29
MUT30
MUT44
MUT46
MUT48
Ex vivo Restimulation
c
% IFNγ+ CD4+ cells
Ex vivo Restimulation

poly(I:C) vaccinations elicited strong CD4+ antigen specific responses but no observable CD8+ responses. While CD8+ T-cells are more commonly known for their effector functions and tumor control abilities, CD4+ T-cells have been implicated in tumor progression control as well [18, 28-31].

*4.11 No survival advantage was experienced by mice treated with the mutanome heterologous prime-boost*

Ultimately, it is not our ability to measure antigen specific T-cell responses that defines whether or not a therapy is successful, but whether the therapy confers a survival advantage. Our hope was that by encoding these mutanome epitopes into an OV and treating the mice with a heterologous prime boost, that mice would benefit from both the oncolytic and anti-tumor immunity aspect of the therapy and have a survival advantage over mice controls. A survival experiment, in which tumor bearing mice were treated with this approach is outlined in **Figure 4.23A**. The positive control in this experiment is the group that was primed with Ad-hDCT and boosted with MG1-hDCT – a treatment previously characterized for its success [111]. Aside from the Ad-hDCT/MG1-hDCT treated mice, none of the mutanome virus treatment combinations conferred any survival advantage upon the mice as shown in **Figure 4.23B**.

*4.12 Prophylactic immunization with mutanome- viruses does not provide any protective effects against lung B16F10 tumors.*

Since it is well understood that prophylactic vaccinations are generally much more efficacious than therapeutic vaccinations [53], we decided to test whether vaccinating mice with the mutanome viruses and subsequently challenging them with B16F10 lung tumors would lead to any reduction in lung tumor burden compared to

**Figure 4.22. Cannot potentiate immune responses to individual mutanome epitopes by priming with an individual peptide and boosting with MG1-MUT virus.**

C57Bl/6 mice were seeded with $7.5x10^4$ B16F10 cells IV. Three days post seeding mice were primed with 50μg mutanome peptide (MUT25, MUT44, or MUT 48) + 50μg poly(I:C) and 7 days later were administered $5x10^8$pfu MG1-MUT, MG1, or peptide + poly(I:C). Seven days later mice were euthanized, spleens were harvested, processed and stained for IFNγ, CD8+ (a, c, e) and CD4+ (a,d,f) responses. Data is presented as means + SEM. N=3.

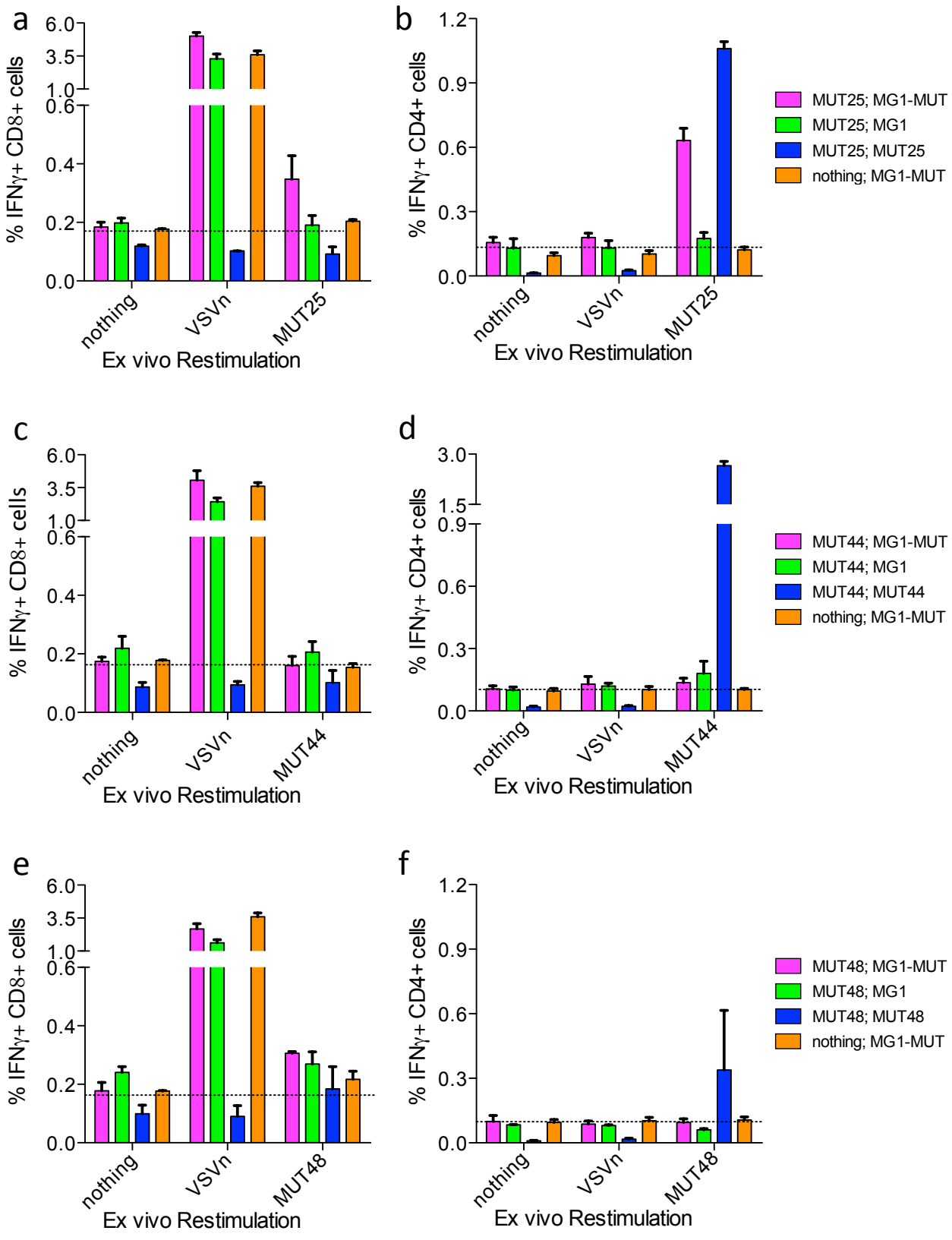
a
% IFNγ+ CD8+ cells
6.0
3.5
1.0
0.6
0.4
0.2
0.0
nothing
VSVn
MUT25
Ex vivo Restimulation
b
% IFNγ+ CD4+ cells
1.2
0.9
0.6
0.3
0.0
nothing
VSVn
MUT25
Ex vivo Restimulation
MUT25; MG1-MUT
MUT25; MG1
MUT25; MUT25
nothing; MG1-MUT
c
% IFNγ+ CD8+ cells
6.0
3.5
1.0
0.6
0.4
0.2
0.0
nothing
VSVn
MUT44
Ex vivo Restimulation
d
% IFNγ+ CD4+ cells
3.0
1.5
0.9
0.6
0.3
0.0
nothing
VSVn
MUT44
Ex vivo Restimulation
MUT44; MG1-MUT
MUT44; MG1
MUT44; MUT44
nothing; MG1-MUT
e
% IFNγ+ CD8+ cells
6.0
3.5
1.0
0.6
0.4
0.2
0.0
nothing
VSVn
MUT48
Ex vivo Restimulation
f
% IFNγ+ CD4+ cells
1.2
0.9
0.6
0.3
0.0
nothing
VSVn
MUT48
Ex vivo Restimulation
MUT48; MG1-MUT
MUT48; MG1
MUT48; MUT48
nothing; MG1-MUT

**Figure 4.23. Heterologous prime-boost with mutanome viruses does not provide any survival advantage for treated mice**

Experimental timeline. C57Bl/6 mice were seeded with $7.5x10^4$ B16F10 cells IV. Three days later mice were treated IM with $1x10^8$pfu Ad-MUT, Ad, or Ad-hDCT. Seven days later, mice received $5x10^8$pfu MG1-MUT, MG1-MUT-UbMut, MG1, MG1-hDCT or nothing as indicated in the treatment timeline. (b) Kaplan Meier curve of mouse survival. No significant trends are present according to log-rank, Mantel-Cox test.

a

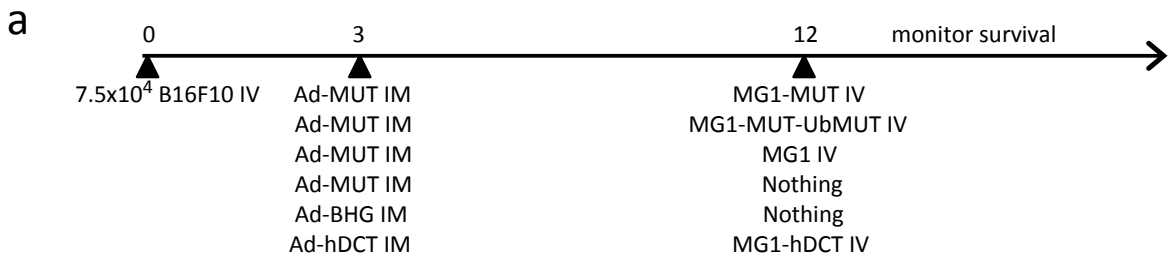
0
3
12
monitor survival
7.5x10^4 B16F10 IV
Ad-MUT IM
Ad-MUT IM
Ad-MUT IM
Ad-MUT IM
Ad-BHG IM
Ad-hDCT IM
MG1-MUT IV
MG1-MUT-UbMUT IV
MG1 IV
Nothing
Nothing
MG1-hDCT IV

b

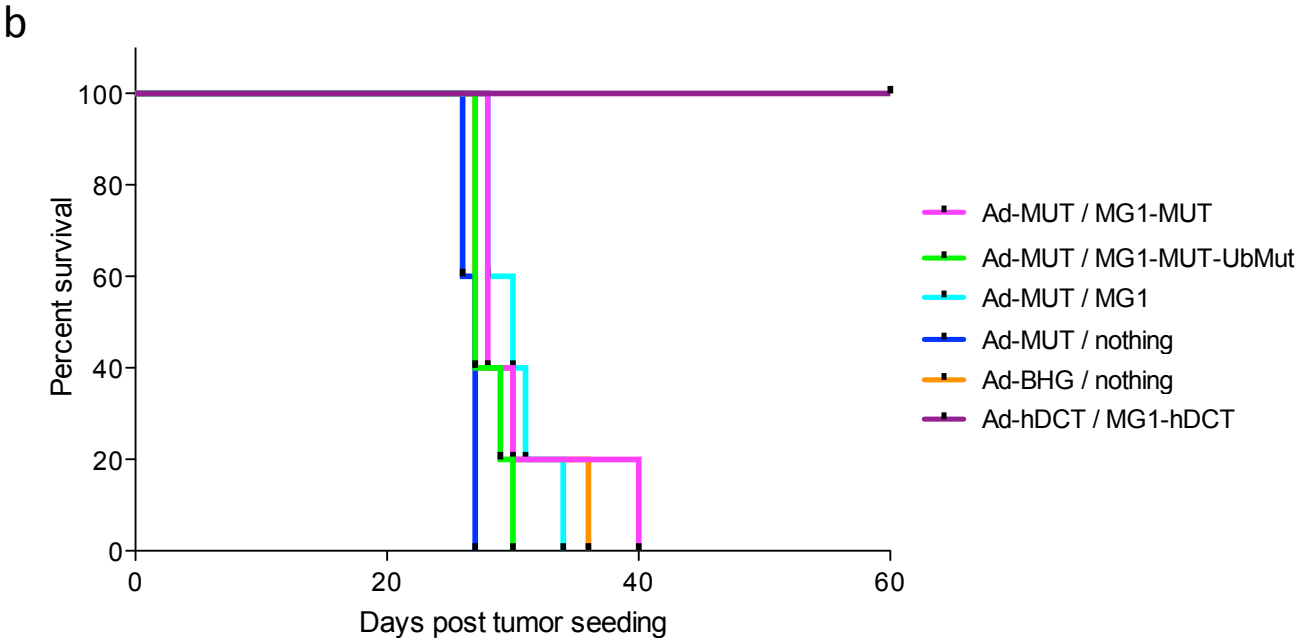
Percent survival
100
80
60
40
20
0
0
20
40
60
Days post tumor seeding
Ad-MUT / MG1-MUT
Ad-MUT / MG1-MUT-UbMut
Ad-MUT / MG1
Ad-MUT / nothing
Ad-BHG / nothing
Ad-hDCT / MG1-hDCT

control treated mice. Mice were treated and challenged according to the timeline displayed in **Figure 4.24A**. One day prior to challenge we did saphenous bleeds on the mice to ensure that immune responses were generated to treatment. We measured immune responses by flow cytometry to *ex vivo* restimulation with VSVn, 9AA DCT, and MUT25 peptides (**Figure 4.24B**) and found that the mice had expected T-cell responses. VSVn peptide induced responses in mice vaccinated with any of the recombinant Maraba viruses, and DCT peptide restimulation induced a strong response in mice vaccinated with Ad-DCT/MG1-DCT. Mice vaccinated with the mutanome viruses also elicited quite significant responses to the MUT25 peptide.

Significantly, on the day of B16F10 challenge the mice that received Ad-MUT/MG1-MUT and Ad-MUT/MG1-MUT-UbMut were smaller and more dehydrated relative to the other groups, however all mice survived. On day 22 post tumor seeding, the mouse lungs and spleens were harvested. Flow cytometry immune analysis on the splenocytes demonstrated that there were significant responses to MUT25 in the Ad-MUT/MG1-MUT, the Ad-MUT/MG1-MUT-UbMut, and the Ad-MUT/MG1 vaccinated mice (**Figure 4.24C**). No other responses were detected against other mutanome peptides. Lung weights (**Figure 4.25B**) and quantification of lung tumors (**Figure 4.25C**) demonstrated that in fact, aside from the peptide only treated groups, the mice that received Ad-MUT/MG1-MUT and Ad-MUT/MG1-MUT-UbMut actually had the greatest lung tumor burden.

**Figure 4.24. Prophylactic prime-boost with mutanome viruses results in T-cell responses to one mutanome epitope as measured in the spleen and blood.**

Experimental timeline. Mice received $1x10^8$pfu Adenovirus IM or 30μg of each mutanome peptide + 50μg poly(I:C) SQ. Seven days later, mice were administered $5x10^8$pfu Maraba virus IV or 30μg of each mutanome peptide + 50μg poly(I:C) SQ. Prime-boost treatment pairings are indicated in timeline. One day prior to lung tumor seeding with $7.5x10^4$ B16F10 cells IV, flow cytometry analysis was performed on blood collected by saph bleeds (b). Twenty-two days after tumor seeding, mice were euthanized and spleens were processed; restimulated with irrB16F10 cells, VSVn peptide, DCT peptides or a mutanome peptides; stained and analyzed by flow cytometry for CD8+ and IFNγ (c). Data is presented as means +SEM.

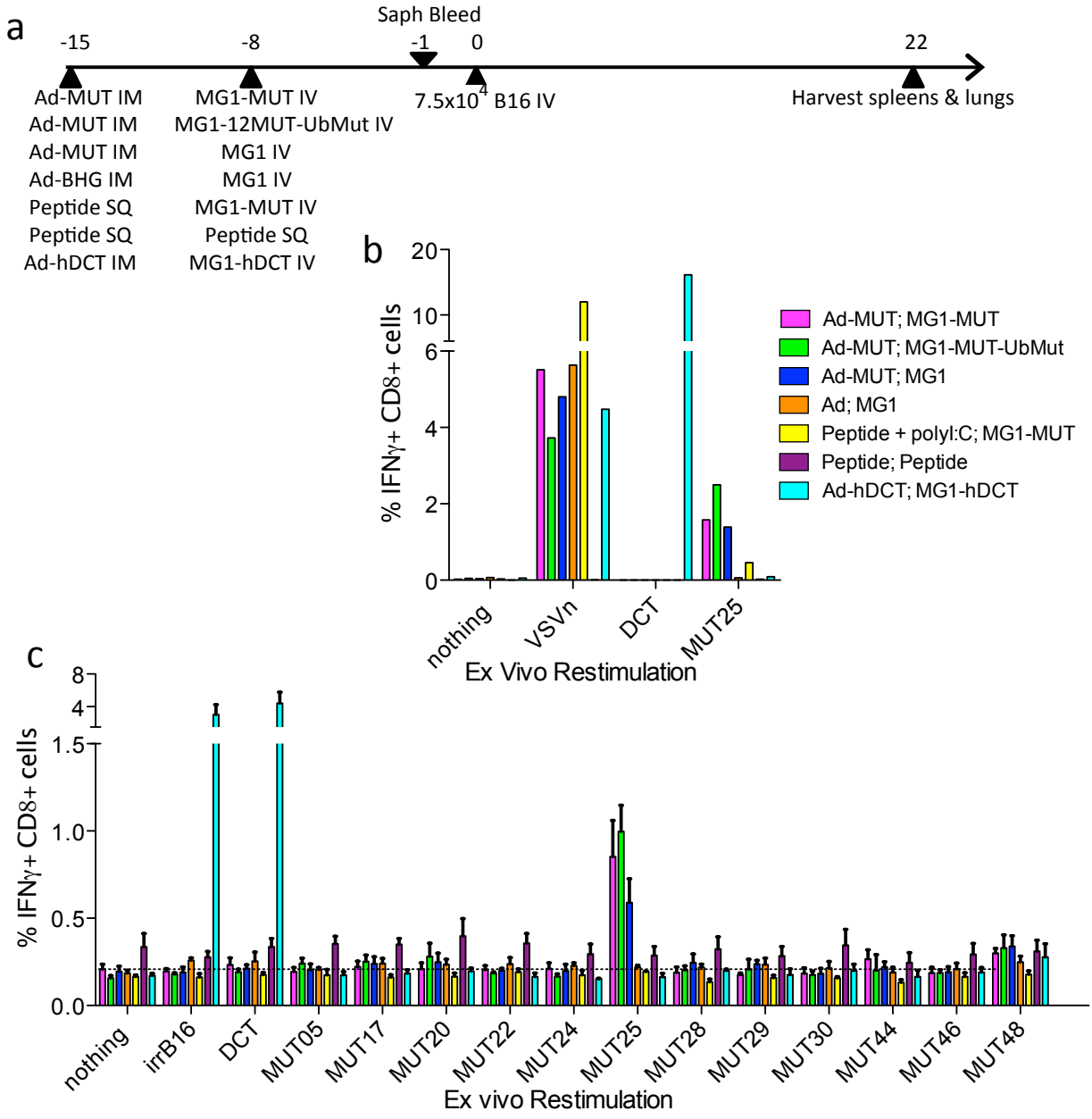
a
Saph Bleed
-15
-8
-1
0
22
Ad-MUT IM
Ad-MUT IM
Ad-MUT IM
Ad-BHG IM
Peptide SQ
Peptide SQ
Ad-hDCT IM
MG1-MUT IV
MG1-12MUT-UbMut IV
MG1 IV
MG1 IV
MG1-MUT IV
Peptide SQ
MG1-hDCT IV
7.5x10^4 B16 IV
Harvest spleens & lungs
b
% IFNγ+ CD8+ cells
Ad-MUT; MG1-MUT
Ad-MUT; MG1-MUT-UbMut
Ad-MUT; MG1
Ad; MG1
Peptide + polyI:C; MG1-MUT
Peptide; Peptide
Ad-hDCT; MG1-hDCT
nothing
VSVn
DCT
MUT25
Ex Vivo Restimulation
c
% IFNγ+ CD8+ cells
nothing
irrB16
DCT
MUT05
MUT17
MUT20
MUT22
MUT24
MUT25
MUT28
MUT29
MUT30
MUT44
MUT46
MUT48
Ex vivo Restimulation

**Figure 4.25. Prime-boost prophylactic vaccinations with mutanome viruses results in greater lung tumor burden than experimental controls.**

Experimental timeline. Mice receive $1x10^8$pfu Adenovirus IM or 30μg of each mutanome peptide + 50μg poly(I:C) SQ. Seven days later, mice were administered $5x10^8$pfu of MG1-MUT, MG1-MUT-UbMUT, MG1 or MG1-hDCT, or 30μg of each mutanome peptide + 50μg poly(I:C) SQ. Prime-boost treatment pairings are indicated in timeline. Twenty-two days after tumor seeding, mice were euthanized and lung weights (b) and number of individual lung metastases (c) were assessed. Data is presented as means +/- SEM. In (b), Peptides; Peptides and Ad-MUT; MG1-MUT-UbMUT treated groups have a significantly greater ($p<0.05$) lung tumor burden relative to Ad;MG1 treated mice. In (c), Peptides;Peptides were found to have a significantly greater ($p<0.01$) lung tumor burden relative to Ad;MG1 treated mice. Statistical analysis in all cases was performed with a One-way ANOVA with Dunnett's Multiple Comparison post-test.

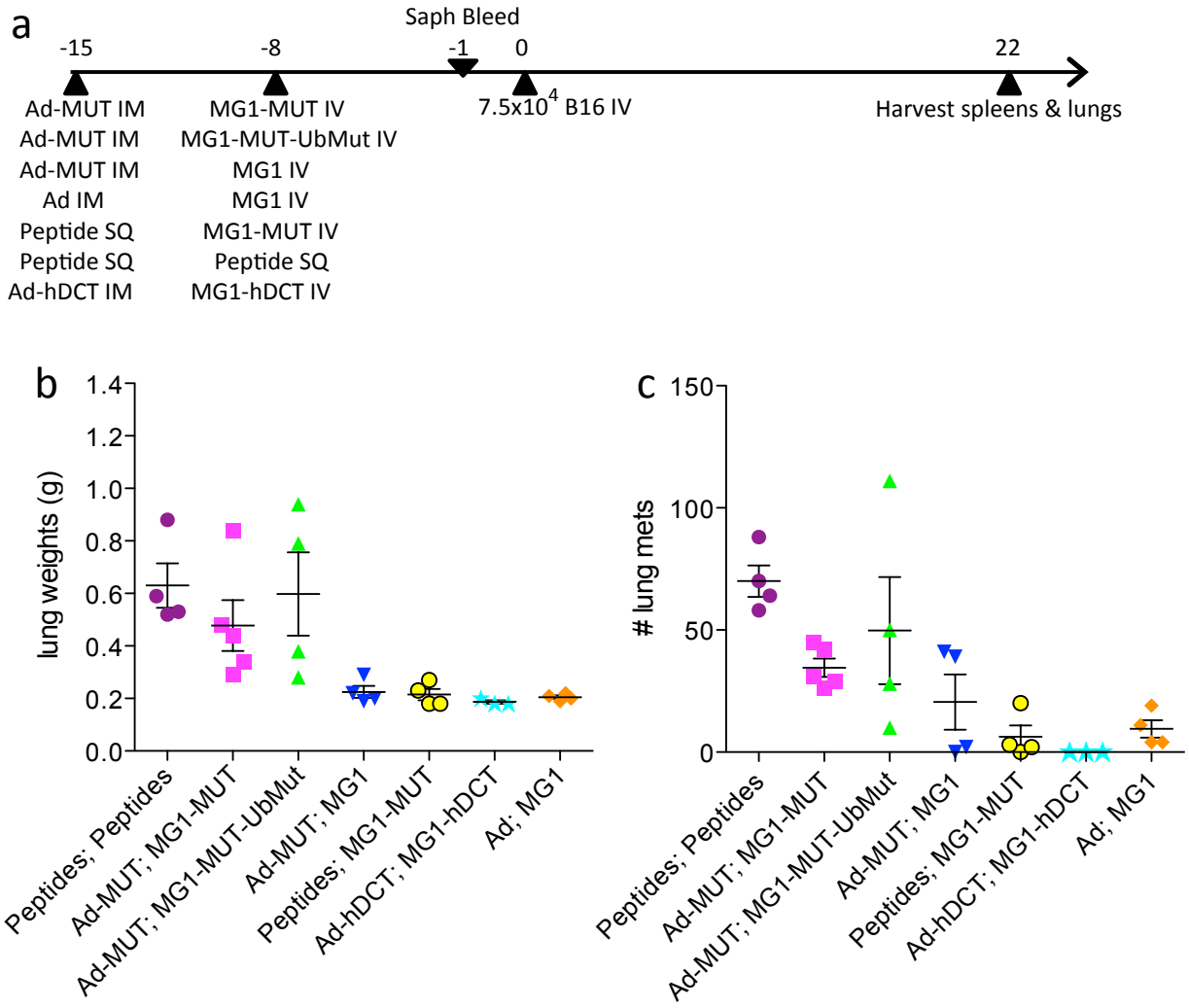
a
Saph Bleed
-15
-8
-1
0
22
Ad-MUT IM
Ad-MUT IM
Ad-MUT IM
Ad IM
Peptide SQ
Peptide SQ
Ad-hDCT IM
MG1-MUT IV
MG1-MUT-UbMut IV
MG1 IV
MG1 IV
MG1-MUT IV
Peptide SQ
MG1-hDCT IV
7.5x10^4 B16 IV
Harvest spleens & lungs
b
lung weights (g)
1.4
1.2
1.0
0.8
0.6
0.4
0.2
0.0
Peptides; Peptides
Ad-MUT; MG1-MUT
Ad-MUT; MG1-MUT-UbMut
Ad-MUT; MG1
Peptides; MG1-MUT
Ad-hDCT; MG1-hDCT
Ad; MG1
c
# lung mets
150
100
50
0
Peptides; Peptides
Ad-MUT; MG1-MUT
Ad-MUT; MG1-MUT-UbMut
Ad-MUT; MG1
Peptides; MG1-MUT
Ad-hDCT; MG1-hDCT
Ad; MG1

## Discussion

Over the last decade there has been substantial progress in OV pre-clinical and clinical studies [88]. A current focus in the OV field is to enhance the induction of anti-tumour immunity following OV therapy [100]. One method used to enhance immune responses is to encode immune modulating cytokines within the oncolytic virus [40, 107, 108, 136]. Another method involves priming the immune system against a tumor associated antigen and then boost this response with an antigen encoding OV. Rhabdoviruses in particular have a strong ability to boost pre-existing T-cell responses towards a tumor antigen and enhance therapeutic benefit [111, 114, 116]. Generating an anti-tumor immune response significantly enhances therapeutic efficacy by lending itself not only to the targeting of the principle tumor but also to any of the tumor metastases [100]. Furthermore the memory responses generated by immune induction can play a pivotal role in preventing tumor relapse [137].

In 2012, Ugur Sahin's group published their exciting findings that therapeutically useful anti-tumor immune responses could be generated to mutant neo-epitopes found within the cancer genome [43]. This thesis is largely based on these key findings presented by Castle *et al.* These tumor specific nonsynonymous somatic point mutations, referred to throughout this text as "mutanome" epitopes, were identified through next generation sequencing (NGS) techniques and subsequent *in vivo* immunological analysis [43]. These B16F10 mutanome antigens, identified to have immunogenic potential, are the mutations we proceeded to investigate throughout this project.

While OVs have shown considerable efficacy on their own, targeting tumor antigens in association with OV therapy has lead to superior therapeutic potential [110-112, 116]. Based on the pre-existing data that the mutanome can be therapeutically targeted to induce tumor immunity [43] and that combination of OV therapy with tumor antigen directed immunotherapy results in superior therapeutic results [116], we hypothesized that combining vaccination against the immunogenic cancer mutanome with oncolytic virus therapy, would surpass the therapeutic potential of either treatment on its own. Additionally we will target multiple mutanome epitopes at once with the intention of minimizing the generation of antigen loss variants [138, 139]

*5.1 Confirmation of the immunogenicity but not the therapeutic potential of the B16F10 cancer mutanome*

Through NGS we were able to confirm that the majority of the immunogenic mutations identified by Castle *et al* were also present in our B16F10 cells (**Table 4.1**) [43]. The four mutations that were found not to be present within our cells were most likely the product of *in vitro* cell passaging [140] and so we focused our efforts on the other 12 mutanome epitopes present in our cells.

In corroboration of previous findings, we successfully were able to generate antigen specific immune responses towards mutanome epitopes through vaccination with synthetic long peptides (SLP) (**Figure 4.5**). Furthermore, the intensity of the T-cell responses generated towards these mutanome peptides also confirmed previous findings that MUT05, MUT17, MUT25, MUT30 and MUT44 were some of most highly immunogenic epitopes [43]. We found that one of the epitopes, MUT29, identified by

Castle *et al* to only induce weak T-cell activation in response to vaccination, did not elicit any immunological response in our hands (**Figure 4.5**)[43]. Since this peptide was only a weak antigen to start with, it is possible we were unable to detect a response due to assay sensitivity. However, since this epitope was previously characterized and the mutation was found to be present in our B16F10 cells, we decided to still include MUT29 in our future experiments.

In contrast to previous findings, we were unable to replicate the result that peptide vaccination using mutanome SLPs confers tumor control against B16F10 tumors (**Figure 4.9** & **4.10**)[43]. All of the experimental conditions used in our study were identical to those previously published in which tumor burden control was attained through a therapeutic treatment approach [43]. While we did not observe this tumor control it is possible that a therapeutic treatment approach was not robust enough to consistently see significant tumor control. In order to replicate their long-term survival of 2 out of 5 mutanome SLP treated mice we should use the prophylactic treatment timeline used in their experiment. While this experiment has not yet been conducted it is an obvious next step to ensure that we can repeat the prophylactic efficacy observed with mutanome SLP vaccination. Although our results demonstrate that therapeutic mutanome SLP vaccination may not confer a survival advantage in mice, this does not mean that other more stimulatory methods of immunotherapy would be unable to do so.

Peptide vaccination with minimal epitopes has long been recognized as a relatively weak therapeutic platform due to the antigen's short period of presentation by APCs to T-cells due to a rapid turnover of MHC molecules as well as the induction of

tolerance [74]. Efforts have been made to extend the potency of peptide vaccination through co-administration with immunogenic adjuvants and vaccination with synthetic long peptides instead of minimal immunodominant epitopes [63, 74]. While there has been major success in enhancing the therapeutic potential of peptides, peptide vaccination is still not as efficient as many other types of therapy. Thus, we propose that presenting the mutanome antigens to the immune system through a different and more stimulatory method, such as with a heterologous prime-boost vaccination using an OV as a boosting vector, could have superior therapeutic effects compared to mutanome SLP vaccination.

We were very motivated by the fact that we were able to confirm that immune responses can be generated towards mutanome neo-antigens in the cancer genome. Neoantigens offer a novel vaccination target that have yet to be fully explored in pre-clinical and clinical studies. In a previous study we demonstrated that peptide vaccination against the immunodominant minimal epitope of dopachrome tautomerase (DCT) was unable to confer tumor burden control in vaccinated mice (data not shown) despite inducing robust antigen specific immune responses (**Figure 4.3** & **Figure 4.4**)[141]. However, vaccination with select viruses encoding DCT leads to a very robust anti-tumor response, significant tumor control and increased survival [110, 111, 116]. This suggested to us that while peptide vaccination against the cancer mutanome may not be robust enough to confer a survival advantage in mice, encoding the mutanome epitopes within an oncolytic virus could be.

*5.2 The multi-epitope mutanome viruses*

The multi-epitope mutanome-encoding viruses were made and designed as described in the *Materials and Methods* and *Results* sections (**Figures 4.16** and **4.17**). Despite encoding 12 immunogenic mutanome epitopes, vaccination with the mutanome containing adenovirus (Ad-MUT) only induced responses to one of the mutanome epitopes: MUT25 (**Figure 4.19**). In contrast, vaccination with the MG1-MUT virus induced responses to two of the mutanome epitopes: MUT25 and MUT48 (**Figure 4.20**). While we cannot compare these findings directly due to different treatment regimens, both the Ad-MUT virus and the MG1-MUT virus encode the same mutanome construct so it is interesting that MG1-MUT would induce responses to more antigens than Ad-MUT. The reason for this is unclear, but it may be because MG1 is a replicating oncolytic virus and could be presenting substantially more antigen to the immune system than the non-replicating Ad-MUT virus. A lack of sufficient antigen presentation may account for why we are not seeing responses to the other mutanome antigens in the multi-epitope string.

It is known that MG1 on its own is not a very strong immune priming vector, but when the immune system is first primed against an antigen then MG1 encoding a tumor antigen has significant boosting potential [111]. Not surprisingly, when the mice were primed by Ad-MUT and boosted by MG1-MUT (**Figure 4.21** and **Figure 4.24)**, only a response to MUT25 was detected.

Based on our previous experiments evaluating epitope competition, we were not expecting immune competition to substantially affect our ability to detect T-cell responses towards multiple epitopes (**Figure 4.6-4.8**). However, it is important to note

that this experiment was conducted with peptide vaccinated mice rather than mice vaccinated with multi-epitope viral constructs. In fact, a study demonstrated that when mice were vaccinated with virally encoded polypeptide a skewed immune response towards just a single epitope was attained [142]. This article reasoned that competition for antigen recognition may be the cause of the skewed immune response. They also showed that vaccinating mice with a higher number of virus infected splenocytes lead to the subsequent boosting of previously undetectable CTL responses to other epitopes in the polypeptide string [142]. While we are not vaccinating mice with infected splenocytes, similar concepts of flooding the immune system with more antigen may apply. To test this, we could inject mice with higher doses of Ad-MUT virus to test if this will induce responses to a greater number of the mutanome epitopes. Testing this strategy with the MG1-MUT virus is less feasible because vaccinating mice with too high of a dose of MG1 is toxic. Another strategy that enabled the boosting of a greater number of CTL epitope responses in this paper was encoding the antigens in individual viruses and treating with a mixture of these viruses instead of with one virus encoding all of the antigens [142]. This too is another strategy that we could test by encoding mutanome sequences into individual viruses and vaccinating mice with a combination of these viruses.

In order for T-cells to generate an immune response to the mutanome antigens encoded within a virus, the multi-epitope construct needs to be effectively processed and loaded onto MHC molecules for presentation [143]. In considering the design of the multi-epitope construct (**Figure 4.16a**), MUT25 is located centrally and MUT48 is located at the C-terminus of the epitope string. The fact that we are able to detect T-

cells responses towards MUT25, and in some cases to MUT48, suggests that the mutanome construct is being expressed upon infection and at least partially processed and presented on the cell surface. However, this still leaves the question of why we are not detecting T-cell activity towards the other mutanome epitopes.

One possibility is that the multi-epitope sequence is not being cleaved between all of the mutanome epitopes as anticipated, or once cleaved, the 27AA peptides are not being degraded into minimal epitopes for MHC cell surface presentation. Epitope flanking residues play important roles in the sequence processing [79] and in how immune stimulatory a given peptide may be [77]. In some cases flanking sequences can actually act to prevent antigen processing so selecting appropriate linkage sequences between peptides in an epitope construct is very important [81, 82]. The AAY linkage sequences used within this study have been well characterized and used effectively in many studies with multi-epitope strings [69, 80]. However, one important consideration is that these linkage sequences have never been used in the context of an OV. Viruses induce substantial changes within the immune system so it is possible that these changes may affect the way in which multi-epitope sequences are processed.

As far as we know, the design used in this study to encode multiple tumor antigens within an oncolytic virus is a completely novel approach. The rational of this approach is explained in great detail in the *Introduction* and *Results* sections of this thesis. The incorporation of cleavage sequences [69, 79] and of ubiquitin for targeting to the proteasome [83, 85] are both well characterized techniques used in DNA vaccination [80]. In order to ensure that the polypeptide is designed appropriately we could test it through DNA vaccination in the absence of virus. A DNA string identical to

the one cloned into the viruses could be used to vaccinate mice for evaluation of subsequent immune responses. If T-cell responses are detected to the majority of our encoded peptides, this will indicate that it is the combination of this sequence with a virus that is ineffective. If however, immune responses are generated only towards MUT25, this would indicate that our multi-epitope strategy needs to be optimized before we can proceed to encode it within an OV.

Optimization of a multi-epitope strategy for encoding multiple antigens within an OV is currently underway. If we are unable to optimize this approach then one option would be to encode individual antigens into multiple viruses and administer them in combination. As previously suggested, this approach should successfully induce comparable immune responses against all of the antigens [142]. However, from a manufacturing and feasibility stand point it is much more efficient to make one virus encoding twelve antigens, than to make twelve viruses encoding one antigen each. While this may be possible for one study and one tumor model, it would be extremely difficult when considering a patient population that contains thousands of different mutations to be targeted.

*5.3 Potential implication of autoimmunity when targeting TAAs*

Despite what was originally hypothesized, the combination of vaccination against the cancer mutanome with oncolytic virus therapy has not yet led to enhanced therapeutic efficacy compared to vaccination with empty virus controls. As shown in **Figure 4.23**, mice that were vaccinated with a heterologous prime boost approach with mutanome viruses experienced no survival advantage over empty-vector control treated mice. In fact, mice treated prophylactically with mutanome viruses actually had

increased lung tumor burden relative to empty vector treated controls (**Figure 4.25**). Another interesting finding of this experiment, was that the mice treated with just one of the mutanome viruses, either the Ad-MUT or the MG1-MUT, in combination with either empty MG1 or peptides respectively, resulted in a relatively lower tumor burden than the mice treated with the prime-boost of Ad-MUT and MG1-MUT. This data is quite surprising given that there has been substantial evidence suggesting that a heterologous virus prime-boost vaccination approach has a significant therapeutic benefit [110, 111, 113, 114]. However, as far as we know there is no evidence suggesting that this approach has had a detrimental effect on therapy. Before any major conclusions are made this experiment should be repeated with a larger number of mice for confirmation of these results.

At the time of tumor challenge (timeline depicted in **Figure 4.25A**) we observed that the mice that had received the prime-boost with Ad-MUT/MG1-MUT or Ad-MUT/MG1-MUT-UbMut were smaller and more dehydrated than the mice from other virus treatment groups. This is significant because if the immune system of the mice was compromised in any way at the time of tumor challenge, this could be why the mice acquired a greater tumor burden.

It is difficult to interpret why the mutanome treated mice were sicker than the others. All viruses were prepared according to the same growth and purification methods and all viruses were titered along side each other. For confirmation however, a repeat experiment should be performed with new virus stocks. If the mice still appear to be less healthy than the other experimental groups then it could be the virally encoded mutanome construct that is contributing to this effect. We could

subsequently test this by injecting mice with a purified mutanome construct and evaluating the health of the mice relative to controls. Another potential cause may be that the MG1 mutanome viruses have altered replication timelines relative to the empty virus control. If the MG1 mutanome viruses were more virulent than the MG1 control virus, this may account for the decreased health of the mice that received these viruses. However, *in vitro* single-step and multi-step growth curves indicate that the three viruses have similar replication cycles so this is unlikely to be the cause (**Figure 4.18**). Furthermore, if MG1-MUT was more virulent we would expect the mice that received mutanome peptides and poly(I:C) followed by MG1-MUT to also have been of poor health, however this was not the case.

Dopachrome tautomerase (DCT) is a melanocyte self-antigen and as a general rule vaccination against self-antigens is more likely to induce autoimmune reactions than vaccination against non-self antigens. Correspondingly, it has been well documented that vaccination with viruses encoding dopachrome tautomerase (DCT) induces vitiligo in mice [117]. Vitiligo is a condition in which the skin/fur loses its colour due an autoimmune reaction against the host's melanocytes. Despite inducing vitiligo, vaccination against DCT was still able to induce prolonged survival [117]. This indicates that even if autoimmunity is observed, it does not necessarily eliminate therapeutic potential. Richard Vile's group has shown that mice vaccinated with VSV encoding a library of cDNA from normal tissue can cure established tumors of the same histological type without inducing any observable autoimmune consequences [113]. This is a good indication that vaccination against mutanome antigens is not likely to induce autoimmune responses, because all of the antigens being vaccinated against in

this study were self-antigens and yet there were no obvious signs of autoimmunity observed.

Although Vile's group did not observe any autoimmune reactions to self-epitopes [113], this does not eliminate the potential for autoimmunity in mice vaccinated against mutanome epitopes. Even though mutanome antigens are technically non-self antigens, there is only a single amino acid differentiating them from their wild-type self-epitopes. Thus there is the potential for cross-reactivity and induction of autoimmunity. In fact, we confirmed (**Figure 4.8B**) previous findings that T-cell responses induced by vaccination with mutanome peptides were also reactive to the wild-type peptide sequences [43]. While we saw no signs of autoimmunity in previous experiments, it is possible that autoimmune responses are the reason why the mice appeared sickly compared to the control mice. In future experiments with mutanome viruses we should carefully observe vaccinated mice for any physiological indicators of autoimmunity throughout the experiments.

*5.4 Future Directions*

As previously mentioned, in order to elucidate why there are only responses being generated to one or two mutanome epitopes there are a number of follow up experiments that should be carried out. 1 – A greater dose of Ad-MUT virus should be given to mice to evaluate whether this induces immune responses to any other mutanome epitopes. 2 – Mutanome sequences should be encoded in individual viruses for comparison with the multi-epitope virus. 3 – Mice should be vaccinated with a DNA string of the mutanome construct, and subsequent immune responses should be evaluated. This will enable us to determine whether the construct needs to be

redesigned. 4 – The experiment in which greater lung tumor burden was observed in mutanome virus vaccinated mice, should be repeated. In addition to lung tumor burden, responses towards wild-type peptides should be examined. 5 – To determine whether it is the mutanome construct that is causing the mice to be sick, mice should be treated with a purified mutanome protein and examined for any negative health effects. 6 – Another immune priming strategy should be adopted so that optimization attempts of the multi-epitope construct can be focused within the context of MG1. 7 – In order to examine whether the mutanome epitopes are reaching the surface of the cell for MHC presentation, we can examine the immunopeptidome – the peptides presented on MHC class I molecules [144]. This can be accomplished by infecting cells with our mutanome viruses, eluting the MHC peptides from the cell surfaces, and analyzing these peptides by mass spectrometry.

One particular aspect of my project that warrants further examination is the comparison of MG1-MUT virus with MG1-MUT-UbMut virus. As explained in the *Results* the only difference between these two viruses is that MG1-MUT-UbMUT has all of the lysines in its ubiquitin, except for lysine 48 (K48), substituted to arginine. Ubiquitin lysines are involved in the targeting of proteins within a cell through ubiquitination. Lysine 48 is the primary lysine involved in proteasome targeting [83]. The hope was that mutating all lysines other than K48 to arginine would favour proteasomal processing over lysosomal degradation, thus resulting in better epitope presentation by MHC molecules and induction of superior T-cell responses to mutanome peptides. Some preliminary data comparing the two viruses was acquired in a survival experiment (**Figure 4.23**), in lung tumor burden post treatment (**Figure 4.25**), and in

immunological analysis (**Figure 4.24B** & **C**), and no significant differences were observed between the two viruses. In order to elucidate whether the mutated ubiquitin is having a positive impact on the multi-epitope construct processing, mice could be primed with mutanome peptides and boosted with the MG1-MUT virus compared to the MG1-MUT-UbMUT virus as was done in **Figure 4.20**. However, given that MUT25 was the only response induced in **Figure 4.24C,** it appears that the factors affecting immune response generation with the MG1-MUT virus are also at play with the MG1-MUT-UbMut virus. Therefore proper processing and presentation of our multi-epitope construct needs to be achieved before we can effectively evaluate the potential of mutated ubiquitin relative to wild-type ubiquitin.

This thesis was focused on targeting neo-antigens formed by point mutations found in the cancer genome within the context of OV therapy. While any non-self segment of the DNA has the potential to induce immune responses, some genomic alterations may be more immunogenic than others. Future studies into the therapeutic potential of neo-antigens could focus on targeting mutations with more immunogenic potential such as frame-shift mutations, deletions or insertion mutations. Studies into if and how these mutations could be incorporated into OV therapy would be necessary.

*5.5 Potential for mutanome encoding oncolytic viruses*

Human cancers have been predicted on average to contain 40 to 60 HLA class I restricted epitopes per patient derived from mutanome sequences [25]. Furthermore it has been demonstrated that these mutations are often the subject of CD4+ and CD8+ T-cell immune responses in human cancers [51, 145]. Targeting multiple epitopes within a cancer from an immunotherapy standpoint limits the likelihood that escape variants

will evade the pressures of the immune response and subsequently result in tumor relapse [6]. Through their study of the B16F10 mutanome, Ugur Sahin's group has demonstrated that next generation sequencing is making it more feasible to sequence a patient's genome to identify immunotherapeutically targetable mutations [43]. While it has been proposed to target these tumor antigen sequences through synthetic long peptides [43], through DNA/RNA transfected dendritic cells [146, 147] or through direct administration of mRNA [44], we propose that stronger and more effective responses will be induced through a heterologous prime-boost vaccination strategy, with an oncolytic virus as the boosting vector. Importantly, in addition to boosting the immune responses, the oncolytic virus will induce other significant anti-tumor effects absent through other mechanisms of vaccination.

The data acquired throughout this thesis was largely preliminary and the approaches used, particularly the multi-epitope construct design, require much more in depth analysis and optimization. However, impressively we were able to confirm previous findings that vaccination with mutanome SLPs are able to induce specific T-cell immune responses, and that the strength of these T-cell responses were comparable to the ones previously described. Furthermore, we proposed and tested a novel approach to targeting multiple tumor antigens within the context of oncolytic virus therapy. Testing this method in a heterologous prime-boost scenario lead to T-cell responses towards 1 of the 12 encoded mutanome antigens. This tells us that the multi-epitope construct is at least being partially expressed, processed and presented. While this approach will still need considerable optimization, the fact that we were

able to detect at least one mutanome specific immune response indicates that it has potential.

In general, the approach we presented in this thesis has the potential to be a very promising cancer therapy once it is optimized. Not only would it involve treatment with an established oncolytic virus, but through the heterologous prime-boost vaccination it could also induce substantial anti-tumor immunity. Furthermore, targeting multiple tumor-unique antigens will hopefully avoid autoimmunity while also reducing the potential of antigen-loss variants and the risk of relapse.

## References


1. Medawar, P.B., *Advice to a young scientist*, ed. A.P.S. Foundation. 1979, United States of America: Basic Groups.
2. *Canadian Cancer Statistics 2013* 2013, Canadian Cancer Society: Toronto, ON.
3. Vogelstein, B. and K.W. Kinzler, *Cancer genes and the pathways they control.* Nat Med, 2004. **10**(8): p. 789-99.
4. Hanahan, D. and R.A. Weinberg, *The hallmarks of cancer.* Cell, 2000. **100**(1): p. 57-70.
5. Hanahan, D. and R.A. Weinberg, *Hallmarks of cancer: the next generation.* Cell, 2011. **144**(5): p. 646-74.
6. Vesely, M.D., *Natural innate and adaptive immunity to cancer* Annual Reviews of Immunology, 2011. **29**: p. 235-271.
7. Schreiber, R.D., L.J. Old, and M.J. Smyth, *Cancer immunoediting: integrating immunity's roles in cancer suppression and promotion.* Science, 2011. **331**(6024): p. 1565-70.
8. Dunn, G.P., et al., *Cancer immunoediting: from immunosurveillance to tumor escape.* Nat Immunol, 2002. **3**(11): p. 991-8.
9. Mittal, D., et al., *New insights into cancer immunoediting and its three component phases-elimination, equilibrium and escape.* Curr Opin Immunol, 2014. **27C**: p. 16-25.
10. Dunn, G.P., L.J. Old, and R.D. Schreiber, *The immunobiology of cancer immunosurveillance and immunoediting.* Immunity, 2004. **21**(2): p. 137-48.
11. Obeid, M., et al., *Calreticulin exposure dictates the immunogenicity of cancer cell death.* Nat Med, 2007. **13**(1): p. 54-61.
12. Ghiringhelli, F., et al., *Links between innate and cognate tumor immunity.* Curr Opin Immunol, 2007. **19**(2): p. 224-31.
13. Matsushita, H., et al., *Cancer exome analysis reveals a T-cell-dependent mechanism of cancer immunoediting.* Nature, 2012. **482**(7385): p. 400-4.
14. Engel, A.M., et al., *Methylcholanthrene-induced sarcomas in nude mice have short induction times and relatively low levels of surface MHC class I expression.* APMIS, 1996. **104**(9): p. 629-39.
15. Svane, I.M., et al., *Chemically induced sarcomas from nude mice are more immunogenic than similar sarcomas from congenic normal mice.* Eur J Immunol, 1996. **26**(8): p. 1844-50.
16. Koebel, C.M., et al., *Adaptive immunity maintains occult cancer in an equilibrium state.* Nature, 2007. **450**(7171): p. 903-7.
17. Teng, M.W., et al., *Opposing roles for IL-23 and IL-12 in maintaining occult cancer in an equilibrium state.* Cancer Res, 2012. **72**(16): p. 3987-96.
18. Dunn, G.P., C.M. Koebel, and R.D. Schreiber, *Interferons, immunity and cancer immunoediting.* Nat Rev Immunol, 2006. **6**(11): p. 836-48.
19. Stern-Ginossar, N., et al., *Human microRNAs regulate stress-induced immune responses mediated by the receptor NKG2D.* Nat Immunol, 2008. **9**(9): p. 1065-73.
20. Wang, T., et al., *Regulation of the innate and adaptive immune responses by Stat-3 signaling in tumor cells.* Nat Med, 2004. **10**(1): p. 48-54.

21. Khong, H.T., Q.J. Wang, and S.A. Rosenberg, *Identification of multiple antigens recognized by tumor-infiltrating lymphocytes from a single patient: tumor escape by antigen loss and loss of MHC expression.* J Immunother, 2004. **27**(3): p. 184-90.
22. Kaplan, D.H., et al., *Demonstration of an interferon gamma-dependent tumor surveillance system in immunocompetent mice.* Proc Natl Acad Sci U S A, 1998. **95**(13): p. 7556-61.
23. Dunn, G.P., et al., *A critical function for type I interferons in cancer immunoediting.* Nat Immunol, 2005. **6**(7): p. 722-9.
24. Boon, T., et al., *Human T cell responses against melanoma.* Annu Rev Immunol, 2006. **24**: p. 175-208.
25. Segal, N.H., et al., *Epitope landscape in breast and colorectal cancer.* Cancer Res, 2008. **68**(3): p. 889-92.
26. Darrasse-Jeze, G., et al., *Feedback control of regulatory T cell homeostasis by dendritic cells in vivo.* J Exp Med, 2009. **206**(9): p. 1853-62.
27. Steinman, R.M., D. Hawiger, and M.C. Nussenzweig, *Tolerogenic dendritic cells.* Annu Rev Immunol, 2003. **21**: p. 685-711.
28. Friedman, K.M., et al., *Tumor-specific CD4+ melanoma tumor-infiltrating lymphocytes.* J Immunother, 2012. **35**(5): p. 400-8.
29. Tran, E., et al., *Cancer immunotherapy based on mutation-specific CD4+ T cells in a patient with epithelial cancer.* Science, 2014. **344**(6184): p. 641-5.
30. Chapuis, A.G., et al., *Transferred melanoma-specific CD8+ T cells persist, mediate tumor regression, and acquire central memory phenotype.* Proc Natl Acad Sci U S A, 2012. **109**(12): p. 4592-7.
31. Church, S.E., et al., *Tumor-specific CD4+ T cells maintain effector and memory tumor-specific CD8+ T cells.* Eur J Immunol, 2014. **44**(1): p. 69-79.
32. Mellman, I., G. Coukos, and G. Dranoff, *Cancer immunotherapy comes of age.* Nature, 2011. **480**(7378): p. 480-9.
33. Steinman, R.M., *Decisions about dendritic cells: past, present, and future.* Annu Rev Immunol, 2012. **30**: p. 1-22.
34. Radford, K.J., K.M. Tullett, and M.H. Lahoud, *Dendritic cells and cancer immunotherapy.* Curr Opin Immunol, 2014. **27**: p. 26-32.
35. Kantoff, P.W., et al., *Sipuleucel-T immunotherapy for castration-resistant prostate cancer.* N Engl J Med, 2010. **363**(5): p. 411-22.
36. Leen, A.M., C.M. Rooney, and A.E. Foster, *Improving T cell therapy for cancer.* Annu Rev Immunol, 2007. **25**: p. 243-65.
37. Porter, D.L., et al., *Chimeric antigen receptor-modified T cells in chronic lymphoid leukemia.* N Engl J Med, 2011. **365**(8): p. 725-33.
38. Kalos, M., et al., *T cells with chimeric antigen receptors have potent antitumor effects and can establish memory in patients with advanced leukemia.* Sci Transl Med, 2011. **3**(95): p. 95ra73.
39. Davila, M.L., et al., *Efficacy and toxicity management of 19-28z CAR T cell therapy in B cell acute lymphoblastic leukemia.* Sci Transl Med, 2014. **6**(224): p. 224ra25.
40. Lemay, C.G., et al., *Harnessing oncolytic virus-mediated antitumor immunity in an infected cell vaccine.* Mol Ther, 2012. **20**(9): p. 1791-9.

41. Atanackovic, D., et al., *Vaccine-induced CD4+ T cell responses to MAGE-3 protein in lung cancer patients.* J Immunol, 2004. **172**(5): p. 3289-96.
42. Melief, C.J. and S.H. van der Burg, *Immunotherapy of established (pre)malignant disease by synthetic long peptide vaccines.* Nat Rev Cancer, 2008. **8**(5): p. 351-60.
43. Castle, J.C., et al., *Exploiting the mutanome for tumor vaccination.* Cancer Res, 2012. **72**(5): p. 1081-91.
44. Kreiter, S., et al., *Tumor vaccination using messenger RNA: prospects of a future therapy.* Curr Opin Immunol, 2011. **23**(3): p. 399-406.
45. Greenman, C., et al., *Patterns of somatic mutation in human cancer genomes.* Nature, 2007. **446**(7132): p. 153-8.
46. Sensi, M. and A. Anichini, *Unique tumor antigens: evidence for immune control of genome integrity and immunogenic targets for T cell-mediated patient-specific immunotherapy.* Clin Cancer Res, 2006. **12**(17): p. 5023-32.
47. Kroemer, G. and L. Zitvogel, *Can the exome and the immunome converge on the design of efficient cancer vaccines?* Oncoimmunology, 2012. **1**(5): p. 579-580.
48. Kreiter, S., et al., *Targeting the tumor mutanome for personalized vaccination therapy.* Oncoimmunology, 2012. **1**(5): p. 768-769.
49. Dubey, P., et al., *The immunodominant antigen of an ultraviolet-induced regressor tumor is generated by a somatic point mutation in the DEAD box helicase p68.* J Exp Med, 1997. **185**(4): p. 695-705.
50. Ikeda, H., et al., *Mutated mitogen-activated protein kinase: a tumor rejection antigen of mouse sarcoma.* Proc Natl Acad Sci U S A, 1997. **94**(12): p. 6375-9.
51. Lennerz, V., et al., *The response of autologous T cells to a human melanoma is dominated by mutated neoantigens.* Proc Natl Acad Sci U S A, 2005. **102**(44): p. 16013-8.
52. Stratton, M.R., *Exploring the genomes of cancer cells: progress and promise.* Science, 2011. **331**(6024): p. 1553-8.
53. Rosenberg, S.A., J.C. Yang, and N.P. Restifo, *Cancer immunotherapy: moving beyond current vaccines.* Nat Med, 2004. **10**(9): p. 909-15.
54. Gudmundsdotter, L., et al., *Therapeutic immunization for HIV.* Springer Semin Immunopathol, 2006. **28**(3): p. 221-30.
55. Pol, S. and M.L. Michel, *Therapeutic vaccination in chronic hepatitis B virus carriers.* Expert Rev Vaccines, 2006. **5**(5): p. 707-16.
56. Harrop, R., J. John, and M.W. Carroll, *Recombinant viral vectors: cancer vaccines.* Adv Drug Deliv Rev, 2006. **58**(8): p. 931-47.
57. Schlom, J., P.M. Arlen, and J.L. Gulley, *Cancer vaccines: moving beyond current paradigms.* Clin Cancer Res, 2007. **13**(13): p. 3776-82.
58. Cavallo, F., et al., *Vaccination for treatment and prevention of cancer in animal models.* Adv Immunol, 2006. **90**: p. 175-213.
59. Rice, J., C.H. Ottensmeier, and F.K. Stevenson, *DNA vaccines: precision tools for activating effective immunity against cancer.* Nat Rev Cancer, 2008. **8**(2): p. 108-20.
60. Gilboa, E., *DC-based cancer vaccines.* J Clin Invest, 2007. **117**(5): p. 1195-203.
61. Tacken, P.J., et al., *Dendritic-cell immunotherapy: from ex vivo loading to in vivo targeting.* Nat Rev Immunol, 2007. **7**(10): p. 790-802.

62. Bijker, M.S., et al., *Design and development of synthetic peptide vaccines: past, present and future.* Expert Rev Vaccines, 2007. **6**(4): p. 591-603.
63. Corradin, G., F. Spertini, and A. Verdini, *Medicinal application of long synthetic peptide technology.* Expert Opin Biol Ther, 2004. **4**(10): p. 1629-39.
64. Schulz, M., R.M. Zinkernagel, and H. Hengartner, *Peptide-induced antiviral protection by cytotoxic T cells.* Proc Natl Acad Sci U S A, 1991. **88**(3): p. 991-3.
65. Knutson, K.L. and M.L. Disis, *Tumor antigen-specific T helper cells in cancer immunity and immunotherapy.* Cancer Immunol Immunother, 2005. **54**(8): p. 721-8.
66. Feltkamp, M.C., et al., *Vaccination with cytotoxic T lymphocyte epitope-containing peptide protects against a tumor induced by human papillomavirus type 16-transformed cells.* Eur J Immunol, 1993. **23**(9): p. 2242-9.
67. Mandelboim, O., et al., *Regression of established murine carcinoma metastases following vaccination with tumour-associated antigen peptides.* Nat Med, 1995. **1**(11): p. 1179-83.
68. Toes, R.E., et al., *Peptide vaccination can lead to enhanced tumor growth through specific T-cell tolerance induction.* Proc Natl Acad Sci U S A, 1996. **93**(15): p. 7855-60.
69. Levy, A., et al., *A melanoma multiepitope polypeptide induces specific CD8+ T-cell response.* Cell Immunol, 2007. **250**(1-2): p. 24-30.
70. Bijker, M.S., et al., *Superior induction of anti-tumor CTL immunity by extended peptide vaccines involves prolonged, DC-focused antigen presentation.* Eur J Immunol, 2008. **38**(4): p. 1033-42.
71. Schnurr, M., et al., *Tumor antigen processing and presentation depend critically on dendritic cell type and the mode of antigen delivery.* Blood, 2005. **105**(6): p. 2465-72.
72. Lefrancois, L., A. Marzo, and K. Williams, *Sustained response initiation is required for T cell clonal expansion but not for effector or memory development in vivo.* J Immunol, 2003. **171**(6): p. 2832-9.
73. Obst, R., et al., *Sustained antigen presentation can promote an immunogenic T cell response, like dendritic cell activation.* Proc Natl Acad Sci U S A, 2007. **104**(39): p. 15460-5.
74. Bijker, M.S., et al., *CD8+ CTL priming by exact peptide epitopes in incomplete Freund's adjuvant induces a vanishing CTL response, whereas long peptides induce sustained CTL reactivity.* J Immunol, 2007. **179**(8): p. 5033-40.
75. Zwaveling, S., et al., *Established human papillomavirus type 16-expressing tumors are effectively eradicated following vaccination with long peptides.* J Immunol, 2002. **169**(1): p. 350-8.
76. Jager, E., et al., *Inverse relationship of melanocyte differentiation antigen expression in melanoma tissues and CD8+ cytotoxic-T-cell responses: evidence for immunoselection of antigen-loss variants in vivo.* Int J Cancer, 1996. **66**(4): p. 470-6.
77. Livingston, B.D., et al., *Optimization of epitope processing enhances immunogenicity of multiepitope DNA vaccines.* Vaccine, 2001. **19**(32): p. 4652-60.

78. Holzhutter, H.G., C. Frommel, and P.M. Kloetzel, *A theoretical approach towards the identification of cleavage-determining amino acid motifs of the 20 S proteasome.* J Mol Biol, 1999. **286**(4): p. 1251-65.
79. Altuvia, Y. and H. Margalit, *Sequence signals for generation of antigenic peptides by the proteasome: implications for proteasomal cleavage mechanism.* J Mol Biol, 2000. **295**(4): p. 879-90.
80. Velders, M.P., et al., *Defined flanking spacers and enhanced proteolysis is essential for eradication of established tumors by an epitope string DNA vaccine.* J Immunol, 2001. **166**(9): p. 5366-73.
81. Yellen-Shaw, A.J., et al., *Point mutation flanking a CTL epitope ablates in vitro and in vivo recognition of a full-length viral protein.* J Immunol, 1997. **158**(7): p. 3227-34.
82. Gileadi, U., et al., *Effect of epitope flanking residues on the presentation of N-terminal cytotoxic T lymphocyte epitopes.* Eur J Immunol, 1999. **29**(7): p. 2213-22.
83. Rodriguez, F., et al., *DNA immunization with minigenes: low frequency of memory cytotoxic T lymphocytes and inefficient antiviral protection are rectified by ubiquitination.* J Virol, 1998. **72**(6): p. 5174-81.
84. Hershko, A., *The ubiquitin pathway for protein degradation.* Trends Biochem Sci, 1991. **16**(7): p. 265-8.
85. Johnson, E.S., et al., *Ubiquitin as a degradation signal.* EMBO J, 1992. **11**(2): p. 497-505.
86. Chau, V., et al., *A multiubiquitin chain is confined to specific lysine in a targeted short-lived protein.* Science, 1989. **243**(4898): p. 1576-83.
87. Lim, K.L., et al., *Parkin mediates nonclassical, proteasomal-independent ubiquitination of synphilin-1: implications for Lewy body formation.* J Neurosci, 2005. **25**(8): p. 2002-9.
88. Russell, S.J., K.W. Peng, and J.C. Bell, *Oncolytic virotherapy.* Nat Biotechnol, 2012. **30**(7): p. 658-70.
89. Brun, J., et al., *Identification of genetically modified Maraba virus as an oncolytic rhabdovirus.* Mol Ther, 2010. **18**(8): p. 1440-9.
90. Roberts, M.S., et al., *Naturally oncolytic viruses.* Curr Opin Mol Ther, 2006. **8**(4): p. 314-21.
91. Dock, G., *The influence of complicating diseases upon leukaemia.* American Journal of the Medical Sciences, 1904. **127**(4): p. 563-592.
92. Bierman, H.R., et al., *Remissions in leukemia of childhood following acute infectious disease: staphylococcus and streptococcus, varicella, and feline panleukopenia.* Cancer, 1953. **6**(3): p. 591-605.
93. Hoster, H.A., R.P. Zanes, Jr., and E. Von Haam, *Studies in Hodgkin's syndrome; the association of viral hepatitis and Hodgkin's disease; a preliminary report.* Cancer Res, 1949. **9**(8): p. 473-80.
94. Barber, G.N., *Vesicular stomatitis virus as an oncolytic vector.* Viral Immunol, 2004. **17**(4): p. 516-27.
95. Lichty, B.D., et al., *Vesicular stomatitis virus: re-inventing the bullet.* Trends Mol Med, 2004. **10**(5): p. 210-6.

96. Yuan, F., et al., *Vascular permeability in a human tumor xenograft: molecular size dependence and cutoff size.* Cancer Res, 1995. **55**(17): p. 3752-6.
97. Mead, D.G., et al., *Transmission of vesicular stomatitis virus from infected to noninfected black flies co-feeding on nonviremic deer mice.* Science, 2000. **287**(5452): p. 485-7.
98. Stojdl, D.F., et al., *Exploiting tumor-specific defects in the interferon pathway with a previously unknown oncolytic virus.* Nat Med, 2000. **6**(7): p. 821-5.
99. Stojdl, D.F., et al., *VSV strains with defects in their ability to shutdown innate immunity are potent systemic anti-cancer agents.* Cancer Cell, 2003. **4**(4): p. 263-75.
100. Melcher, A., et al., *Thunder and lightning: immunotherapy and oncolytic viruses collide.* Mol Ther, 2011. **19**(6): p. 1008-16.
101. Mastrangelo, M.J., et al., *Intratumoral recombinant GM-CSF-encoding virus as gene therapy in patients with cutaneous melanoma.* Cancer Gene Ther, 1999. **6**(5): p. 409-22.
102. Prestwich, R.J., et al., *Immune-mediated antitumor activity of reovirus is required for therapy and is independent of direct viral oncolysis and replication.* Clin Cancer Res, 2009. **15**(13): p. 4374-81.
103. Cramer, D.W., et al., *Mumps and ovarian cancer: modern interpretation of an historic association.* Cancer Causes Control, 2010. **21**(8): p. 1193-201.
104. Bianchi, M.E., *DAMPs, PAMPs and alarmins: all we need to know about danger.* J Leukoc Biol, 2007. **81**(1): p. 1-5.
105. Novellino, L., C. Castelli, and G. Parmiani, *A listing of human tumor antigens recognized by T cells: March 2004 update.* Cancer Immunol Immunother, 2005. **54**(3): p. 187-207.
106. Dranoff, G., et al., *Vaccination with irradiated tumor cells engineered to secrete murine granulocyte-macrophage colony-stimulating factor stimulates potent, specific, and long-lasting anti-tumor immunity.* Proc Natl Acad Sci U S A, 1993. **90**(8): p. 3539-43.
107. Li, H., et al., *Oncolytic measles viruses encoding interferon beta and the thyroidal sodium iodide symporter gene for mesothelioma virotherapy.* Cancer Gene Ther, 2010. **17**(8): p. 550-8.
108. Kirn, D.H., et al., *Targeting of interferon-beta to produce a specific, multi-mechanistic oncolytic vaccinia virus.* PLoS Med, 2007. **4**(12): p. e353.
109. Willmon, C.L., et al., *Expression of IFN-beta enhances both efficacy and safety of oncolytic vesicular stomatitis virus for therapy of mesothelioma.* Cancer Res, 2009. **69**(19): p. 7713-20.
110. Bridle, B.W., et al., *Potentiating cancer immunotherapy using an oncolytic virus.* Mol Ther, 2010. **18**(8): p. 1430-9.
111. Pol, J.G., et al., *Maraba virus as a potent oncolytic vaccine vector.* Mol Ther, 2014. **22**(2): p. 420-9.
112. Diaz, R.M., et al., *Oncolytic immunovirotherapy for melanoma using vesicular stomatitis virus.* Cancer Res, 2007. **67**(6): p. 2840-8.
113. Kottke, T., et al., *Broad antigenic coverage induced by vaccination with virus-based cDNA libraries cures established tumors.* Nat Med, 2011. **17**(7): p. 854-9.

114. Pulido, J., et al., *Using virally expressed melanoma cDNA libraries to identify tumor-associated antigens that cure melanoma.* Nat Biotechnol, 2012. **30**(4): p. 337-43.
115. Bridle, B.W., et al., *Vesicular stomatitis virus as a novel cancer vaccine vector to prime antitumor immunity amenable to rapid boosting with adenovirus.* Mol Ther, 2009. **17**(10): p. 1814-21.
116. Bridle, B.W., S. Hanson, and B.D. Lichty, *Combining oncolytic virotherapy and tumour vaccination.* Cytokine Growth Factor Rev, 2010. **21**(2-3): p. 143-8.
117. Bridle, B.W., et al., *Immunotherapy can reject intracranial tumor cells without damaging the brain despite sharing the target antigen.* J Immunol, 2010. **184**(8): p. 4269-75.
118. Vliet, P.C. and J.S. Sussenbach, *An adenovirus type 5 gene function required for initiation of viral DNA replication.* Virology, 1975. **67**(2): p. 415-26.
119. Ghosh, S. and G.J. Duigou, *Decreased replication ability of E1-deleted adenoviruses correlates with increased brain tumor malignancy.* Cancer Res, 2005. **65**(19): p. 8936-43.
120. Bett, A.J., et al., *An efficient and flexible system for construction of adenovirus vectors with insertions or deletions in early regions 1 and 3.* Proc Natl Acad Sci U S A, 1994. **91**(19): p. 8802-6.
121. Tatsis, N. and H.C. Ertl, *Adenoviruses as vaccine vectors.* Mol Ther, 2004. **10**(4): p. 616-29.
122. Yang, T.C., et al., *The CD8+ T cell population elicited by recombinant adenovirus displays a novel partially exhausted phenotype associated with prolonged antigen presentation that nonetheless provides long-term immunity.* J Immunol, 2006. **176**(1): p. 200-10.
123. Pol, J.G., et al., *Panorama from the oncolytic virotherapy summit.* Mol Ther, 2013. **21**(10): p. 1814-8.
124. Schultz, E.S., et al., *A MAGE-A3 peptide presented by HLA-DP4 is recognized on tumor cells by CD4+ cytolytic T lymphocytes.* Cancer Res, 2000. **60**(22): p. 6272-5.
125. Poulin, K.L., et al., *Retargeting of adenovirus vectors through genetic fusion of a single-chain or single-domain antibody to capsid protein IX.* J Virol, 2010. **84**(19): p. 10074-86.
126. Ross, P.J. and R.J. Parks, *Construction and characterization of adenovirus vectors.* Cold Spring Harb Protoc, 2009. **2009**(5): p. pdb prot5011.
127. Wan, Y., et al., *Dendritic cells transduced with an adenoviral vector encoding a model tumor-associated antigen for tumor vaccination.* Hum Gene Ther, 1997. **8**(11): p. 1355-63.
128. Boudreau, J., et al., *Culture of myeloid dendritic cells from bone marrow precursors.* J Vis Exp, 2008(17).
129. Lutz, M.B., et al., *An advanced culture method for generating large quantities of highly pure dendritic cells from mouse bone marrow.* J Immunol Methods, 1999. **223**(1): p. 77-92.
130. Li, H. and R. Durbin, *Fast and accurate short read alignment with Burrows-Wheeler transform.* Bioinformatics, 2009. **25**(14): p. 1754-60.

131. Li, H., et al., *The Sequence Alignment/Map format and SAMtools.* Bioinformatics, 2009. **25**(16): p. 2078-9.
132. Robinson, J.T., et al., *Integrative genomics viewer.* Nat Biotechnol, 2011. **29**(1): p. 24-6.
133. Wang, K., M. Li, and H. Hakonarson, *ANNOVAR: functional annotation of genetic variants from high-throughput sequencing data.* Nucleic Acids Res, 2010. **38**(16): p. e164.
134. Dale, R.K., B.S. Pedersen, and A.R. Quinlan, *Pybedtools: a flexible Python library for manipulating genomic datasets and annotations.* Bioinformatics, 2011. **27**(24): p. 3423-4.
135. Robertson, G., et al., *De novo assembly and analysis of RNA-seq data.* Nat Methods, 2010. **7**(11): p. 909-12.
136. Boudreau, J.E., et al., *IL-15 and type I interferon are required for activation of tumoricidal NK cells by virus-infected dendritic cells.* Cancer Res, 2011. **71**(7): p. 2497-506.
137. Saffran, D.C., et al., *Immunotherapy of established tumors in mice by intratumoral injection of interleukin-2 plasmid DNA: induction of CD8+ T-cell immunity.* Cancer Gene Ther, 1998. **5**(5): p. 321-30.
138. Dunbar, P.R., et al., *A shift in the phenotype of melan-A-specific CTL identifies melanoma patients with an active tumor-specific immune response.* J Immunol, 2000. **165**(11): p. 6644-52.
139. Marincola, F.M., et al., *Escape of human solid tumors from T-cell recognition: molecular mechanisms and functional significance.* Adv Immunol, 2000. **74**: p. 181-273.
140. Wang, Y., et al., *Long-term cultured mesenchymal stem cells frequently develop genomic mutations but do not undergo malignant transformation.* Cell Death Dis, 2013. **4**: p. e950.
141. Davila, E., R. Kennedy, and E. Celis, *Generation of antitumor immunity by cytotoxic T lymphocyte epitope peptide vaccination, CpG-oligodeoxynucleotide adjuvant, and CTLA-4 blockade.* Cancer Res, 2003. **63**(12): p. 3281-8.
142. Palmowski, M.J., et al., *Competition between CTL narrows the immune response induced by prime-boost vaccination protocols.* J Immunol, 2002. **168**(9): p. 4391-8.
143. Guermonprez, P., et al., *Antigen presentation and T cell stimulation by dendritic cells.* Annu Rev Immunol, 2002. **20**: p. 621-67.
144. Caron, E., et al., *The MHC I immunopeptidome conveys to the cell surface an integrative view of cellular regulation.* Mol Syst Biol, 2011. **7**: p. 533.
145. Chen, L., et al., *Tumor immunogenicity determines the effect of B7 costimulation on T cell-mediated tumor immunity.* J Exp Med, 1994. **179**(2): p. 523-32.
146. Holtkamp, S., et al., *Modification of antigen-encoding RNA increases stability, translational efficacy, and T-cell stimulatory capacity of dendritic cells.* Blood, 2006. **108**(13): p. 4009-17.
147. Boudreau, J.E., et al., *Engineering dendritic cells to enhance cancer immunotherapy.* Mol Ther, 2011. **19**(5): p. 841-53.

**Contributions of Collaborators**

Dr. Kyle Stephenson scanned all of the ELISPOT plates quantified throughout this thesis with the ImmunoSpot plate reader (McMaster University, Hamilton ON). Spencer Martin, of Dr. Brad Nelson's Lab, conducted all of the Next Generation Genome Sequencing (BC Cancer Agency, Victoria BC), RNA-seq and subsequent analysis as described in detail in the *Materials and* Methods. Dr. Robin Parks cloned and rescued AdRP2014, referred to throughout this text as "Ad", and AdRP3117, referred to throughout this text as "Ad-MUT". Carmen Wong grew, purified and titered the AdRP2014 virus, and Kathrin Poulin grew, purified and titered the AdRP3117 (Ottawa Hospital Research Institute, Ottawa ON). Dr. Brian Lichty provided the Ad-hDCT and MG1-hDCT viruses (McMaster University). Dr. David Stojdl provided the MG1 shuttle vector and backbone (Children's Hospital of Eastern Ontario, Ottawa ON). Dr. Marie-Claude Bourgeois Daigneault provided the VSV-IFNγ, and Dr. Chantal Lemay provided the VSV-gmcsf, both used in Figure 4.12 (OHRI). Dr. Marie-Claude Bourgeois Daigneault successfully rescued the MG1-MUT-UbMUT virus. Dr. Victoria Jennings performed the flow cytometry for the experiment found in Appendix I. Dr. Rebecca Auer (OHRI), Dr. Brian Lichty and Dr. Kyle Stephenson were close collaborators throughout the entire project.

## Appendices

### Appendix I – No significant difference observed in T-cell response between a 1.5 hour and a 4 hour co-incubation with synthetic long peptide.

Mice were vaccinated with 100ug 27AA DCT peptide, with 50ug poly(I:C) on day 0 and with MG1 (1E8pfu) on day 7. On day 14 mice were euthanized and spleens were restimulated with nothing, VSVn, 9AA DCT or 27AA DCT peptide. Spleens were left to incubate with the restimulation peptide for the regular 1.5 hours or for 4hours prior to adding Golgi Plug to the cultures. Spleens were then further processed and stained for CD8+ and IFNγ and analyzed by flow cytometry. Data is presented as means + SEM.

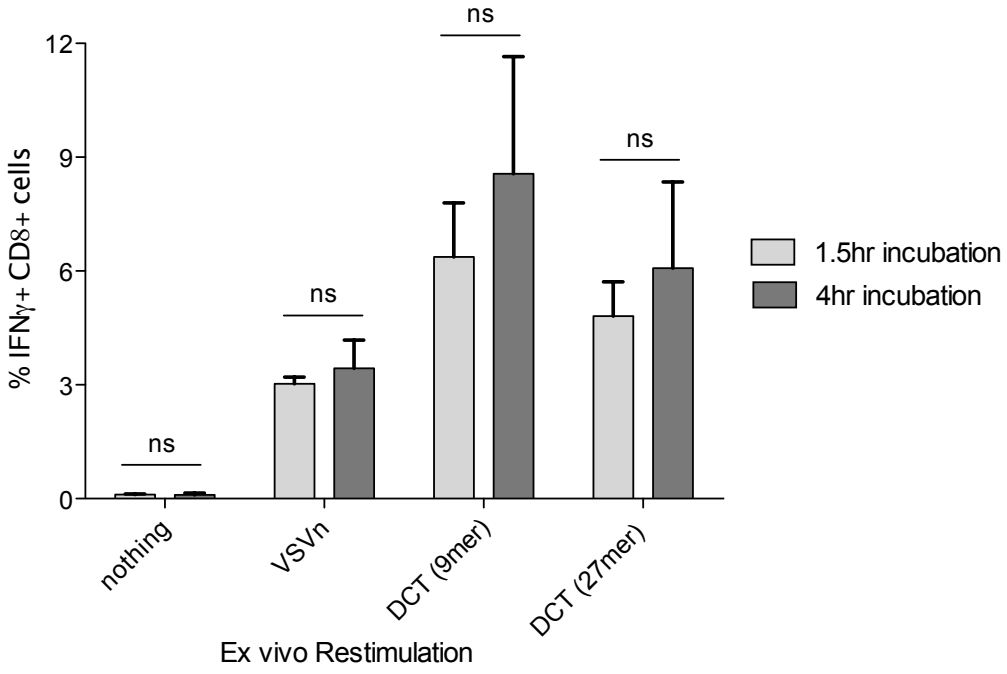
ns
ns
ns
ns
12
9
6
3
0
% IFNγ+ CD8+ cells
nothing
VSVn
DCT (9mer)
DCT (27mer)
Ex vivo Restimulation
1.5hr incubation
4hr incubation

**Appendix II. Immune responses generated to the mutanome peptides when vaccinated with differing doses of peptide.**

IFNγ ELISPOT analysis of splenocytes from mice vaccinated with the mutanome peptide cocktail and restimulated *ex vivo* against each individual peptide. C57Bl/6 mice were immunized with a cocktail of 100ug, 60ug or 30ug of each of the mutanome peptides with 50ug poly(I:C). All groups have an N of 3 mice per group but spleens were pooled among groups for the immune analysis. Columns represent means +SEM. Data is normalized to the unstimulated controls.

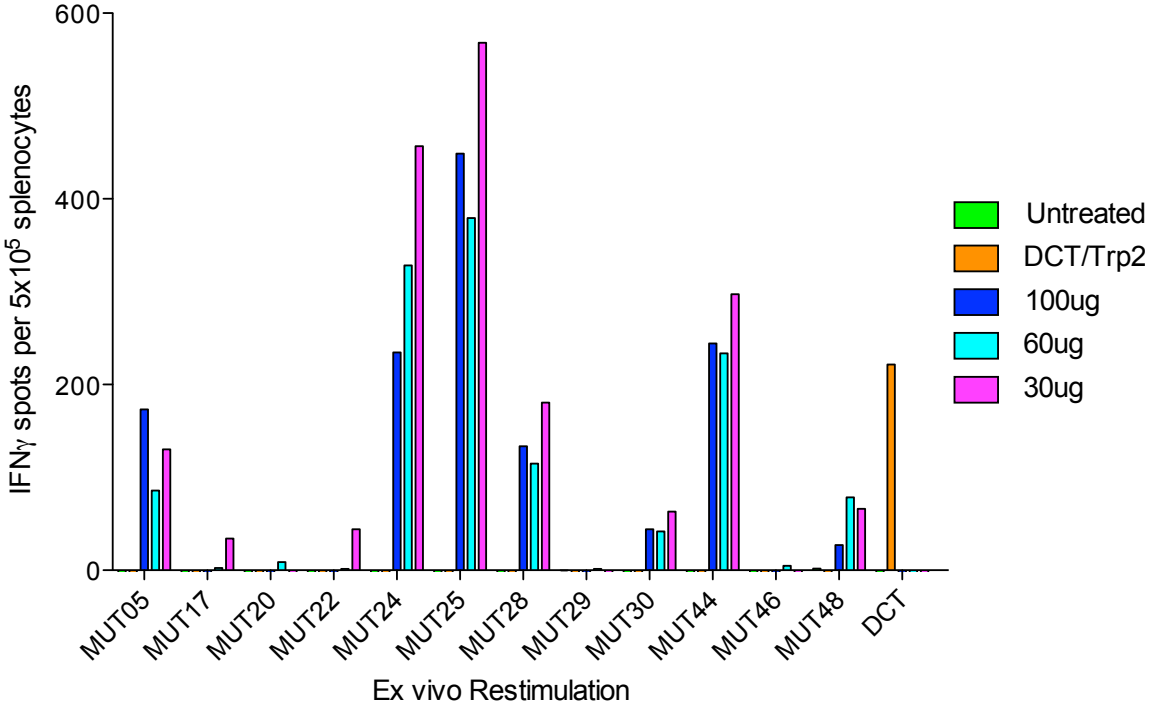
600
400
200
0
IFNγ spots per 5x10^5 splenocytes
MUT05
MUT17
MUT20
MUT22
MUT24
MUT25
MUT28
MUT29
MUT30
MUT44
MUT46
MUT48
DCT
Ex vivo Restimulation
Untreated
DCT/Trp2
100ug
60ug
30ug

**Appendix III – Reciprocal cellular cross-talk within the tumor microenvironment promotes oncolytic virus activity**

*Contributions of author:* M Marguerie was an ongoing collaborator on this project. M Marguerie conducted some select *in vitro* experiments, performed all of the flow cytometry analysis and aided in some of the *in vivo* mouse studies.

***Submitted:*** Nature Medicine, February 2014

Currently conducting some *in vivo* experiments to address the reviewers' comments

**Reciprocal cellular cross-talk within the tumor microenvironment promotes oncolytic virus activity**

Carolina S. Ilkow[1,2], Monique Marguerie[1,2], Cory Batenchuk[1,2], Daniela Ben Neriah[1], Sophie Cousineau[1], Theresa Falls[1], Christiano Tanese de Souza[1], Fabrice LeBoeuf[1,2], Rozanne Arulanandam[1,2], Lawton Stubbert[1,2], Steve Thorne[3], Piriya Paramanthan[4], Avijit Chatterjee[4], Christina Addison[1,2], David Stojdl[2,5], Jean-Simon Diallo[1], Brian Lichty[6], and John C. Bell[1,2,4]

[1]Centre for Innovative Cancer Therapeutics, Ottawa Hospital Research Institute, Ottawa, ON, Canada

[2]Departments of Biochemistry, Immunology and Microbiology, University of Ottawa, Ottawa, ON, Canada

[3]University of Pittsburgh Cancer Institute and Departments of Surgery and Immunology, University of Pittsburgh, Pittsburgh, Pennsylvania, USA

[4]The Ottawa Hospital, Division of Gastroenterology, Ottawa, ON, Canada.

[5]Children's Hospital of Eastern Ontario Research Institute, Ottawa, ON, Canada

[6]McMaster Immunology Research Centre, McMaster University, Hamilton, ON, Canada

Corresponding author: John C. Bell

Running Title: The tumor microenvironment enhances virotherapy through FGF-2

dependent modulation of antiviral innate responses

**Appendix IV – Panorama from the oncolytic virotherapy summit**

*Contributions of author:* M Marguerie attended the Seventh International Meeting on Replicating Oncolytic Virus Therapeutics, took detailed notes during the sessions, researched and wrote the manuscript in collaboration with JG Pol and R Arulanandam and under the supervision of JC Bell and BD Lichty.

***Published:*** Molecular Therapy, October 2013

doi:10.1038/mt.2013.207

# Panorama From the Oncolytic Virotherapy Summit

## *7th International Summit on Oncolytic Viral Therapeutics*

**Quebec, Canada, 15–18 June 2013**

Jonathan G Pol[1], Monique Marguerie[2], Rozanne Arulanandam[2], John C Bell[2] and Brian D Lichty[1]

In June, the historical heart of Quebec City welcomed the 7th International Summit on Oncolytic Viral Therapeutics for an excellent opportunity to witness the growth of the field, in both size and maturity. Efforts are being made to better characterize interactions between oncolytic viruses (OVs) and host components, both inside and outside the tumor bed, with their relative contribution to the overall therapeutic efficacy. New approaches in improving OV delivery, tumor selectivity, spreading, and killing continue to flourish. Clinical evaluations, ongoing and upcoming, have never been this numerous. The present review draws on some of the unpublished and recently published findings reported during the meeting.

Oncolytic virotherapy appears to be a promising contender for the treatment of neoplasms that fail to respond to approved therapies. Encouraging responses with minimal side effects have already been reported against cancers considered to be incurable, such as glioblastoma multiforme (GBM). With a 15-month median survival and a 5-year survival rate of <10% under standard care, it is the most aggressive primary brain malignancy. Several OVs have demonstrated a tolerable safety profile in phase I trials against GBM. At this summit, related efficacy data were unveiled. It was reported that 52% of the 24 patients who received a single intratumoral injection of the adenovirus (Ad) DNX-2401 as first-line therapy showed stabilization or partial or complete regression of their disease. Six patients are still alive, one reaching 4 years posttreatment (Frank Tufaro, DNAtrix). Clinical activity and benefits have also been reported in GBM patients treated with the replicating lentivirus Toca511 (in combination with the prodrug TocaFC) (Doug Jolly, Tocagen) or with the poliovirus PVS-RIPO (Matthias Gromeier, Duke University). Both viruses were administered locally, as a first-line treatment or as a second-line therapy in combination with resection, respectively. Results are very promising with many complete responses so far. Impressively, three of the seven patients who received the PVS-RIPO so far have already displayed complete response.

Three viral oncolytics have reached phases IIB–III of clinical evaluation, giving hope for a first OV approval in Western countries: the modified vaccinia virus (VACV) Pexa-vec/JX-594 (Caroline Breitbach, Jennerex), the wild-type reovirus Reolysin, and the engineered herpes simplex virus (HSV) T-VEC.[1] Results from the phase III OPTiM trial, involving T-VEC for the treatment of unresected stages IIIb/c and IV melanoma, were presented. T-VEC, an oncolytic HSV-1 expressing granulocyte–macrophage colony-stimulating factor (GM-CSF), was administered into primary or nodal lesions, while the control arm received subcutaneous injections of GM-CSF. The primary end point was met, with a durable response (objective response lasting 6 months or more) observed in 16.3% of patients treated with T-VEC vs. 2.1% in the GM-CSF cohort. The difference was even more striking when only stage IIIb/c patients were considered: 33% vs. 0%, respectively. Several secondary end points were also met, including overall response (26.4% vs. 5.7%). Overall survival analysis was not finalized but showed a trend in favor of T-VEC.

Because of tumor evasion and metastasis, efficient treatment of advanced-stage neoplasms will probably require systemic delivery of the oncolytic agent. Through this route, OVs must overcome numerous barriers to reach the tumor, such as antibody neutralization, macrophage capture, and off-target tissue adsorption. Two years ago, Pexa-Vec/JX-594 first demonstrated antitumor activity following a single intravenous injection in 12 of 22 patients with advanced treatment-refractory solid tumors.[2] Ever since, several OVs—including Reolysin, the Ad chimera ColoAd1, the VACV GL-ONC1, and the Seneca valley virus NTX-010—have been reported as being suitable for safe blood infusion in phase I human trials. Their therapeutic efficacy is currently under clinical investigation. The list is rapidly extending as additional candidates are translating into the clinic (e.g., measles virus MV-NIS, parvovirus H-1 ParvOryx, rhabdoviruses VSV-hIFN-β, and Maraba MG1-hMAGE-A3).

Efficacy of oncolytic virotherapy relies not only on viral oncolysis of infected cells but also on the induction of antitumor immunity. Immune mediators contributing to OV-induced antitumor immunity and their dynamics of action are subject to particular attention. Treatment with oncolytic reovirus typically induces the secretion of proinflammatory cytokines and the recruitment of antigen-presenting cells, natural killer (NK) cells, and T lymphocytes within the tumor environment.[3,4] Additionally, a recent study described concomitant inhibition of the infiltration and protumor effects of myeloid-derived suppressor cells and regulatory T cells.[5] In a murine melanoma model, reovirus-mediated priming of an antitumor cytotoxic response was independent of both virus replication and oncolysis.[6] A similar

[1]*McMaster Immunology Research Center, Department of Pathology and Molecular Medicine, McMaster University, Hamilton, Ontario, Canada;* [2]*Ottawa Hospital Research Institute, Centre for Innovative Cancer Research, Ottawa, Ontario, Canada*

***Correspondence:*** *Brian D Lichty, Department of Pathology and Molecular Medicine, MDCL 5023, McMaster University, 1280 Main Street West, Hamilton, Ontario L8S 4K1, Canada. E-mail: lichtyb@mcmaster.ca*

observation has recently been reported for the attenuated Maraba virus MG1 in the same model. Indeed, administration of MG1 resulted in a replication-independent, rapid, and intense activation of NK cells (Jiqing Zhang, Ottawa). For at least these two RNA viruses, the adjuvant role of virus-associated molecular patterns determined therapeutic efficacy. Such properties may be of particular interest in a perioperative setting. Indeed, the immunosuppression that follows surgery is associated with high risk of metastatic cancer recurrence.[7] It is speculated that activation of immune cells such as NK cells by replication-incompetent viruses has the potential to prevent tumor recurrence.[8]

The adaptive antitumor immune response is commonly generated within a few weeks after OV administration, but a clinical impact of immunotherapy may not become apparent in short-term follow-up. Intriguingly, an ongoing human clinical trial involving the engineered poliovirus PVS-RIPO for the treatment of high-grade glioma appears to fit this emerging paradigm (Matthias Gromeier, Duke University)—tumor shrinkage was delayed to several months after local infusion of PVS-RIPO. Biopsy samples illustrated massive cancer cell necrosis and infiltration of macrophages and lymphocytes. Involvement of OV oncolysis at that time point was excluded, as viral clearance was achieved within 2 weeks postinjection because of a strong humoral response. Mechanisms in understanding these results will probably require better characterization of the interactions among poliovirus, infected brain tumor cells, and the immune system.

OVs have been armed over the years with immunomodulatory factors to enhance their immunotherapeutic ability. Regardless of the protein expressed from the virus, such strategies allow for tumor-localized delivery at high local concentrations while avoiding toxicity that potentially arises from systemic administration. Transgenes encoding cytokines such as GM-CSF or interleukin-12 (IL-12) have been inserted into various OV backbones. One research group recently found that expressing IL-12 from an oncolytic HSV increased interferon-γ (IFN-γ) release, inhibited angiogenesis, and reduced the number of immunosuppressive regulatory T cells within the tumor.[9]

Expression of trastuzumab, a monoclonal antibody targeting HER2, from an oncolytic Ad resulted in improved efficacy in HER2-positive cancers (Paula Savola, Helsinki). New studies are investigating the ability of measles virus (MV) armed with CTLA4 or PD-L1 antibodies to prolong survival (Guy Ungerechts, Heidelberg). Other research groups have armed VACV with TRAIL (Rinat Maksyutov, Koltsovo) or CD40L (Karolina Autio and Suvi Parvainen, Helsinki) to induce apoptosis and promote T-cell expansion, respectively. The presence of the VACV-soluble type I IFN-neutralizing protein B18R within the tumor environment has previously been shown to enhance HSV and vesicular stomatitis virus (VSV) antitumor activity.[10–12] Recently, B18R has been expressed from a new immunomodulatory platform, the nonpathogenic commensal bacterium *Escherichia coli*. Tumor "preconditioning" with B18R expressing *E. coli* followed by treatment with VSV led to enhanced OV infection and greater therapeutic efficacy (Michelle Cronin, Cork).

Overexpression of tumor-associated antigens (TAAs) from OV genomes has also been exploited to generate potent tumor-specific T-cell responses. To extend the strategy to different types of tumors, corresponding immunogenic TAAs will need to be identified. The TAA dopachrome tautomerase has been targeted for OV-mediated murine melanoma immunotherapy.[13] Dopachrome tautomerase is currently being investigated for the treatment of glioma in murine models together with the glioma-associated antigens EphrinRA2 and ED-B. Oncolytic VSV[13] and Maraba virus both display potent vaccine booster ability. In macaques, a prime-boost strategy involving an oncolytic Maraba MG1 vaccine to boost Ad-primed response against the human tumor antigen MAGE-A3 generated remarkably strong MAGE-A3–specific responses (Jonathan Pol, McMaster University). This approach will be translated into patients with advanced MAGE-A3$^+$ tumors in the coming months. In addition to targeting one highly immunogenic TAA, it has been proposed that targeting multiple TAAs, even if individual responses are weak, could have therapeutic benefit by generating a significant overall antitumor response. As an illustration, mice with brain melanoma displayed prolonged survival following treatment with a VSV–complementary DNA (VSV-cDNA) library derived from human melanoma cells.[14] Such an approach applied early enough could prevent emergence of antigen-loss variants and thus recurrence. Indeed, the antigenic profile of recurring tumors differed from that of primary tumors. As a consequence, recurring tumors could only be cured by treating them with VSV-cDNA libraries derived from recurring tumors but not from parental tumors. Another interesting finding resided in the possibility of treating recurring melanoma tumors with cDNA libraries from recurring prostate cancer and vice versa. A comparative analysis led to the identification of shared TAAs specific to tumor recurrence (Richard Vile, Mayo Clinic).

Recent progress in the field of oncolytic virotherapy has been focused on circumventing the tumor microenvironment barriers that constitute the dense extracellular matrix (ECM), the tortuous tumor vasculature, and various immune-cell populations to improve delivery, dissemination, and efficacy. In a different light, it was revealed that the natural ability of oncolytic VACV to infect resident tumor endothelial cells and induce vascular shutdown is enhanced with the maturity of the developing vasculature.[15] The alternative strategy adopted by this OV, and potentially others, to "bite the hand that feeds" may be due to elevated levels of vascular endothelial growth factor, a key driver of vessel maturation recently found to have a direct immunosuppressive effect on the tumor vascular bed (Andrea McCart, Toronto). The tumor-associated stroma was recognized as another compartment conducive to OV infection due to an elegant interplay of growth factor signaling between activated, cancer-associated fibroblasts and tumor cells (Carolina Ilko, Ottawa).

These data combined, revealing the inherent immunosuppressive, OV-sensitizing effects of certain soluble growth factors within the tumor microenvironment, prompt us to consider whether this compartment can instead be exploited to reap the full benefits of OV therapy. Besides, it is known that components of the ECM can be natural targets for VACV and/or myxomavirus (MYXV) attachment.[16] On the other hand, in the context of oncolytic Ad, treatment of tumors with ECM-digesting enzymes, such as hyaluronidase, can improve spread and efficacy.[17] Researchers have extended these findings to show that in resistant models of pancreatic adenocarcinoma, an oncolytic Ad expressing hyaluronidase (VCN-01), had potent antitumor cytotoxicity when combined with gemcitabine, a first-line chemotherapy

for this cancer type (Miriam Bazam-Peregrino, Barcelona). Another group is also observing improved antitumor efficacy upon combining hyaluronidase with two additional proteolytic enzymes—chondroitinase and proteinase K—in conditionally replicating Ad (Alison Tedcastle, Oxford). Switching gears to brain cancers, microglial cells, which contribute up to one-third of the tumor mass, were shown to proliferate after administration of HSV and to interfere with HSV oncolysis. RAMBO virus, an oncolytic HSV expressing the antiangiogenic fragment vasculostatin (Vstat120), was able to reduce microglia activation and inflammation by suppressing its expression or secretion of tumor necrosis factor-α, as observed both *in vitro* and in mice with intracranial tumors (Balveen Kaur, Ohio State University).

Only a few OVs currently researched are naturally tumor-tropic in terms of their receptor specificity (e.g., Sindbis virus, coxsackievirus A21).[18–20] Research in the field is progressing toward identifying and exploiting inherent OV cell entry pathways and systematically modulating receptor specificity to increase tumor selectivity. VSV displays pantropic infectivity mediated by its coat protein (G), and its cellular port of entry was very recently identified as the low-density-lipoprotein receptor.[21] New studies revealed that the inherent neurotoxicity of VSV can be markedly reduced when G is replaced with MV H and F glycoproteins without affecting the rapid spread of the virus.[22] In a similar vein, others have replaced VSV-G with the lymphocytic choriomeningitis virus glycoprotein to render it nonneurotoxic.[23] With the additional use of mesenchymal stem cells as carrier cells, dampened antibody-mediated neutralization has been observed while achieving significant efficacy in orthotopic models of ovarian cancer (Catherine Dold, Innsbruck). Complement-mediated neutralization of VSV-G, which is far greater in human than mouse serum, can also be circumvented through pseudotyping with the less immunogenic Maraba virus G protein (Steven Russell, Mayo Clinic). In the case of Ads, chimeras have been generated by exchanging the Ad5 hexon with hexons from different serotypes to reduce Kupffer cell capture in the liver and lower antibody neutralization (e.g., Ad3, 6, 11, or 48). However, the field has started to move from a linear to a more systematic synthesis of novel OVs to accelerate identification of tumor-selective candidates. One group developed a platform of about 60 different Ads in which about 60% of the genome can be replaced (Clodagh O'Shea, Salk Institute). The aim will be to craft therapies specific for different tumor types by swapping coat proteins from Ads that naturally target the organ of interest.

Another strategy commonly applied to improve OV tumor selectivity consists of placing OV genome replication under tumor-restricted transcriptional regulators. This can be achieved by incorporating microRNA response elements (MREs) specific to microRNAs (miRs) overexpressed in normal tissues or downregulated in tumor cells. This approach is of particular interest when OVs are delivered systemically so as to limit off-target replication. MREs complementary to miRs specifically expressed in liver, muscle, and macrophages were recently introduced in the genome of Sindbis virus (Gray Kueberuwa, Oxford). Intravenous injection of the engineered virus appeared safe and demonstrated antitumor activity in a murine metastatic melanoma model.

A few studies are currently being conducted with OVs targeting cancer stem cells (CSCs). Whereas CSCs' origin and nature remain controversial, their dual role as tumor-initiating cells and as a source of treatment-resistant cells is recognized.[24] CD133 is commonly thought to be a CSC marker. An oncolytic MV has been retargeted to $CD133^+$ cells by modifying the hemagglutinin (H) protein so that it displays a CD133-specific single-chain antibody fragment.[25] Another team has restricted HSV replication to CSCs by placing ICP4 expression under control of the CD133 promoter. In mice treated with this engineered HSV, whole-tumor shrinkage was observed despite targeting only $CD133^+$ cells, representing as little as 30% of the tumor mass (Kaoru Terai). With regard to these promising preclinical results, this targeted approach deserves further investigation and testing.

A constant focus for the field is to look for ways to predict how a certain tumor is going to react to a given OV and whether therapeutic success will be achieved. Human pancreatic ductal adenocarcinoma cells showed high heterogeneity in their permissiveness to VSV. Resistant cells demonstrated retention of type I IFN responses, constitutive high-level expression of IFN-stimulated genes, and defects in apoptosis (Valery Grdzelishvili, North Carolina). Introduction of JAK/STAT inhibitors resulted in increased viral infection, replication, and oncolysis.[26] Measles vaccine strain binds to both CD46 and signaling lymphocytic activation molecule (SLAM), often coexpressed in hematological malignancies.[27] Using NIS-expressing MV vectors able to recognize either receptor and high-resolution imaging, investigators found that SLAM-dependent entry led to more efficient tumor regression and survival in a mouse model of mantle cell lymphoma.[28] SLAM may be further exploited as a positive predictive marker for therapy. In the case of HSV-1, short hairpin RNA knockdown of histone deacetylase 6 (HDAC6) reduced degradation of HSV virions in glioma cell lines. This resulted in an increased HSV-1 oncolysis on primary glioma samples (Hiroshi Nakashima, Brigham & Women's Hospital).

Although treatment with short hairpin RNA may not be realistic *in vivo*, drug-targeted inhibition of HDAC6 may improve HSV efficacy against GBM. Seneca valley virus (SVV) is an oncolytic picornavirus with inherent tumor selectivity. By screening a large number of small-cell lung cancer lines, a research group found that the messenger RNA ratio of late neurogenic transcription factor NEUROD1 to early neurogenic transcription factor ASCL1 correlated with the degree of cell permissivity to SVV infection.[29] This ratio could be used as a predictive marker in the clinic for oncolytic SVV efficacy. Recently it was shown that Mnk kinase activity potentiated the efficacy of PVS-RIPO treatment (Michael Brown, Duke University). Interestingly, Mnk kinases are active in a variety of cancers and have been implicated in the development of chemoresistance.[30,31] This finding is encouraging for patients whose cancer failed to respond to chemotherapy and positions OV therapy as a promising complement to standard care strategies.

OV therapy also appeared as a precious add-on to standard-of-care stem cell transplantation (ASCT) for patients with diseases such as multiple myeloma (MM). Associated common concerns with ASCT are the development of graft-vs.-host disease (GvHD) and reintroduction of MM cells from the bone marrow samples. Therefore, one group has pretreated stem cell samples *ex vivo* with MYXV and successfully eliminated malignant cells before transplantation.[32–35]

Moreover, they have shown that infecting bone marrow with MYXV resulted in the infection of activated but not naive human T cells, abrogating GvHD post-ASCT.[36]

When standard monotherapies fail because of tumor resistance, combination strategies offer great promise. Targeting multiple cellular or molecular checkpoints that are vital for malignant cells could be one key to success. In this regard, synergistic efficacy between oncolytic virotherapy and chemotherapy has been reported in preclinical studies. With proper dosing, as well as route and timing of administration, all classes of anticancer drugs tested demonstrated positive interactions with OVs. As an example, combining the adenovirus Ad5/3-D24-GMCSF with the alkylating agents ifosfamide and the anthracycline doxorubicin significantly prolonged survival of immunocompetent rodents with sarcoma, in comparison to single agents (Mikko Siurula, Helsinki). Therapeutic improvement was associated with enhanced cell-death immunogenicity. In a hamster model of pancreatic adenocarcinoma, intratumoral administration of the oncolytic Ad VCN-01 allowed chemosensitization to the nucleoside analogue gemcitabine. In addition, a delayed antiviral humoral response was observed (Miriam Bazan-Peregrino, Barcelona). Both phenomena contributed to increased tumor growth control. Chemical agents affecting the microtubule network (e.g., docetaxel) also benefited from combination with OVs such as VSVΔM51 (Jean-Simon Diallo, Ottawa) or the coxsackievirus A21 (Min Yuan Quah, Newcastle) in ovarian and lung murine tumor models. The topoisomerase inhibitors irinotecan and mitoxanthrone improved antitumor efficacy when administered in combination with an oncolytic VACV (Kathryn Ottoline-Perry, Toronto) or HSV-1 (Samuel Workenhe, McMaster University) in colorectal peritoneal carcinomatosis and a mammary murine tumor model, respectively. Finally, a number of tyrosine and serine/threonine kinase inhibitors have displayed synergy with OVs in rodent tumor models. These include erlotinib with HSV-1 in the context of pancreatic cancer (Kazuo Yamamura, Nagoya), sorafenib in combination with reovirus in hepatitis C virus–associated hepatomas (Adel Jabar, Leeds), and mammalian target of rapamycin inhibitors together with HSV-1 in breast cancer models (Tommy Alain, McGill University).

Mutual benefits have also been reported between radiation therapy and OV therapy. For example, whole-brain irradiation has been shown to disrupt the blood–brain barrier. Therefore, one group demonstrated that head irradiation before systemic administration of reovirus enhanced virus delivery to intracranial tumors in mice (Liz Ilett, Leeds). This strategy will be evaluated in patients with recurrent high-grade brain tumors. Another approach consists of combining administration of $^{131}$I with OV-mediated expression of the sodium-iodide symporter NIS. Enhanced antitumor activity has been confirmed with several OV backbones, including MV, VSV, and VACV. Furthermore, NIS-driven uptake of the radionuclide inside the tumor bed not only increases cytotoxicity but also permits noninvasive tracking of OV infection sites.[37–39]

The ability to track OVs *in vivo* through reporter protein expression enables identification of permissive sites and visualization of the extent of viral replication. Such information may be helpful to design delivery optimization strategies or readministration schedules. With computer assistance, it has even been possible to make a three-dimensional model of the inoculum. However, several factors can alter the quality of the signal, such as rapid virus clearance, high background in the tissue hosting the tumor (e.g., liver), or nonspecific uptake in surrounding organs. For example, using positron emission tomography imaging, monitoring of VSV-NIS delivery to murine liver tumors was not feasible because of iodine uptake in the stomach. Depending on the tissue targeted, replacement of the reporter protein and/or the associated radionuclide may solve the issue. In the present case, VSV imaging was achieved by switching from [$^{131}$I]/NIS to the enhanced HSV-1 thymidine kinase sr39tk–[$^{18}$F]FHBG tracker system (Kim Bentrup, Munich).

For practical reasons (and despite their immunogenicity), green fluorescent protein and luciferase remain the most common reporter proteins used for visualizing OV-infected tissues. However, tissue components strongly interact with visible light, quickly annealing the signal emitted by such bioluminescent reporters as the number of cell layers increases. Cold substitutes are emerging, such as the fluorogen-activating proteins (FAPs). FAPs can be fused to proteins of interest and are poorly immunogenic. Coupled to fluorogens that emit in near infrared, they already demonstrated sensitive *in vivo* imaging in preclinical models (Steve Thorne, Pittsburgh). The use of reporter-expressing OVs has also been proposed as a cancer diagnostic tool. A demonstration of this application was performed on blood samples treated with Ad TRAD-F35–142–3pT. This modified Ad possesses: (i) an Ad35 fiber (F35) that binds to the leukocyte receptor CD46, (ii) an E1 gene expressed under the control of the telomerase promoter that is constitutively active in malignant cells (TRAD), and (iii) green fluorescent protein expression silenced in the presence of miR-142–3p—a miR expressed only in normal blood cells (142–3pT). This approach showed impressive sensitivity, being able to detect a single malignant cell out of millions of normal ones (Fuminori Sakurai, Osaka). By reducing the number of false-negative test results, this application of OVs would allow for earlier treatment, increasing the likelihood of success.

As numerous neoplasms fail to respond to standards of care, there is an urgent need for efficient alternatives. There is hope that some OVs will join the arsenal of approved anticancer therapies in the near future. As mentioned, there has been a remarkable expansion of our knowledge of OV biology inside and outside the tumor bed in the past few years. Subsequent development of new-generation OVs and combination strategies should contribute to expand the list of promising candidates significantly. However, definition of a "promising candidate" must be qualified, as this term has tended to be used to refer to an OV that displayed therapeutic efficacy in preclinical studies. Unfortunately, OV preclinical evaluation is mostly performed in the same imperfect rodent models that conducted several first-generation "good candidates" to clinical failure owing to a lack of therapeutic benefits.

Because evaluation in human patients is a long and costly process, a more reliable preclinical selection is required. In this regard, a method of *ex vivo* short-term culture of patient tumor biopsy samples with maintained high viability has been developed. This methodology, based on staining assays, allows evaluation of oncolytic activity, with characterization of the type of tumor cell death induced, as well as identification of the various immune components present inside the tumor section (e.g., cell subsets,

cytokines). Such a model is obviously still imperfect because it cannot address certain issues, such as OV delivery. However, it could be useful to quickly compare the oncolytic activity of distinct viruses on the same patient tumor sample. Preclinical comparison of multiple OVs in one particular tumor model should help to identify which OVs best treat a defined type of cancer and thus help prioritize its translation into the clinic for a particular neoplasm. Such comparative studies have recently been performed and are likely to multiply in the future. Because it is not always possible for a research group to achieve such comparisons, a good alternative could reside in defining consensus tumor models and relative parameters for each type of neoplasm that then would enable researchers to evaluate their own OV and compare it within the community.

## REFERENCES


1. Sheridan, C (2013). Amgen announces oncolytic virus shrinks tumors. *Nat Biotechnol* **31**: 471–472.
2. Breitbach, CJ, Burke, J, Jonker, D, Stephenson, J, Haas, AR, Chow, LQ *et al.* (2011). Intravenous delivery of a multi-mechanistic cancer-targeted oncolytic poxvirus in humans. *Nature* **477**: 99–102.
3. Gujar, SA, Marcato, P, Pan, D and Lee, PW (2010). Reovirus virotherapy overrides tumor antigen presentation evasion and promotes protective antitumor immunity. *Mol Cancer Ther* **9**: 2924–2933.
4. Gujar, SA, Pan, D, Marcato, P, Garant, KA and Lee, PW (2011). Oncolytic virus-initiated protective immunity against prostate cancer. *Mol Ther* **19**: 797–804.
5. Gujar, S, Dielschneider, R, Clements, D, Helson, E, Shmulevitz, M, Marcato, P *et al.* (2013). Multifaceted therapeutic targeting of ovarian peritoneal carcinomatosis through virus-induced immunomodulation. *Mol Ther* **21**: 338–347.
6. Prestwich, RJ, Ilett, EJ, Errington, F, Diaz, RM, Steele, LP, Kottke, T *et al.* (2009). Immune-mediated antitumor activity of reovirus is required for therapy and is independent of direct viral oncolysis and replication. *Clin Cancer Res* **15**: 4374–4381.
7. Tai, LH, de Souza, CT, Bélanger, S, Ly, L, Alkayyal, AA, Zhang, J *et al.* (2013). Preventing postoperative metastatic disease by inhibiting surgery-induced dysfunction in natural killer cells. *Cancer Res* **73**: 97–107.
8. Tai, LH, Zhang, J, Scott, KJ, Tanese de Souza, C, Alkayyal, AA, Ananth, AA *et al.* (2013). Perioperative influenza vaccination reduces post-operative metastatic disease by reversing surgery-induced dysfunction in natural killer cells. *Clin Cancer Res*; e-pub ahead of print 30 August 2013.
9. Zhang, W, Fulci, G, Wakimoto, H, Cheema, TA, Buhrman, JS, Jeyaretna, DS *et al.* (2013). Combination of oncolytic herpes simplex viruses armed with angiostatin and IL-12 enhances antitumor efficacy in human glioblastoma models. *Neoplasia* **15**: 591–599.
10. Fu, X, Rivera, A, Tao, L and Zhang, X (2012). Incorporation of the B18R gene of vaccinia virus into an oncolytic herpes simplex virus improves antitumor activity. *Mol Ther* **20**: 1871–1881.
11. Paglino, JC and van den Pol, AN (2011). Vesicular stomatitis virus has extensive oncolytic activity against human sarcomas: rare resistance is overcome by blocking interferon pathways. *J Virol* **85**: 9346–9358.
12. Le Boeuf, F, Diallo, JS, McCart, JA, Thorne, S, Falls, T, Stanford, M *et al.* (2010). Synergistic interaction between oncolytic viruses augments tumor killing. *Mol Ther* **18**: 888–895.
13. Bridle, BW, Stephenson, KB, Boudreau, JE, Koshy, S, Kazdhan, N, Pullenayegum, E *et al.* (2010). Potentiating cancer immunotherapy using an oncolytic virus. *Mol Ther* **18**: 1430–1439.
14. Pulido, J, Kottke, T, Thompson, J, Galivo, F, Wongthida, P, Diaz, RM *et al.* (2012). Using virally expressed melanoma cDNA libraries to identify tumor-associated antigens that cure melanoma. *Nat Biotechnol* **30**: 337–343.
15. Ottolino-Perry, K, Tang N, Head R, Ng, C, Arulanandam, R, Angarita, FA *et al.* (2013). Tumor vascularization is critical for oncolytic vaccinia virus treatment of peritoneal carcinomatosis. *Int J Cancer*; e-pub ahead of print 29 August 2013.
16. Chan, WM, Bartee, EC, Moreb, JS, Dower, K, Connor, JH and McFadden, G (2013). Myxoma and vaccinia viruses bind differentially to human leukocytes. *J Virol* **87**: 4445–4460.
17. Ganesh, S, Gonzalez-Edick, M, Gibbons, D, Van Roey, M and Jooss, K (2008). Intratumoral coadministration of hyaluronidase enzyme and oncolytic adenoviruses enhances virus potency in metastatic tumor models. *Clin Cancer Res* **14**: 3933–3941.
18. Wang, KS, Kuhn, RJ, Strauss, EG, Ou, S and Strauss, JH (1992). High-affinity laminin receptor is a receptor for Sindbis virus in mammalian cells. *J Virol* **66**: 4992–5001.
19. Berno, V, Porrini, D, Castiglioni, F, Campiglio, M, Casalini, P, Pupa, SM *et al.* (2005). The 67 kDa laminin receptor increases tumor aggressiveness by remodeling laminin-1. *Endocr Relat Cancer* **12**: 393–406.
20. Shafren, DR, Au, GG, Nguyen, T, Newcombe, NG, Haley, ES, Beagley, L *et al.* (2004). Systemic therapy of malignant human melanoma tumors by a common cold-producing enterovirus, coxsackievirus a21. *Clin Cancer Res*;**10**(Pt 1): 53–60.
21. Finkelshtein, D, Werman, A, Novick, D, Barak, S and Rubinstein, M (2013). LDL receptor and its family members serve as the cellular receptors for vesicular stomatitis virus. *Proc Natl Acad Sci USA* **110**: 7306–7311.
22. Ayala-Breton, C, Barber, GN, Russell, SJ and Peng, KW (2012). Retargeting vesicular stomatitis virus using measles virus envelope glycoproteins. *Hum Gene Ther* **23**: 484–491.
23. Muik, A, Kneiske, I, Werbizki, M, Wilflingseder, D, Giroglou, T, Ebert, O *et al.* (2011). Pseudotyping vesicular stomatitis virus with lymphocytic choriomeningitis virus glycoproteins enhances infectivity for glioma cells and minimizes neurotropism. *J Virol* **85**: 5679–5684.
24. Frame, FM and Maitland, NJ (2011). Cancer stem cells, models of study and implications of therapy resistance mechanisms. *Adv Exp Med Biol* **720**: 105–118.
25. Bach, P, Abel, T, Hoffmann, C, Gal, Z, Braun, G, Voelker, I *et al.* (2013). Specific elimination of CD133$^+$ tumor cells with targeted oncolytic measles virus. *Cancer Res* **73**: 865–874.
26. Moerdyk-Schauwecker, M, Shah, NR, Murphy, AM, Hastie, E, Mukherjee, P and Grdzelishvili, VZ (2013). Resistance of pancreatic cancer cells to oncolytic vesicular stomatitis virus: role of type I interferon signaling. *Virology* **436**: 221–234.
27. Noyce, RS, Bondre, DG, Ha, MN, Lin, LT, Sisson, G, Tsao, MS *et al.* (2011). Tumor cell marker PVRL4 (nectin 4) is an epithelial cell receptor for measles virus. *PLoS Pathog* **7**: e1002240.
28. Miest, TS, Frenzke, M and Cattaneo, R (2013). Measles virus entry through the signaling lymphocyte activation molecule governs efficacy of mantle cell lymphoma radiovirotherapy. *Mol Ther;* e-pub ahead of print 5 August 2013.
29. Poirier, JT, Dobromilskaya, I, Moriarty, WF, Peacock, CD, Hann, CL and Rudin, CM (2013). Selective tropism of Seneca valley virus for variant subtype small cell lung cancer. *J Natl Cancer Inst* **105**: 1059–1065.
30. Altman, JK, Glaser, H, Sassano, A, Joshi, S, Ueda, T, Watanabe-Fukunaga, R *et al.* (2010). Negative regulatory effects of Mnk kinases in the generation of chemotherapy-induced antileukemic responses. *Mol Pharmacol* **78**: 778–784.
31. Zhao, Y, Shen, S, Guo, J, Chen, H, Greenblatt, DY, Kleeff, J *et al.* (2006). Mitogen-activated protein kinases and chemoresistance in pancreatic cancer cells. *J Surg Res* **136**: 325–335.
32. Bartee, E, Chan, WS, Moreb, JS, Cogle, CR and McFadden, G (2012). Selective purging of human multiple myeloma cells from autologous stem cell transplant grafts using oncolytic myxoma virus. *Biol Blood Marrow Transplant* **18**: 1540–1551.
33. Rahman, MM, Madlambayan, GJ, Cogle, CR and McFadden, G (2010). Oncolytic viral purging of leukemic hematopoietic stem and progenitor cells with myxoma virus. *Cytokine Growth Factor Rev* **21**: 169–175.
34. Kim, M, Madlambayan, GJ, Rahman, MM, Smallwood, SE, Meacham, AM, Hosaka, K *et al.* (2009). Myxoma virus targets primary human leukemic stem and progenitor cells while sparing normal hematopoietic stem and progenitor cells. *Leukemia* **23**: 2313–2317.
35. Madlambayan, GJ, Bartee, E, Kim, M, Rahman, MM, Meacham, A, Scott, EW *et al.* (2012). Acute myeloid leukemia targeting by myxoma virus *in vivo* depends on cell binding but not permissiveness to infection *in vitro*. *Leuk Res* **36**: 619–624.
36. Bartee, E, Meacham, A, Wise, E, Cogle, CR and McFadden, G (2012). Virotherapy using myxoma virus prevents lethal graft-versus-host disease following xeno-transplantation with primary human hematopoietic stem cells. *PLoS One* **7**: e43298.
37. Belin, LJ, Ady, JW, Lewis, C, Marano, D, Gholami, S, Mojica, K *et al.* (2013). An oncolytic vaccinia virus expressing the human sodium iodine symporter prolongs survival and facilitates SPECT/CT imaging in an orthotopic model of malignant pleural mesothelioma. *Surgery* **154**: 486–495.
38. Li, H, Nakashima, H, Decklever, TD, Nace, RA and Russell, SJ (2013). HSV-NIS, an oncolytic herpes simplex virus type 1 encoding human sodium iodide symporter for preclinical prostate cancer radiovirotherapy. *Cancer Gene Ther* **20**: 478–485.
39. Li, H, Peng, KW and Russell, SJ (2012). Oncolytic measles virus encoding thyroidal sodium iodide symporter for squamous cell cancer of the head and neck radiovirotherapy. *Hum Gene Ther* **23**: 295–301.

## Appendix V – Permission from CCC to publish Vesley *et al* figure (Figure 1.1)

Copyright Clearance Center

1 PAYMENT 2 REVIEW 3 CONFIRMATION

### Step 3: Order Confirmation

**Thank you for your order!** A confirmation for your order will be sent to your account email address. If you have questions about your order, you can call us at +1.855.239.3415 Toll Free, M-F between 3:00 AM and 6:00 PM (Eastern), or write to us at info@copyright.com. This is not an invoice.

**Confirmation Number: 11217368**
**Order Date: 06/05/2014**

If you paid by credit card, your order will be finalized and your card will be charged within 24 hours. If you choose to be invoiced, you can change or cancel your order until the invoice is generated.

**Payment Information**

Monique Marguerie

**Order Details**

**Annual Review of Immunology**

| | |
|---|---|
| **Order detail ID:** | 65041660 |
| **Order License Id:** | 3402620737056 |
| **ISBN:** | 9780824330293 |
| **Publication Type:** | Book |
| **Publisher:** | Annual Reviews |

**Permission Status:** Granted
**Permission type:** Republish or display content
**Type of use:** Republish in a thesis/dissertation

| | |
|---|---|
| **Requestor type** | Academic institution |
| **Format** | Print, Electronic |
| **Portion** | chart/graph/table/figure |
| **Number of charts/graphs/tables/figures** | 1 |
| **Title or numeric reference of the portion(s)** | Natural innate and adaptive immunity to cancer. Figure 1. |
| **Title of the article or chapter the portion is from** | Natural innate and adaptive immunity to cancer |
| **Editor of portion(s)** | N/A |

| | |
|---|---|
| **Author of portion(s)** | Matthew D. Vesely, Michael H. Kershaw, Robert D. Schreiber, and Mark J. Smyth |
| **Volume of serial or monograph** | 29 |
| **Page range of portion** | 238 |
| **Publication date of portion** | 2011 |
| **Rights for** | Main product |
| **Duration of use** | Current edition and up to 5 years |
| **Creation of copies for the disabled** | no |
| **With minor editing privileges** | no |
| **For distribution to** | Canada |
| **In the following language(s)** | Original language of publication |
| **With incidental promotional use** | no |
| **Lifetime unit quantity of new product** | 0 to 499 |
| **Made available in the following markets** | Education |
| **The requesting person/organization** | Monique Marguerie |
| **Order reference number** | None |
| **Author/Editor** | Monique Marguerie |
| **The standard identifier** | 4859558 |
| **Title** | Combining the immunogenic cancer mutanome with oncolytic virus therapy |
| **Publisher** | University of Ottawa |

| | |
|---|---|
| **Expected publication date** | Jun 2014 |
| **Estimated size (pages)** | 200 |

**Note:** This item will be invoiced or charged separately through CCC's **RightsLink** service. More info **$ 0.00**

**This is not an invoice.**

**Total order items: 1**

**Order Total: $ 0.00**

# Monique Marguerie

## Education

**MSc. Biochemistry - Specialization in Human and Molecular Genetics** 2012 - present

- Graduate Admissions Scholarship
- CIHR *Frederick Banting and Charles Best* Masters Award

**Honours Bachelor of Science, Major Biology, Major Psychology** 2007 – 2011
University of Ottawa, Ontario

- Admission Scholarship; NSERC Undergraduate Research Scholarship; Honours Thesis project; Deans Honours List; Graduated with "magna cum laude"

## Publications/ Working Papers

**"Panorama from the Oncolytic Virotherapy Summit"**

Pol JG, Marguerie M, Arulanandam R, Bell JC, Lichty BD
Meeting Review. *Molecular Therapy*. 2013. 21(10): 1814-1818

**"Reciprocal cellular cross-talk within the tumor microenvironment promotes oncolytic virus activity"**

Carolina S. Ilkow[1,2], Monique Marguerie[1,2], Cory Batenchuk[1,2], Daniela Ben Neriah[1], Sophie Cousineau[1], Theresa Falls[1], Christiano Tanese de Souza[1], Fabrice LeBoeuf[1,2], Rozanne Arulanandam[1,2], Lawton Stubbert[1,2], Steve Thorne[3], Piriya Paramanthan[4], Avijit Chatterjee[4], Christina Addison[1,2], David Stojdl[2,5], Jean-Simon Diallo[1], Brian Lichty[6], and John C. Bell[1,2,4]
Research Paper. Submitted to *Nature Medicine* in February 2014. Currently working to address reviewers comments and suggestions.

**"Modulation of complement activity improves systemic delivery of oncolytic Vaccinia virus to tumors"**

Evgin L, Acuna S, Tanese de Souza C, Marguerie M, Lemay C, Falls T, Ilkow C, Parato K, Breitbach C, Kirn D, Atkins H, Stahl G, Thurman J, Holers M, Lambris J, McCart A, Bell J
Research Paper. Paper in preparation. Expected submission: August 2014.

## Funding

**CIHR Masters Award: Frederick Banting & Charles Best Canada Graduate Scholarship**

- Canadian Institutes of Health Research, 2013 –2014. Value of $17,500

**Graduate Admissions Scholarship**

- University of Ottawa, Sept 2012 – Aug 2014. Value of $15,000

**NSERC Undergraduate Student Research Award**

- NSERC, May 2011 – Aug 2011. Value of $4,500

**Undergraduate Admissions Scholarship**

- University of Ottawa, Sept 2007 – May 2008. Value of $3,000

## Major Projects/Presentations

**Poster Presentation at the Terry Fox Research Institute Conference** 2014
Montreal QC, Canada. May 7 – May 10, 2014

**Verbal Presentation for University of Ottawa BMI Seminar Day** 2014
Ottawa ON, Canada. March 7, 2014

**Poster Presentation at the Canadian Cancer Research Conference** 2013
Toronto ON, Canada. November 4 – November 6, 2013.

**Poster Presentation at the 7th International Meeting of Replicating Oncolytic Virus Therapeutics** 2013
Quebec City, QC, Canada. June 15 – June 18, 2013.

**Poster Presentation at the Cancer Immunology and Immunotherapy Conference (Keystone)** 2013
Vancouver, BC, Canada. January 27-February 1, 2013.

**Poster Presentation at the Ottawa Hospital Research Institute Research Day** 2012 &2013
Ottawa, ON, Canada November 15 2012, November 14 2013.

**Verbal Presentation at the Canadian Oncolytic Virus Consortium (CovCo) Retreat** 2012
Huntsville, ON, Canada. September 28 – October 1, 2012.

**Undergraduate Honours Thesis Project** 2010 – 2011
Supervisors: Dr Harold Atkins & Dr Scott Findlay
The Ottawa Hospital Cancer Centre/University of Ottawa, Ottawa, ON

- Developed statistical models to examine how tumour heterogeneity arises by assessing the outcomes of bone marrow transplants and chemotherapy treatments in multiple myeloma patients

**Fund allocation for species at risk in Canada** 2010
University of Ottawa/Parks Canada, Ottawa, ON

- Prepared a database and a report analysing species funding and the risk statuses for species found in Canada, for Dr. Briar Howes of Parks Canada

## Work Experience

**Research Technician** 2011 –2012
Jennerex Biotherapeutics, Ottawa, ON

- Participated in a collaborative effort with McMaster University to develop and optimize a rhabdovirus purification system to be used in virus purification for clinical trials

**Summer Research Student** 2011
Canadian Institute of Cancer Research, OHRI, Bell Lab, Ottawa, ON

- Funded by NSERC Undergraduate Student Research Award

**Research Assistant** 2010
Agri-Food and Agriculture Canada, Ottawa, ON

## Volunteer Experience

**Lets Talk Science: Classroom Mentor & Aboriginal Mentorship Program** 2012 – 2014
Carson Grove & Alta Vista Elementary School, Ottawa; Opeongo Highschool, Douglas ON

**Making Waves Ottawa President** 2013 - 2014
Jack Purcell & Lowertown Pool, Ottawa

**Making Waves Ottawa Swim Instructor & Fundraising Executive** 2011 - 2013
Jack Purcell & Lowertown Pool, Ottawa

**Child and Playroom Monitor** 2008 - 2013
Children's Hospital of Eastern Ontario, Ottawa

**Volunteer at orphanage for street children (ages 8-18)** 2010
Children for Children's Future, Arusha, Tanzania

**Emergency room research program recruiter, SUPPORT program** 2010
Children's Hospital of Eastern Ontario, Ottawa

## Extra-Curricular Activities/Other

**Kickboxing** 2012 – present
Therien Jiu-Jitsu & Kickboxing, Ottawa ON

**Recreational Ball Hockey League** 2011 – present
Ottawa Sport & Social Club, Ottawa ON

**Ottawa Race Weekend Half Marathon** 2010 & 2011
Run Ottawa, Ottawa ON

**PADI Certified Open Water Diver** 2008-present
PADI, Jamaica

**Standard First Aid, and CPR "C" Certified** 2006-present
Red Cross/St. Johns Ambulance